

New results on small- x resummation for splitting functions

Marco Bonvini,^a Stefano Frixione,^{b,c} Giovanni Stagnitto^{b,d}

^a*INFN, Sezione di Roma, Piazzale Aldo Moro 5, I-00185, Rome, Italy*

^b*INFN, Sezione di Genova, Via Dodecaneso 33, I-16146, Genoa, Italy*

^c*CERN, Theoretical Physics Department, CH-1211 Geneva, Switzerland*

^d*Università degli Studi di Genova, Via Dodecaneso 33, I-16146 Genoa, Italy*

E-mail: Marco.Bonvini@roma1.infn.it, Stefano.Frixione@cern.ch,
Giovanni.Stagnitto@ge.infn.it

ABSTRACT: We revisit the basic steps necessary to obtain next-to-leading-logarithmic accurate small- x results for the DGLAP splitting functions, and their implementations within the [HELL](#) framework. We derive new analytical all-order results for the leading-logarithmic gg anomalous dimension, the qg and gg finite Green functions, and most importantly for the qg anomalous dimension, which allows us to arrive for the first time at a properly resummed qg splitting kernel. We use these results as cornerstones of a new implementation of small- x splitting-function resummation which is more solid and numerically better behaved with respect to those available thus far. All of these novelties are included in the upcoming 4.0 version of [HELL](#).

KEYWORDS: Parton Distribution Functions, Resummation, Small- x

Contents

1	Introduction	2
2	Generalities on small-x resummation	5
2.1	Resummation of γ_+	6
2.2	Resummation of γ_{qg}	8
2.3	Synopsis of new analytical results	12
3	All-order resummation of P_{qg}	12
3.1	All-order result in conjugate Mellin space	13
3.2	Perturbative coefficients	16
3.3	Resummation of subleading running coupling effects	19
4	Resummed DGLAP evolution to large α_s	22
4.1	Improvements to employ large α_s values in γ_+	22
4.2	Numerical results for P_{qg} and comparison with previous predictions	24
4.3	Results for the singlet splitting function matrix	27
4.4	When subleadingness ceases to be a useful concept	29
5	Future directions: results for the qg Green function	32
6	Conclusions	36
A	New analytical all-order results for γ_s	37
A.1	Perturbative coefficients	37
A.2	Integral representations	39
A.3	Fixed-point representation	42
B	Solving equations for the resummation of γ_{qg}	44
B.1	Determining the function Ω	44
B.2	Coefficients of the bare quark Green function $\hat{\mathcal{G}}_{qg}^{(0)}$	47
B.3	Extraction of the h_k coefficients and construction of the function h_{qg}	49
B.4	Alternative closed-form expression for t_n coefficients	52
B.5	Construction of finite quark Green function \mathcal{G}_{qg}	52
C	Details on numerical implementation	55
C.1	Numerical integrations for P_{qg}	55
C.2	Approximate fixed-order anomalous dimension at large α_s	57
C.3	A modified approximation for the resummation of running coupling effects in γ_+	58
C.4	Solution to the branch-change problem in γ_+	61
	References	63

1 Introduction

Predictions for high-energy hadron colliders rely on the collinear factorization formula

$$d\sigma_{h_1 h_2 \rightarrow X}(Q^2, s) = \sum_{ij} \int dx_1 dx_2 f_{i/h_1}(x_1, \mu_F^2) f_{j/h_2}(x_2, \mu_F^2) d\hat{\sigma}_{ij \rightarrow X}(x_1, x_2, Q^2, s, \mu_F^2), \quad (1.1)$$

where s denotes the centre-of-mass energy squared, f_{i/h_1} and f_{j/h_2} are non-perturbative Parton Distribution Functions (PDFs), that encode the longitudinal momentum distribution of partons i and j inside the incoming hadrons h_1 and h_2 , respectively, and $d\hat{\sigma}_{ij \rightarrow X}$ is the short-distance cross section (a.k.a. coefficient function) that models the hard scattering of the incoming partons for the sufficiently inclusive production of a generic final state X . The symbol Q^2 denotes a hard scale squared, typical of the scattering process, e.g. the invariant mass squared M^2 of the final state X . The factorization in eq. (1.1), namely the separation of long- and short-distance effects, is associated with a scale μ_F , thus called factorisation scale: the dependence of PDFs on such a scale is dictated by the DGLAP equations [1–3], whose kernels (also called splitting functions in configuration space and anomalous dimensions in a space Mellin-conjugated to the latter one) are known exactly up to next-to-next-to-leading order (NNLO) [4, 5]. At the N³LO, the currently available partial and approximate results [6–16] already enable phenomenological applications.

While a factorization formula such as that of eq. (1.1) originally stems from a careful analysis of QCD colour dynamics¹, a formally identical expression underpinned by QED interactions and much better understood perturbatively can be employed in the case of high-energy *lepton* colliders, like LEP or the proposed FCC-ee or CEPC. There, it serves the primary purpose of resumming potentially-large logarithmic terms of m_ℓ^2/Q^2 (m_ℓ being the mass of the colliding leptons) that are associated with initial-state collinear radiation, and which emerge order-by-order in perturbative computations, whose predictions might thus be spoiled by them. Technically, the resummation is achieved by introducing lepton (antilepton) PDFs f_{i/ℓ^-} (f_{i/ℓ^+}), which are the strict analogues of their QCD counterparts; indeed, as in QCD, such PDFs evolve perturbatively according to a DGLAP equation, thereby achieving the sought resummation — currently, the state of the art is a next-to-leading logarithmic (NLL) evolution [17, 18]. Importantly, at variance with the hadronic case, the initial conditions for the evolution at $\mu_0^2 \sim m_\ell^2$ are fully perturbative: at the leading-order they are trivially given by $f_{\ell^\pm/\ell^\pm}(x, \mu_0^2) = \delta(1-x)$ for the lepton themselves, and are equal to zero for all of the other partons. At the next-to-leading order, the photon acquires a nonzero initial condition [19]. The next-to-next-to-leading order initial conditions have recently also become available (see refs. [20, 21] and ref. [22] for an earlier work on the non-singlet contribution).

Among possible future lepton colliders, one interesting option is constituted by a muon collider. Thanks to its reduced synchrotron radiation, such a machine could potentially reach energies of order 10-30 TeV. Muon PDFs relevant to muon-collider predictions have attracted some recent interest [23–25]. As it will be discussed more extensively later, owing to its much larger centre-of-mass energy (w.r.t. that of an e^+e^- collider), a muon collider will be sensitive to much smaller values of parton momentum fractions. In that regime, two things happen: firstly, the fixed-order perturbative approach of DGLAP is liable to become unstable owing to the presence of $\log x$ terms in the splitting kernels (small- x effects, i.e. the main argument of this paper). And secondly, QCD dynamics inside the incoming leptons cannot be neglected any longer. Indeed, although quark radiation first appears at relative $\mathcal{O}(\alpha^2)$ through photon splitting, with gluon radiation kicking in at $\mathcal{O}(\alpha^2\alpha_s)$, the resulting PDFs appear to be non-negligible at the end of the evolution, with the gluon large in size at small values of $x < 10^{-2}$ – 10^{-3} , second only to the photon PDF². This is due to the interplay between the enhancement of QCD radiation at small energies and the significant

¹And it is in fact unproved.

²At large values of x , the muon-in-muon PDF f_{μ^\pm/μ^\pm} remains the only relevant contribution at any final scale.

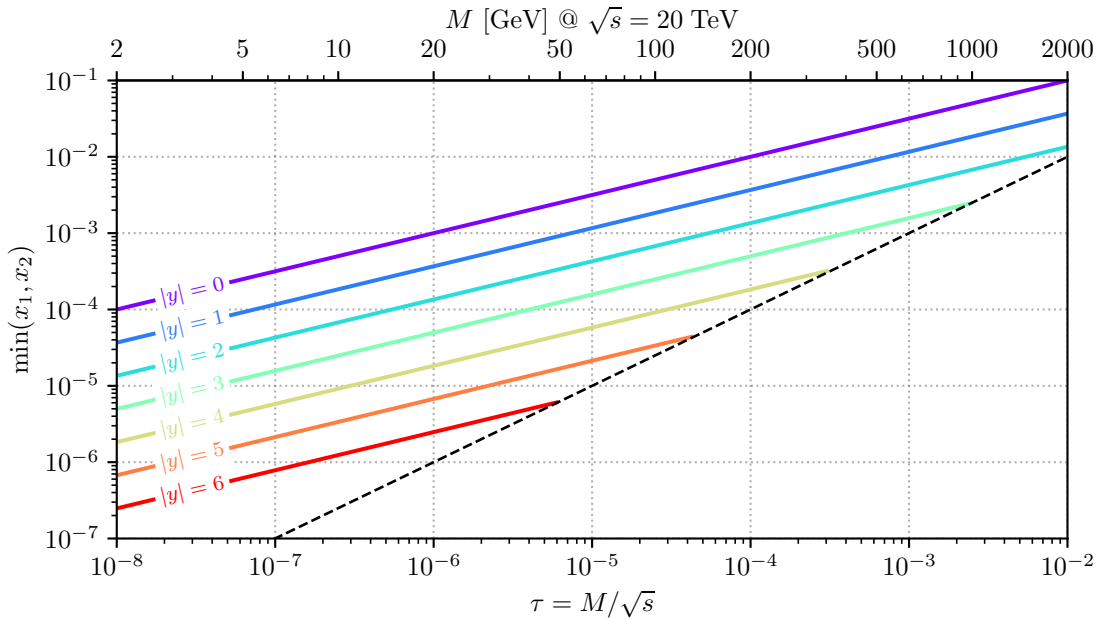


Figure 1. Momentum fractions probed at high-energy colliders as a function of $\tau = M/\sqrt{s}$ for various rapidities. On the secondary axis on the top, the value of M for $\sqrt{s} = 20$ TeV is indicated as reference. Note that the largest accessible rapidity is determined by τ , with $|y| < 1/2 \log(1/\tau)$, as marked by the black dashed line.

evolution range, which spans at least three order of magnitudes from the muon mass $m_\mu \sim 100$ MeV to the electroweak scale. Because of this, refs. [23–25] all deal with QCD radiation, although by means of vastly different approaches.

We now return to the first item mentioned before, i.e. the relevance of small- x effects in high-energy collisions. In fact, since such effects are driven by kinematics, they are equally relevant to hadron as well as to lepton collisions, and can thus be discussed by means of the same language in these two cases. The starting point is the observation that, in the context of a factorisation theorem, the production of a final state with invariant mass M entails that the PDFs will be evaluated (in leading-order kinematics) at the following x values

$$x_{1,2} = \frac{M}{\sqrt{s}} e^{\pm y} = \sqrt{\tau} e^{\pm y}, \quad (1.2)$$

with y the laboratory-frame rapidity of that final state, and $\tau \equiv M^2/s$. To illustrate the kinematical regions that emerge from eq. (1.2), in fig. 1 we plot eq. (1.2) as a function of τ for given values of y . The main message of fig. 1 is that, over a large part of the phase space, small values of x are probed. For example, at a $\sqrt{s} = 20$ TeV collider, assuming the onset of the small- x regime at $x \sim 10^{-3}$ (i.e. the regime in which there could possibly be a breakdown of a fixed-order-based DGLAP PDF evolution), this corresponds to the central ($y = 0$) production of a system with $M = 20$ GeV; at $|y| = 2$ that value increases to about $M = 180$ GeV, while production of any final state with absolute rapidity larger than 3 will involve the small- x region.

The presence of potentially large $\log x$ terms in PDF evolution (and in the coefficient functions) calls for their all-order resummation. Small- x (or high-energy) resummation is a longstanding topic in QCD, and has been addressed with a variety of methods; for a pedagogical introduction we

refer the reader to textbooks [26, 27]. The small- x resummation of DGLAP evolution is known to next-to-leading logarithmic accuracy (NLL) and it is based on the BFKL equation [28–32]. After the computation of the two-loop BKFL kernel [33, 34]³, it has been realised that the BFKL evolution kernel is perturbative unstable, making its implementation in phenomenological applications non trivial. The problem of constructing resummed anomalous dimensions for PDF evolution has been tackled by several groups, see refs. [42–47], refs. [48–51], and refs. [52–55]. More recently, further progress has been made in refs. [56–58], where the Altarelli-Ball-Forte (ABF henceforth) approach [42–47] has been exploited to obtain state-of-the-art resummed predictions for DGLAP splitting functions, publicly available through the [HELL](#) code.

We reiterate that fig. 1 implies that small- x resummation is also relevant for muon collider physics, and therefore one should include it at least in (but not necessarily limited to) the QCD-evolution sector of lepton densities. However, in doing so, one faces a problem whose analogue is not relevant to hadronic-PDF evolution. Namely, muon-PDF evolution starts at a scale of the order of the muon mass, i.e. smaller than Λ_{QCD} , that is a regime where hadron PDFs are not evolved by means of DGLAP equations. Therefore, with muon PDFs one is forced to either artificially switch off QCD dynamics [23, 24] without a proper dynamical mechanism to do so⁴, or to extend the validity of $\alpha_s(\mu^2)$ down to $\mu^2 = 0$. The latter option has been suggested by two of us in ref. [25], where it is achieved by means of the adoption of a simple analytical parametrisation of α_s , inspired by a dispersive approach [59]. With such a parametrisation, at small scales the coupling behaves as⁵

$$\alpha_s(\mu) \sim \frac{1}{\beta_0} \left[\alpha_s^{\text{pert}} \left(\frac{\mu^2}{\Lambda_{\text{QCD}}^2} \right) + \alpha_s^{\text{np}} \left(\frac{\mu^2}{\Lambda_{\text{QCD}}^2} \right) \right], \quad (1.3)$$

with β_0 the first coefficient of the QCD β function and

$$\alpha_s^{\text{pert}}(X) = \frac{1}{\log(X)}, \quad \alpha_s^{\text{np}}(X) = \frac{X+b}{(1-X)(1+b)} \left(\frac{1+c}{X+c} \right)^p. \quad (1.4)$$

When $\mu^2 \rightarrow \Lambda_{\text{QCD}}^2$, both $\alpha_s^{\text{pert}}(X)$ and $\alpha_s^{\text{np}}(X)$ behave as $1/(1-X)$ with opposite signs, canceling the divergence. Elsewhere, this functional form guarantees the smooth transition between an RGE-driven evolution relevant to large and intermediate values of μ^2 , and its low-energy parametrised small-scale counterpart. In general, it is this smooth behaviour coupled with the requirement that RGE dynamics be used as much as is sensible (i.e. down to around the charm-quark mass) which implies a rapid growth of $\alpha_s(\mu^2)$ for decreasing μ before non-perturbative effects turn it around. In particular, with the default values for the parameters of α_s^{np} adopted in ref. [25] ($p = 4$, $b = 0.25$ and $c = 4$) $\alpha_s(\mu^2)$ can be as large as 0.8 (this happens for $\mu \sim 0.3$ GeV).

The bottom line is that, on top of the small- x resummation procedure which is common to both hadron and lepton PDFs, the physics of a muon collider (and, in fact, that of an e^+e^- collider whose physics program is based on the ability of reaching extremely large precision where all ingredients must be controlled to the minutest details) forces one to consider a large- α_s regime as well. This regime has been largely ignored in the literature and in the resulting computer codes such as [HELL](#), which will be prominent in this paper.

By using the large- α_s argument as a motivation, in this work we address and solve the problem it poses. In doing so, we achieve what are nominally by-product ingredients in such a solution, but which are in fact of general greater importance than the ability to carry out small- x , large- α_s evolution. Specifically, we have obtained for the first time in the literature analytical all-order results for, among other things, the so called γ_s and h_{qg} functions, as well as for the complete $\mathcal{O}(\epsilon^0)$ \mathcal{G}_{qg}

³The calculation of the three-loop BFKL kernel is in progress [35–41].

⁴This implies the necessity of introducing a switch-off scale upon which PDF predictions will depend in an inherently infrared-unstable manner.

⁵Expressions valid at two-loop, as well as with quark-mass thresholds, can be found in ref. [25].

Green function. We stress that the h_{qg} result is of particular importance, since it leads to a properly all-order resummed expression for the P_{qg} kernel, which currently is resummed to all orders only in an approximate manner that is, as we shall show, liable to extremely large instabilities. We use these novel results as a basis for improving the `HELL` code, which thus becomes more robust (importantly, also in the context of hadron-collision applications), and capable of dealing with large- α_s evolution. In view of this, the present paper has a broader and more technical scope than muon-PDF small- x evolution — the results for the latter topic are therefore postponed to a forthcoming work [60].

The paper is organised as follows: in sect. 2 we give a brief overview of the small- x resummation procedure we follow (sects. 2.1 and 2.2), and of the new analytical results we have obtained in this work (sect. 2.3). In sect. 3 we present our findings relevant to the P_{qg} splitting kernel, in both its all-order and perturbative-expansion forms. The implications of the new analytical results we have found, and of the new approach for the inclusion of subleading-logarithmic effects, including those stemming from strong-coupling running, are discussed in sect. 4. Sect. 5 reports the analytical results for the $\mathcal{O}(\epsilon^0)$ qg and gg Green functions, which do not enter any of the numerical predictions we have obtained, but are nevertheless useful to elucidate the all-order structure emerging from high-energy factorisation. Finally, in sect. 6 we give our conclusions. Additional technical material is reported in the appendices: sect. A deals with the LL gg anomalous dimension, sect. B with the qg anomalous dimension and Green function, and sect. C with the numerical implementation relevant to the new version of `HELL`.

2 Generalities on small- x resummation

We begin by broadly summarizing the strategy used to perform small- x resummation of the DGLAP splitting functions. For pedagogical purposes, in the present section we keep technical details to a minimum.

Leading small- x logarithms arise only in the singlet sector⁶, and we therefore consider a 2×2 evolution matrix that couples together the quark singlet and the gluon. Small- x resummation is typically performed in a conjugate (Mellin) space. We define the Mellin transformation following the standard small- x conventions, where the entries γ_{ij} of the anomalous dimension 2×2 matrix are defined as

$$\gamma_{ij}(\alpha_s, N) = \int_0^1 dx x^N P_{ij}(\alpha_s, x), \quad (2.1)$$

so that the leading-power small- x logarithms that have the generic form $\frac{1}{x} \log^n x$ correspond to poles at $N = 0$ (rather than at $N = 1$, which one would obtain by using the standard Mellin-transform conventions). Specifically, the leading logarithmic (LL) contributions are defined to be all terms that behave as $\frac{1}{x} \alpha_s^n \log^{n-1} x$ for any n , which correspond to $(\alpha_s/N)^n$ structures in the Mellin space, while next-to-leading logarithmic (NLL) terms are suppressed by an overall power of α_s w.r.t. the LL ones, and so on. Once the all-order functions of α_s/N are constructed in the Mellin space, the resummed splitting functions $P_{ij}(x)$ are then obtained in the configuration space by Mellin inversion.

The NLL resummation of anomalous dimensions in the singlet sector requires just two resummed ingredients. Historically, one of them is taken to be the eigenvalue $\gamma_+(\alpha_s, N)$ of the matrix in eq. (2.1), that is defined as the one containing *all* small- N singularities, while the other, γ_- , is nonsingular at $N = 0$. In addition to that, one needs to include information on the rotation back to flavour space, which is carried out for instance by the entry γ_{qg} . At the NLL all of the other

⁶The non-singlet sector is affected by small- x logarithmic enhancements only starting at the next-to-leading power. As such, it is not of relevance to us for the current work.

matrix entries can be derived from these two ingredients according to the following relations⁷

$$\gamma_{gg}^{\text{NLL}'}(\alpha_s, N) = \gamma_+^{\text{NLL}'}(\alpha_s, N) - \frac{C_F}{C_A} \gamma_{qq}^{\text{NLL}'}(\alpha_s, N), \quad (2.2a)$$

$$\gamma_{gq}^{\text{NLL}'}(\alpha_s, N) = \frac{C_F}{C_A} \gamma_{gg}^{\text{NLL}'}(\alpha_s, N), \quad (2.2b)$$

$$\gamma_{qq}^{\text{NLL}'}(\alpha_s, N) = \frac{C_F}{C_A} \gamma_{gg}^{\text{NLL}'}(\alpha_s, N). \quad (2.2c)$$

We stress that the resummation procedure of $\gamma_+^{\text{NLL}'}$ and $\gamma_{gg}^{\text{NLL}'}$ that we are about to review actually contains a number of contributions in addition to the pure LL and NLL small- x terms, chiefly emerging from the running of the strong coupling, that, despite being subleading w.r.t. the indicated logarithmic accuracy, are necessary for the perturbative stability of the result. This is what informs the notation used in eq. (2.2), i.e. the fact that we have written NLL' rather than simply NLL. This an example of a notation which we shall systematically adopt in the paper, by following the

Notation rule: for any given resummed quantity ς , the symbol ς itself denotes the all-order function that includes all small- x logarithmic towers. By $\varsigma|_{\text{LL}}$ and $\varsigma|_{\text{NLL}}$ we denote the corresponding quantities which strictly contain all and only the leading and the leading plus next-to-leading small- x logarithms, respectively. Finally, by $\varsigma^{\text{LL}'}$ and $\varsigma^{\text{NLL}'}$ we denote $\varsigma|_{\text{LL}}$ and $\varsigma|_{\text{NLL}}$ augmented by logarithmic contributions beyond the leading and the next-to-leading ones, respectively, as well as by power-suppressed terms.

Clearly, there are infinite ways to include beyond-accuracy logarithmic contributions into a strictly logarithmically-ordered quantity; the precise definition of such extra contributions will be clear from the context.

We also stress that the results that we are going to present are in a factorization scheme which is a variant of the $\overline{\text{MS}}$ scheme usually called $Q_0\overline{\text{MS}}$ [61–64]. We also recall that all resummed results, however they are obtained, must then be matched to the known exact fixed-order results. This is usually performed by using an additive matching: from the resummed result its α_s expansion up to the desired order is subtracted, and this “resummed contribution” (after a suitable damping⁸ at large x) is added to the corresponding fixed-order complete result.

Small- x resummation in Mellin space is performed differently for the eigenvalue γ_+ and the γ_{gg} entry: the former is resummed through duality with BFKL (see sect. 2.1), while the latter is obtained through the collinear factorization of the quark Green function in the high-energy limit (see sect. 2.2).

2.1 Resummation of γ_+

The core of the resummation of the anomalous dimension matrix is the eigenvalue γ_+ . At the LL, it is the only object needed for resummation, and it thus coincides with γ_{gg} and (up to a color factor) γ_{gq} , while the quark entries γ_{gq} and γ_{qq} are of NLL. Its resummation is driven by the consistency between DGLAP and BFKL equations, which leads to an all-order duality relation between $\gamma_+(\alpha_s, N)$ and the BFKL kernel $\chi_{\text{BFKL}}(\alpha_s, \gamma)$ ⁹. By ignoring running coupling effects, the

⁷While formally eq. (2.2b) is valid only at LL, we can still define $\gamma_{gq}^{\text{NLL}'}$ as in eq. (2.2b) since as far as PDF evolution is concerned the yet unknown NLL component of γ_{gq} is irrelevant because that kernel is multiplied by the quark PDF, which is itself a NLL object.

⁸We remind the reader that, while not mandatory, damping is common practice in matched results whose resummation components are potentially anomalously large in regions where resummation should actually not be necessary.

⁹Note that $\chi_{\text{BFKL}}(\alpha_s, \gamma)$ is sometimes called the eigenvalue or characteristic function of the BFKL equation, obtained by Mellin transformation from the BFKL kernel in momentum space, with γ being the Mellin conjugate variable. The choice of using γ as the generic name for this variable, often adopted in the literature, is motivated by the fact that by duality the kernel is computed with argument γ coinciding with the anomalous dimension.

duality takes generally the form

$$\chi_{\text{BFKL}}(\alpha_s, \gamma_+(\alpha_s, N)) = N, \quad (2.3)$$

namely the two functions are the inverse of one another. By using the LO expression of the kernel, namely $\chi_{\text{BFKL}}(\alpha_s, \gamma) = \alpha_s \chi_0(\gamma) + \mathcal{O}(\alpha_s^2)$, one obtains the resummation of the pure LL contributions to γ_+ . Indeed, eq. (2.3) becomes

$$\alpha_s \chi_0(\gamma_+(\alpha_s, N)) + \mathcal{O}(\alpha_s^2) = N, \quad (2.4)$$

which, neglecting the $\mathcal{O}(\alpha_s^2)$ contributions, clearly gives as solution for γ_+ an all-order function of α_s/N . Explicitly, we can therefore write

$$\chi_0(\gamma) = \frac{C_A}{\pi} \chi(\gamma), \quad (2.5)$$

$$\chi(\gamma) \equiv 2\psi_0(1) - \psi_0(\gamma) - \psi_0(1-\gamma) = \frac{1}{\gamma} + \sum_{k=1}^{\infty} 2\zeta_{2k+1} \gamma^{2k}, \quad (2.6)$$

with ψ_0 the digamma function and ζ_{2k+1} the Riemann ζ constants. We can thus rewrite the duality at this order, eq. (2.4), as

$$1 = \alpha_N \chi(\gamma_s(\alpha_N)), \quad (2.7)$$

where for convenience we have introduced the symbol (in four dimensions — for a d -dimensional definition see eq. (3.2))

$$\alpha_N \equiv \frac{C_A \alpha_s}{\pi N}. \quad (2.8)$$

The anomalous dimension γ_s emerging from eq. (2.7) corresponds to the pure LL part of γ_+ , and resums all and only the $(\alpha_s/N)^k$ terms¹⁰. Solving the implicit equation (2.7) is complicated due to the functional form of $\chi(\gamma)$, and indeed so far in the literature only fairly limited analytical information had been available. Conversely, in this work, we have been able to solve eq. (2.7) perturbatively to all orders, thus finding an explicit series representation. While the former cannot be resummed in a closed form directly in terms of elementary functions, we have managed to do so through an integral representation; an all-order fixed-point solution is reported later as well. A detailed discussion of these novel results is given in appendix A.1.

Unfortunately, the resummation in terms of γ_s , despite being a useful tool for perturbative analytic manipulations, is not suitable for obtaining phenomenological results numerically. Indeed, when moving to the NLL, which in turns requires the usage of the NLO BFKL kernel, the solution of the duality equation has a completely different behaviour at small N w.r.t. the pure LL one, thus exposing a problem of perturbative stability of the resummation procedure. Such an instability in the resummed perturbative progression is induced by a severe perturbative instability of the fixed-order BFKL kernel. In particular, in the “physical region” of the kernel, $0 < \gamma < 1$, NLO corrections change completely the behaviour near $\gamma = 0$ and $\gamma = 1$, owing to the novel presence of higher poles with opposite signs. Therefore, in order to achieve a sensible resummation, the instability of the fixed-order BFKL kernel has to be addressed first.

The achievement of perturbatively-stable resummed results took several years in the late 90s and early 2000s. The strategy towards this goal, used by most groups with some differences in the practical implementations, is based on the following steps.

- Firstly, the duality eq. (2.3) is employed “in reverse”, namely by using the knowledge of the fixed-order anomalous dimension to solve the duality equation for the BFKL kernel, thereby leading to the resummation of the poles of such kernel located at $\gamma = 0$.

¹⁰Therefore, according to our conventions it should be denoted by $\gamma_+|_{\text{LL}}$; the use γ_s instead of that symbol is in keeping with the conventions of the literature.

- This procedure does not cure the instability at $\gamma = 1$. In order to achieve this, the symmetry property of the BFKL kernel for $\gamma \rightarrow 1 - \gamma$ is exploited to extend the stabilisation of the pole at $\gamma = 0$ to $\gamma = 1$ as well.
- At this point the fixed-order BFKL kernel has been stabilised by the resummation of its leading singularities. After further imposing a constraint due to momentum conservation, the duality can be used again to obtain a resummed anomalous dimension, usually dubbed double-leading, because *both* (hence the “double”) the kernel and its dual anomalous dimension are accurate to (N)LO+(N)LL accuracy.
- Finally, the resummation of a class of subleading terms originating from the running of the strong coupling is also included. Despite being subleading, these terms are very important because they change the kind of the leading small- N singularity (from a branch point to a simple pole), thus impacting the leading small- x behaviour of the splitting functions.

The concrete realisation of this procedure as proposed by the ABF group is what has been implemented in the `HELL` code, with various improvements detailed in refs [56–58]. As a result, the perturbatively stable resummed anomalous dimensions contain, in addition to the purely LL and NLL contributions, several subleading logarithmic and subleading power terms. Thus, we can write

$$\gamma_+^{\text{LL}'}(\alpha_s, N) = \gamma_s(\alpha_N) + \text{subleading log} + \text{subleading power} \quad (2.9)$$

$$\gamma_+^{\text{NLL}'}(\alpha_s, N) = \gamma_s(\alpha_N) + \alpha_s \gamma_{ss}(\alpha_N) + \text{subleading log} + \text{subleading power}, \quad (2.10)$$

where $\gamma_{ss}(\alpha_N)$ is another all-order function of α_s/N representing all purely NLL contributions to γ_+ . The subleading contributions, despite formally being beyond accuracy, are a crucial part of the resummed result, and cannot be neglected.

Unfortunately, explicit expressions for the subleading terms (or equivalently for the full $\gamma_+^{(\text{N})\text{LL}'}$) are very difficult (if not impossible) to obtain, given that part of the anomalous dimension comes from the solution of the duality equation with a kernel which is much more complicated than the LO one of eq. (2.5) and (2.6). The standard approach, also adopted in the `HELL` code, is to compute the solution to the duality relation numerically, a procedure that has some criticalities (we discuss some of them in sect. 4.1). Our findings on the explicit forms of γ_s presented in appendix A.1 may provide some insight on this procedure, possibly paving the way for an alternative, more robust determination of the resummed anomalous dimension $\gamma_+^{(\text{N})\text{LL}'}$.

We conclude this section by noting that eq. (2.7) allows one to trivially express α_N in terms of γ_s as follows¹¹

$$\alpha_N = \frac{1}{\chi(\gamma_s)} = \gamma_s + \mathcal{O}(\gamma_s^2). \quad (2.11)$$

We stress that this is an exact relationship between two given quantities (α_N and γ_s), which has nothing to do with the logarithmic accuracy at which one is working. This property allows one to recast any perturbative expansion in α_N as an expansion in γ_s ; it will be extensively exploited in sect. 3, since γ_s enters as a building block in the resummation of γ_{qg} . Given the intricate nature of γ_s as is outlined above and detailed in appendix A, being able to express results in terms of γ_s rather than α_N simplifies the analytical expressions.

2.2 Resummation of γ_{qg}

The resummation of the γ_{qg} element of the splitting matrix relies on the collinear factorization of the quark Green function in the high-energy limit [62]. As we shall come back to this factorization later in sect. 3 we refrain from giving additional details here, and focus instead on available results

¹¹The full perturbative expansion of α_N in terms of γ_s is provided in eq. (A.26).

and on how they have been used. We limit ourselves to stressing that this factorisation procedure has been employed so far in the literature only to extract the perturbative expansion of γ_{qg} in an iterative manner (thus in practice for a limited number of them).

The qg anomalous dimension is enhanced at small x starting at NLL, which means that its leading small- x dependence can be written as a simple α_s prefactor, times an all-order function of α_s/N . More explicitly, from ref. [62], we have

$$\gamma_{qg}(\alpha_s, N)|_{\text{NLL}} = \frac{\alpha_s}{3\pi} T_R \left[1 + \frac{5}{3}\alpha_N + \frac{14}{9}\alpha_N^2 + \left(\frac{82}{81} + 2\zeta_3 \right) \alpha_N^3 + \dots \right]. \quad (2.12)$$

A complete all-order expression for γ_{qg} has never been fully achieved so far. Available implementations of the resulting resummation therefore must rely on a finite number of coefficients of the γ_{qg} expansion in α_s : ref. [62] presented the analytical results for the first six coefficients of such an expansion, and later in the context of ref. [47] about thirty-five coefficients have been computed numerically. As we shall show, the numerical extraction leads one to significant deviations w.r.t. to the actual analytical result, which we shall present later. The authors of ref. [62] have also been able to derive an all-order expression for the rational part of the coefficients, which is however insufficient to obtain an improved numerical approximation, as the transcendental ζ terms are as important as (if not more than) the rational ones.

Even though any implementation of the resummation of γ_{qg} based on a finite number of coefficients is necessarily approximate, in the literature some additional manipulations have been introduced in order to obtain a result which is as good as possible. These include on the one hand methods to try and improve the convergence properties of the series, in order to make the most out of the few coefficients which were known, and on the other hand to include in the resummed formula additional contributions due to the running of the coupling, which are important¹² for a more reliable description of the small- N regime (as is the case for γ_+).

The first of these manipulations stems from introducing [47] a new function, h_{qg} , such that the anomalous dimension γ_{qg} at the NLL can be rewritten as

$$\gamma_{qg}(\alpha_s, N)|_{\text{NLL}} = \frac{\alpha_s}{3\pi} T_R h_{qg}(\gamma_s(\alpha_N)), \quad (2.13)$$

in terms of the pure LL anomalous dimension $\gamma_s(\alpha_N)$, defined in eq. (2.7). The idea behind this way of writing the resummed form of γ_{qg} , which resembles that of coefficient functions [62], is that the anomalous dimension γ_s captures the essence of the irreducible complexity of the resummed result, so that the function h_{qg} is expected to be simpler, and with better convergence properties, w.r.t. the original function γ_{qg} . In particular, by making use of eq. (2.11), it is easy to extract the coefficients of the expansion of h_{qg} in powers of γ_s from those of γ_{qg} in powers of α_N : truncating the series expansion of the function h_{qg} at a given order γ_s^k is likely less impactful than truncating the expansion of γ_{qg} at the corresponding order α_N^k , owing to the expected better convergence properties of the former w.r.t. the latter.

The second manipulation consists in introducing the resummation of subleading running coupling contributions. This is more easily achieved in terms of the function h_{qg} . One simple (but insufficient) step is to compute the function h_{qg} in terms of the full resummed γ_+ rather than simply in terms of γ_s , so that the resummation of running coupling effects in γ_+ is automatically included. Technically, at this order, it is sufficient to use $\gamma_+^{\text{LL}'}$; however, ABF [47] suggest to use the NLL anomalous dimension $\gamma_+^{\text{NLL}'}$ so that the leading N pole is in the same position for all entries of

¹²Of course, the improvement given by the resummation of subleading running coupling effects may be irrelevant in comparison with the irreducible uncertainty due to the missing higher order coefficients. However, as we shall see in sect. 4.3, there are kinematical regimes in which the approximation obtained from the limited number of coefficients is good enough to justify the inclusion of the running coupling corrections.

the singlet anomalous dimension matrix. For the rest of the section we simply write γ_+ without specifying the order, but keeping in mind that in practical implementations (like in [HELL](#)) it is to be intended as $\gamma_+^{\text{NLL}'}$.

In order to actually resum all leading running-coupling contributions (those proportional to powers of β_0), it is also necessary to change the way the function h_{qg} depends on γ_+ [[47](#), [65](#)]. By introducing the series expansion of h_{qg} ,

$$h_{qg}(z) = \sum_{k=0}^{\infty} h_k z^k, \quad (2.14)$$

the resummed NLL' anomalous dimension appearing in eq. (2.2) is computed according to the formula

$$\gamma_{qg}^{\text{NLL}'}(\alpha_s, N) = \frac{\alpha_s}{3\pi} T_R \sum_{k=0}^{\infty} h_k [\gamma_+^k(\alpha_s, N)], \quad (2.15)$$

where we have introduced the notation $[\gamma_+^k]$ defined by the following recursive procedure [[47](#)]

$$[\gamma_+^{k+1}] = (\gamma_+ - k r(\alpha_s, N)) [\gamma_+^k], \quad [\gamma_+^0] = 1. \quad (2.16)$$

The quantity $r(\alpha_s, N)$, in its simplest realisation, is given by $r(\alpha_s, N) = \alpha_s \beta_0$. This expression stems from approximating the dependence on α_s of γ_+ as if it were linear (like at the LO). ABF also suggest an alternative form of $r(\alpha_s, N)$ such that the coefficient of α_s is the actual derivative of γ_+ . We shall come back to this point shortly.

Note that eq. (2.15) cannot straightforwardly be written as an all-order closed expression (a non-trivial integral expression will be presented in sect. 3.3). Paradoxically, this has not posed a significant problem, since in any case the number of known h_k coefficients was quite limited. Indeed, at this stage, in order to obtain a resummed expression one had to decide what to do with the limited knowledge available. This problem is even more severe after the inclusion of running coupling effects, because the convergence of the series in eq. (2.15) is worse than the original one of eq. (2.14), due to the presence of the factor k in the recursion eq. (2.16), which reduces the radius of convergence. To tame this problem, in ref. [[47](#)] the Borel summation of the series was considered, supplementing the asymptotic behaviour of the Borel transform with a guessed functional form. Later, in ref. [[56](#)] this procedure has been modified by computing a Padé approximant of the Borel transform and using it in its place, which leads to a more robust result. The [HELL](#) implementation prior to this paper is based on the latter approach, and employs just the first 16 coefficients of the expansion of h_{qg} ¹³. The quality of such an approximation can be assessed indirectly by comparing it with the exact resummed result presented for the first time in this paper (see sect. 4.3).

Before concluding this section, we give some extra detail about this resummed formula that will be useful later in this work. We start by reporting an alternative form of eq. (2.15), derived in ref. [[56](#)], which reads

$$\gamma_{qg}^{\text{NLL}'}(\alpha_s(Q^2), N) = \frac{\alpha_s(Q^2)}{3\pi} T_R \sum_{k=0}^{\infty} h_k [\partial_\nu^k U(N, Q^2 e^\nu, Q^2)]_{\nu=0}. \quad (2.17)$$

This equation coincides with eq. (2.15) for a specific form of the function U , but it is more general than that for a generic U , and in particular it allows one to incorporate the β_0 terms to all orders without making any approximation. The function U represents the leading DGLAP evolution at small x , given by

$$U(N, \mu^2, \mu_0^2) = \exp \left[\int_{\mu_0^2}^{\mu^2} \frac{dq^2}{q^2} \gamma_+(\alpha_s(q^2), N) \right]. \quad (2.18)$$

¹³The choice of using 16 coefficients was based on an analysis of the stability of the result upon variations of several parameters (the number of coefficients used, the order of the Padé approximant, the order of the Borel transform).

In order to be able to compute the integral analytically, some approximation must be introduced. The most drastic one consists in neglecting the running of the strong coupling altogether, namely to use

$$U(N, \mu^2, \mu_0^2) \stackrel{\text{f.c.}}{=} \left(\frac{\mu^2}{\mu_0^2} \right)^{\gamma_+(\alpha_s, N)}, \quad (2.19)$$

so that the derivatives in this fixed-coupling (f.c.) case become

$$[\partial_\nu^k U(N, Q^2 e^\nu, Q^2)]_{\nu=0} \stackrel{\text{f.c.}}{=} \gamma_+^k(\alpha_s, N), \quad (2.20)$$

thus reproducing the power series of h_{qg} computed in $\gamma_+(\alpha_s, N)$ (to fully recover the fixed-coupling result eq. (2.13), one should also replace $\gamma_+(\alpha_s, N)$ with its fixed-coupling expression $\gamma_s(\alpha_N)$). A less drastic approximation leading to the ABF result of eq. (2.15) is

$$\gamma_+(\alpha_s(q^2), N) \stackrel{\text{ABF}}{=} \frac{\gamma_+(\alpha_s(\mu_0^2), N)}{1 + r(\alpha_s(\mu_0^2), N) \log \frac{q^2}{\mu_0^2}}, \quad (2.21)$$

whence

$$U(N, \mu^2, \mu_0^2) \stackrel{\text{ABF}}{=} U_{\text{ABF}}(N, \mu^2, \mu_0^2) \equiv \left(1 + r(\alpha_s(\mu_0^2), N) \log \frac{\mu^2}{\mu_0^2} \right)^{\gamma_+(\alpha_s(\mu_0^2), N)/r(\alpha_s(\mu_0^2), N)}. \quad (2.22)$$

Note that the ABF-approximate evolution operator in eq. (2.22) depends only on $\alpha_s(\mu_0^2)$, while the μ dependence is explicit. It is easy to see [56] that the derivatives in eq. (2.17) applied to this function reproduce the same recursion pattern as in eq. (2.16), namely

$$[\partial_\nu^k U_{\text{ABF}}(N, Q^2 e^\nu, Q^2)]_{\nu=0} = [\gamma_+^k(\alpha_s(Q^2), N)]. \quad (2.23)$$

The dependence on $\log(q^2/\mu_0^2)$ of eq. (2.21) resembles that of a function which depends linearly on α_s and with one-loop running. In this case, the function r would simply be $r(\alpha_s, N) = \alpha_s \beta_0$, which is what we already discussed. Since in this approximation the anomalous dimension has the right value but the wrong slope at $q^2 = \mu_0^2$, ABF suggest a possibly improved version that reproduces the correct derivative. This is achieved by choosing $r(\alpha_s, N) = \alpha_s^2 \beta_0 \frac{d}{d\alpha_s} \log \gamma_+(\alpha_s, N)$. This variant, which has been used to obtain the default resummed predictions in previous HELL works, is clearly more complicated as it requires the α_s -derivative of the resummed anomalous dimension. We shall come back to this point in sect. 4.1.

Another interesting result of ref. [56] is that, if a function (or a distribution) $\mathcal{P}_{qg}(\xi)$ exists such that

$$h_{qg}(\gamma) = \gamma \int_0^\infty d\xi \xi^{\gamma-1} \mathcal{P}_{qg}(\xi), \quad (2.24)$$

then it is possible to rewrite eq. (2.17) as follows:

$$\gamma_{qg}^{\text{NLL}'}(\alpha_s(Q^2), N) = \frac{\alpha_s(Q^2)}{3\pi} T_R \int_0^\infty d\xi \frac{d}{d\xi} U(N, Q^2 \xi, Q^2) \mathcal{P}_{qg}(\xi). \quad (2.25)$$

This expression reminds one of the k_t factorization of ref. [62]¹⁴, and indeed a form of this kind has been used extensively for the resummation of coefficient functions in the HELL literature. The actual function $\mathcal{P}_{qg}(\xi)$ has never been introduced before in the literature because it is impossible to obtain it without the full knowledge of the function $h_{qg}(z)$.

¹⁴In particular, it reproduces the k_t factorization expressions of ref. [62] in the LL fixed-coupling limit, where the evolution function is replaced by its fixed-coupling expression eq. (2.19) and the anomalous dimension γ_+ by γ_s .

2.3 Synopsis of new analytical results

Before closing this section, we briefly summarize the main new analytical results of this paper for the reader's convenience. These results are detailed in sects. 3 and 5 and in appendices A and B, and here we limit ourselves to refer to the relevant equations. They constitute the basic ingredients through which we revisit and improve several aspects of what has been outlined in sects. 2.1 and 2.2.

A first set of results give different expressions for γ_s , the pure LL part of the γ_+ eigenvalue, introduced in eq. (2.7). Firstly, in eq. (A.18), we write $\gamma_s(a)$ as a perturbative expansion in its argument a , with coefficients in closed analytical form; its inverse relationship, namely the argument a written as a series in γ_s , is presented in eq. (A.26), which thus reports the exact expressions for the terms collectively denoted by $\mathcal{O}(\gamma_s^2)$ in eq. (2.11). In eq. (A.19), we provide a closed-form non-integral implicit expression for γ_s . In eq. (A.31) and eq. (A.32), γ_s is written through equivalent integral representations featuring both a Borel and a Hankel integral. It is possible to perform the Borel integrals analytically, and in this way one obtains pure-Hankel integral representations, as in eqs. (A.37) and (A.39). Finally, in eq. (A.51), $\gamma_s(a)$ is expressed as a fixed point of a function, parametrically dependent on a , directly related to the LO BFKL kernel.

Concerning the resummation of the anomalous dimension γ_{qg} , the main result of the paper presented in eq. (3.24) is an all-order closed-form expression for the function h_{qg} introduced in eq. (2.13). A closed-form non-recursive expression for the coefficients h_k of the expansion of h_{qg} in terms of γ , eq. (2.14), is provided in eq. (3.30). It is also possible to find expressions for the coefficients of the series when h_{qg} is expanded in terms of α_N : two alternative analytical expressions for such coefficients are given in eq. (3.34) and eq. (B.58), with the former more compact than the latter.

Further ancillary results related to the resummation of the anomalous dimension γ_{qg} are presented in appendix B: in particular, they concern closed-form expressions for the perturbative expansions of some objects introduced in sect. 3. The coefficients of the expansion of the bare quark Green function $\mathcal{G}_{qg}^{(0)}$ (introduced in eq. (3.1)) in terms of α_N/ϵ , see eq. (B.18), are given in eqs. (B.37)–(B.39) or alternatively in eq. (B.45).

Finally, we present new results for the finite Green function \mathcal{G}_{qg} and its gg counterpart, \mathcal{G}_{gg} . In eq. (5.1), we provide a closed and all-order form for the $\epsilon = 0$ part of \mathcal{G}_{qg} . Eq. (5.5) gives a relationship between the $\mathcal{O}(\epsilon^0)$ contributions to \mathcal{G}_{qg} and \mathcal{G}_{gg} . Finally, the analytical non-recursive coefficients of the expansion of \mathcal{G}_{qg} and \mathcal{G}_{gg} in terms of γ_s are reported in eqs. (5.13) and (5.14), respectively.

As a concluding comment for this section, we point out that many of the all-order results we have just introduced stem from a methodology which entails some guesswork; typically, by computing exactly the first few (up to twenty, in some cases) elements of a sequence, and by using them to establish a parametric pattern, eventually employed to resum the series formed by the elements of that sequence. Therefore, while in number theory such results would be referred to as “conjectures”, as physicists we feel confident that this method has allowed us to find the true all-order functions we needed for our small- x studies; in all cases, this has meant comparing the re-expansion of the all-order results with as many perturbative coefficients as we could evaluate, whose numbers were always larger than those upon which the original pattern-extrapolations had been based.

3 All-order resummation of P_{qg}

The goal of this section is to obtain a resummed expression for the qg splitting function P_{qg} . Specifically, in sect. 3.1 we first determine the function h_{qg} of eq. (2.13) to all orders. In sect. 3.2 we then provide closed-form expressions for the coefficients of the power series expansion of h_{qg} in

terms of both γ_s and α_N , and we compare our results with the coefficients previously known in the literature. Finally, in sect. 3.3 we discuss how to use the new h_{qg} result to obtain a complete resummation of P_{qg} that includes subleading running-coupling effects.

3.1 All-order result in conjugate Mellin space

The way to determine the function h_{qg} is through the collinear factorization of the quark Green function in the high-energy limit [62]. The bare (i.e. divergent in four dimensions) quark Green function $\mathcal{G}_{qg}^{(0)}$ can be factorized as follows,

$$\mathcal{G}_{qg}^{(0)} = \mathcal{G}_{qg} \Gamma_{gg} + \Gamma_{qg}, \quad (3.1)$$

where \mathcal{G}_{qg} represent the $\epsilon \rightarrow 0$ finite (factorized) Green function, and Γ_{gg} and Γ_{qg} are the transition functions (or collinear counterterms) in the high-energy limit. Eq. (3.1) is valid in $d = 4 + 2\epsilon$ dimensions, and the functions in eq. (3.1) depend on N , α_s and ϵ . As we are working with d -dimensional quantities, we find it convenient to extend the definition of α_N in eq. (2.8) to¹⁵

$$\alpha_N \equiv \frac{C_A \alpha_s S_\epsilon}{\pi N}, \quad S_\epsilon = \left(\frac{e^{\gamma_E}}{4\pi} \right)^\epsilon. \quad (3.2)$$

For the purpose of the algebraic manipulations that we shall perform, we factor out the term $\frac{T_R N}{3C_A}$ from γ_{qg} , the Green functions and the qg transition function¹⁶

$$\gamma_{qg}|_{\text{NLL}} = \frac{T_R N}{3C_A} \hat{\gamma}_{qg}(\alpha_N), \quad (3.3a)$$

$$\mathcal{G}_{qg}^{(0)}|_{\text{NLL}} = \frac{T_R N}{3C_A} \hat{\mathcal{G}}_{qg}^{(0)}(\alpha_N, \epsilon), \quad (3.3b)$$

$$\mathcal{G}_{qg}|_{\text{NLL}} = \frac{T_R N}{3C_A} \hat{\mathcal{G}}_{qg}(\alpha_N, \epsilon), \quad (3.3c)$$

$$\Gamma_{qg}|_{\text{NLL}} = \frac{T_R N}{3C_A} \hat{\Gamma}_{qg}(\alpha_N, \epsilon), \quad (3.3d)$$

so that the functions with a hat depend on α_s and N only through α_N . Note that γ_{qg} lives in 4 dimensions, whereas the functions $\mathcal{G}_{qg}^{(0)}$, \mathcal{G}_{qg} and Γ_{qg} live in d dimensions, and so they also depend on ϵ , both explicitly and implicitly (through α_N , per eq. (3.2)). We also observe that, according to eq. (3.3a) and eq. (2.13), the functions $\hat{\gamma}_{qg}$ and h_{qg} are related by

$$\hat{\gamma}_{qg}(\alpha_N) = \alpha_N h_{qg}(\gamma_s(\alpha_N)). \quad (3.4)$$

With these definitions, we can rewrite eq. (3.1) as

$$\hat{\mathcal{G}}_{qg}^{(0)} = \hat{\mathcal{G}}_{qg} \Gamma_{gg} + \hat{\Gamma}_{qg}, \quad (3.5)$$

with¹⁷

$$\begin{aligned} \hat{\Gamma}_{qg}(\alpha_N, \epsilon) &= \frac{1}{\epsilon} \int_0^{\alpha_N} \frac{da}{a} \hat{\gamma}_{qg}(a) \Gamma_{gg}(a, \epsilon)|_{\text{LL}} \\ &= \frac{1}{\epsilon} \int_0^{\alpha_N} da h_{qg}(\gamma_s(a)) \Gamma_{gg}(a, \epsilon)|_{\text{LL}}, \end{aligned} \quad (3.6)$$

$$\Gamma_{gg}(\alpha_N, \epsilon)|_{\text{LL}} = \exp \left[\frac{1}{\epsilon} \int_0^{\alpha_N} \frac{da}{a} \gamma_s(a) \right], \quad (3.7)$$

¹⁵In case of 4-dimensional quantities, eq. (3.2) coincides with eq. (2.8) since $S_\epsilon = 1$ for $\epsilon = 0$.

¹⁶In order to avoid any possible misunderstanding, we have explicitly indicated on the r.h.s. of eqs. (3.3b)-(3.3d), the dependence of the functions which appear there on two different arguments in order to make explicit the fact that the dependence upon ϵ is not entirely captured by α_N . In the following this dependence will often be understood.

¹⁷Note that there is a typo in the definition of the function Γ_{qg} in ref. [62]: in equation (4.13) of that paper, the first argument of $\Gamma_{qg,N}$ should read α/S_ϵ rather than α .

For later convenience, we introduce the function

$$\Omega(z) \equiv \int_0^{1/\chi(z)} \frac{da}{a} \gamma_s(a), \quad (3.8)$$

where $\chi(z)$ is the LO BFKL kernel, eq. (2.6). We observe that when Ω is computed in $\gamma_s(\alpha_N)$ we can use eq. (2.7) to rewrite the upper limit of the integral as α_N , thus leading to

$$\Omega(\gamma_s(\alpha_N)) = \int_0^{\alpha_N} \frac{da}{a} \gamma_s(a). \quad (3.9)$$

This observation allows us to rewrite eq. (3.7) as

$$\Gamma_{gg}(\alpha_N, \epsilon)|_{\text{LL}} = \exp \left[\frac{1}{\epsilon} \Omega(\gamma_s(\alpha_N)) \right]. \quad (3.10)$$

We stress that we have made the choice of defining Ω such that it depends on α_N through the function $\gamma_s(\alpha_N)$ ¹⁸ for a good reason. Indeed, this choice will play a crucial role in the following, as working in terms of γ_s instead of α_N simplifies analytical derivations. Moreover, this function will also appear in our all-order results for h_{qg} and $\hat{\mathcal{G}}_{qg}$. Further results on the function $\Omega(z)$, and in particular explicit expressions depending only on the BFKL kernel χ , are collected in appendix B.1.

In eq. (3.5) both the factorized Green function $\hat{\mathcal{G}}_{qg}$ and the anomalous dimension $\hat{\gamma}_{qg}$ appearing implicitly through eq. (3.6) are unknowns. The way to extract both functions from a single equation relies on the fact that $\hat{\mathcal{G}}_{qg}$ is finite in the limit $\epsilon \rightarrow 0$. Indeed, we can write eq. (3.5) in the form

$$\hat{\mathcal{G}}_{qg} = \left[\hat{\mathcal{G}}_{qg}^{(0)} - \hat{\Gamma}_{qg} \right] \Gamma_{gg}^{-1}, \quad (3.11)$$

so that it is clear that the constraint that the left-hand side be finite in the $\epsilon \rightarrow 0$ limit imposes the cancellation of the ϵ poles on the right-hand side, allowing an order-by-order extraction of $\hat{\gamma}_{qg}$ and thus of $\hat{\mathcal{G}}_{qg}$ ¹⁹. A fundamental ingredient in this computation is $\hat{\mathcal{G}}_{qg}^{(0)}$, whose form is straightforward but extremely involved [62]. Here in the main text we therefore assume that this function is known, and proceed to computing the quantities of primary interest. The details of the computation of $\hat{\mathcal{G}}_{qg}^{(0)}$, and its results, are reported in appendix B.2.

We now turn to the determination of h_{qg} to all orders. We begin by rewriting eq. (3.11) as

$$\hat{\mathcal{G}}_{qg} \Gamma_{gg} = F(\Omega) \Gamma_{gg} - \hat{\Gamma}_{qg}, \quad F(\Omega) \equiv \hat{\mathcal{G}}_{qg}^{(0)} \Gamma_{gg}^{-1}, \quad (3.12)$$

where we have introduced the quantity F , which we assume to be a function of Ω , eq. (3.8). This assumption is actually innocuous, since it is always possible to trade a dependence on α_N for a dependence on Ω : one first writes α_N as a function of γ_s by exploiting eq. (2.11), and then one writes γ_s as a function of Ω by exploiting eq. (B.10). More generally, regardless of the details of the specific linear transformation, any perturbative series in α_N can equivalently be given as a series in either γ_s or (importantly) Ω . Thus, the dependence of F upon Ω is not meant to be exclusive of other possible dependences (e.g., ϵ), which are understood, but it merely indicates that one assumes Ω to be an appropriate expansion parameter.

By deriving both sides of eq. (3.12) with respect to α_N and by solving for h_{qg} the resulting expression, one obtains

$$h_{qg}(\gamma_s) = \gamma_s \chi(\gamma_s) \left(\epsilon \frac{dF}{d\Omega} + F(\Omega) \right) - \left(\epsilon \frac{d\hat{\mathcal{G}}_{qg}}{d\alpha_N} + \gamma_s \chi(\gamma_s) \hat{\mathcal{G}}_{qg} \right), \quad (3.13)$$

¹⁸This is always possible, as we commented already in sect. 2.1, thanks to eq. (2.11).

¹⁹In particular, at each order in α_s the largest power of the ϵ pole determines the corresponding order of $\hat{\gamma}_{qg}$, and the lower powers provide consistency conditions with lower orders.

where we have used eq. (2.11) and

$$\frac{d\Omega}{d\alpha_N} = \gamma_s \chi(\gamma_s). \quad (3.14)$$

Note that the right-hand-sides of eq. (3.13) and eq. (3.14) are meant to be evaluated at $\gamma_s = \gamma_s(\alpha_N)$ and $\Omega = \Omega(\gamma_s(\alpha_N))$. In order to proceed, we note that owing to eqs. (3.6), (3.7), and to the general characteristics of the coefficients of $\hat{\mathcal{G}}_{qg}^{(0)}$ (whose details are reported in appendix B.2), the structure of eq. (3.12), as far as the ϵ dependence is concerned, is the following,

$$\hat{\mathcal{G}}_{qg} = F(\Omega) - \hat{\Gamma}_{qg} \Gamma_{gg}^{-1} \iff \sum_{k=0}^{\infty} A_k \epsilon^k = \sum_{k=-\infty}^{\infty} B_k \epsilon^k - \sum_{k=-\infty}^{-1} C_k \epsilon^k, \quad (3.15)$$

where A_k , B_k , and C_k are ϵ -independent parameters (except for the implicit dependence through α_N)²⁰, whose precise definition is unimportant here. Therefore,

$$B_k = C_k, \quad k < 0, \quad (3.16)$$

$$B_k = A_k, \quad k \geq 0. \quad (3.17)$$

This immediately shows that the C_k coefficients, containing the information on $\hat{\gamma}_{qg}$, are fully determined by the singular part of F , while they are completely independent of $\hat{\mathcal{G}}_{qg}$, which is in turn determined by the non-singular part of F . Bearing this in mind, we separate the ϵ dependence of $F(\Omega)$ into three contributions, respectively divergent, finite, and vanishing in the $\epsilon \rightarrow 0$ limit, as follows:

$$F = F^{\text{div}} + F^0 + F^{\text{reg}} \equiv \sum_{k=-\infty}^{-1} B_k \epsilon^k + B_0 + \sum_{k=1}^{\infty} B_k \epsilon^k. \quad (3.18)$$

Since h_{qg} is IR-finite, and we are interested in its form in four dimensions, eqs. (3.13) and (3.18) imply

$$\begin{aligned} h_{qg}(\gamma_s) &= \gamma_s \chi(\gamma_s) \left(\epsilon \frac{dF^{\text{div}}}{d\Omega} + F^{\text{div}}(\Omega) + B_0 - A_0 \right) + \mathcal{O}(\epsilon) \\ &= \gamma_s \chi(\gamma_s) \left(\epsilon \frac{dF^{\text{div}}}{d\Omega} + F^{\text{div}}(\Omega) \right) + \mathcal{O}(\epsilon), \end{aligned} \quad (3.19)$$

which is consistent with the known fact that $\hat{\gamma}_{qg}$ can be obtained by only considering the divergent part of the eq. (3.11). Crucially in eq. (3.19) the explicit dependence on α_N has disappeared, with h_{qg} depending only on γ_s , possibly through Ω .

With an explicit computation which uses eqs. (B.19), (B.20), and (B.37)–(B.39) (or (B.45)) we can infer the all-order behaviour of the coefficients in the expansion of F^{div} in Ω , which reads thus:

$$F^{\text{div}}(\Omega) = \frac{3}{4} \sum_{k=1}^{\infty} \sum_{j=k}^{\infty} \frac{(-)^{k-1}}{j!} 2^{j-k} \frac{\Omega^j}{\epsilon^k} + \frac{1}{4} \sum_{k=1}^{\infty} \sum_{j=k}^{\infty} \frac{(-)^{k-1}}{j!} \frac{2^{j-k}}{3^{j-k}} \frac{\Omega^j}{\epsilon^k} \quad (3.20)$$

$$\begin{aligned} &= \sum_{k=1}^{\infty} \frac{(-)^{k+1} 3}{2^{k+2}} \frac{e^{2\Omega}}{\epsilon^k} + \sum_{k=1}^{\infty} \sum_{j=0}^{k-1} \frac{(-)^k 3}{2^{k+1}} \frac{2^{j-1} \Omega^j}{j! \epsilon^k} \\ &+ \sum_{k=1}^{\infty} \frac{(-)^{k+1} 3^k}{2^{k+2}} \frac{e^{2/3\Omega}}{\epsilon^k} + \sum_{k=1}^{\infty} \sum_{j=0}^{k-1} \frac{(-)^k 3^k}{2^{k+1}} \frac{2^{j-1} \Omega^j}{3^j j! \epsilon^k}. \end{aligned} \quad (3.21)$$

²⁰The fact that the S_ϵ dependence is implicit through α_N is crucial to simplify the expressions. Indeed, if we had expanded also that dependence, the $\hat{\Gamma}_{qg} \Gamma_{gg}^{-1}$ would produce also positive powers of ϵ , hampering the separation between the various terms.

By summing the series we finally obtain

$$F^{\text{div}}(\Omega) = \frac{3e^{2\Omega}}{4(1+2\epsilon)} - \frac{3e^{-\Omega/\epsilon}}{4(1+2\epsilon)} + \frac{3e^{\frac{2}{3}\Omega}}{4(3+2\epsilon)} - \frac{3e^{-\Omega/\epsilon}}{4(3+2\epsilon)}, \quad (3.22)$$

whence

$$\epsilon \frac{dF^{\text{div}}}{d\Omega} + F^{\text{div}}(\Omega) = \frac{1}{4} \left(3e^{2\Omega} + e^{\frac{2}{3}\Omega} \right). \quad (3.23)$$

We note that, as a function of Ω , F^{div} turns out to only have rational coefficients, which is remarkable given that transcendental coefficients proportional to odd Riemann ζ constants appear when expanding in α_N . Moreover, we observe that eq. (3.23) is independent of ϵ and finite, despite the fact that the function F^{div} contains only divergent contributions. By plugging eq. (3.23) into eq. (3.19), we obtain the sought result in four dimensions,

$$h_{qg}(z) = \frac{z \chi(z)}{4} \left(3e^{2\Omega(z)} + e^{\frac{2}{3}\Omega(z)} \right), \quad (3.24)$$

whence, using eqs. (3.3a), (3.4), and (2.11),

$$\gamma_{qg}(\alpha_s, N)|_{\text{NLL}} = \frac{T_{RN}}{3C_A} \frac{\gamma_s(\alpha_N)}{4} \left(3e^{2\Omega(\gamma_s(\alpha_N))} + e^{\frac{2}{3}\Omega(\gamma_s(\alpha_N))} \right). \quad (3.25)$$

Eq. (3.24), or equivalently eq. (3.25), is our main new result. Eq. (3.24) is explicitly written as a function of a generic z to stress the fact that it is valid for any (complex) value of z and not just for $z = \gamma_s(\alpha_N)$. We note that by replacing the functions with their expansions to lowest order, $z \chi(z) = 1 + \mathcal{O}(z)$ and $\Omega(z) = z + \mathcal{O}(z^2)$, we reproduce the result of ref. [62] for the rational coefficients of $\hat{\gamma}_{qg}$ ²¹.

As we can see, the all-order expression for $h_{qg}(\gamma)$ depends on the function $\Omega(\gamma)$. Since its definition, eq. (3.8), is based on an integral with complex variables, its evaluation is not straightforward. Unfortunately, we have not been able to compute the integral in terms of elementary functions. Nevertheless, in appendix B.1 we have been able to manipulate it such that its form is easier to handle numerically, e.g. by expressing it in terms of the BFKL kernel χ without involvement of the function γ_s , and by recasting all integrals in the real domain.

3.2 Perturbative coefficients

Thanks to eq. (3.24), the computation of the coefficients of the expansion of h_{qg} in terms of z is straightforward. We rewrite that equation as follows

$$h_{qg}(z) = \frac{1}{4} \left[3 \exp \left(2\tilde{h}_{\frac{1}{2}}(z) \right) + \exp \left(\frac{2}{3}\tilde{h}_{\frac{3}{2}}(z) \right) \right], \quad (3.26)$$

where, from eq. (B.4),

$$\begin{aligned} \tilde{h}_b(z) &\equiv \Omega(z) + b \log(z\chi(z)) \\ &= z - (z-b) \log(1 + \hat{\chi}(z)) + \int_0^1 dy \log(1 + \hat{\chi}(yz)), \end{aligned} \quad (3.27)$$

with $\hat{\chi}$ related to the BFKL LO kernel, see eq. (A.16) and eq. (A.17). Then, by using the expression of the generating function of the complete exponential Bell polynomials B_n , we obtain

$$\exp \left(b\tilde{h}_{\frac{1}{b}}(z) \right) = \sum_{n=0}^{\infty} \frac{z^n}{n!} B_n \left(\hat{Z}_b \right), \quad (3.28)$$

²¹The rational part of the coefficients of the expansion of $\hat{\gamma}_{qg}$ are the same of those of h_{qg} , because the relation between the two is given by the relation between α_N and γ_s , which differs from an identity only by terms proportional to (odd) ζ constants — see eq. (2.11) and eq. (2.6).

where the k^{th} element of the vector \widehat{Z}_b is

$$\widehat{Z}_b^{[k]} = b \left(\delta_{k,1} + \frac{1}{b} \sum_{j=1}^k (-)^{j+1} (j-1)! B_{k,j}(Z) - (k-1) \sum_{j=1}^{k-1} (-)^{j+1} (j-1)! B_{k-1,j}(Z) \right), \quad (3.29)$$

with Z being the vector defined in eq. (A.14) and by $B_{k,j}$ we denote the incomplete exponential Bell polynomials. By re-expanding eq. (3.26) in powers of z through eq. (3.28), and by equating the resulting expression to that of a generic perturbative expansion of $h_{qg}(z)$ as in eq. (2.14), one obtains a closed-form, non-recursive expression for the coefficients h_n . Explicitly, that is:

$$h_n = \frac{1}{n!} \left[\frac{3}{4} B_n \left(\widehat{Z}_2 \right) + \frac{1}{4} B_n \left(\widehat{Z}_{\frac{2}{3}} \right) \right]. \quad (3.30)$$

For convenience, we report the explicit form of the first ten coefficients which emerge from eq. (3.30)

$$h_0 = 1, \quad (3.31a)$$

$$h_1 = \frac{5}{3}, \quad (3.31b)$$

$$h_2 = \frac{14}{9}, \quad (3.31c)$$

$$h_3 = \frac{82}{81} + 2\zeta_3, \quad (3.31d)$$

$$h_4 = \frac{122}{243} + \frac{5}{6}\zeta_3, \quad (3.31e)$$

$$h_5 = \frac{146}{729} - \frac{14}{9}\zeta_3 + 2\zeta_5, \quad (3.31f)$$

$$h_6 = \frac{2188}{32805} - \frac{205}{81}\zeta_3 + \frac{5}{9}\zeta_5, \quad (3.31g)$$

$$h_7 = \frac{13124}{688905} - \frac{488}{243}\zeta_3 - \frac{15}{7}\zeta_3^2 - \frac{56}{27}\zeta_5 + 2\zeta_7, \quad (3.31h)$$

$$h_8 = \frac{1406}{295245} - \frac{803}{729}\zeta_3 - \frac{1}{2}\zeta_3^2 - \frac{82}{27}\zeta_5 + \frac{5}{12}\zeta_7, \quad (3.31i)$$

$$h_9 = \frac{11810}{11160261} - \frac{15316}{32805}\zeta_3 + \frac{41}{14}\zeta_3^2 - \frac{1708}{729}\zeta_5 - \frac{125}{27}\zeta_3\zeta_5 - \frac{7}{3}\zeta_7 + 2\zeta_9. \quad (3.31j)$$

With the result of eq. (3.30), we can readily obtain its analogue for the expansion of $\hat{\gamma}_{qg}$ itself, which reads (see appendix B.4 for an explicit derivation)

$$\hat{\gamma}_{qg}(\alpha_N) = \frac{\gamma_s(\alpha_N)}{4} \left(3e^{2\Omega(\gamma_s(\alpha_N))} + e^{\frac{2}{3}\Omega(\gamma_s(\alpha_N))} \right) \quad (3.32)$$

$$= \sum_{k=0}^{\infty} t_k \alpha_N^{k+1}, \quad (3.33)$$

$$t_k = \frac{1}{k!} \sum_{n=0}^k h_n n! B_{k,n}(\hat{G}) = \frac{1}{k!} \sum_{n=0}^k \left(\frac{3}{4} B_n \left(\widehat{Z}_2 \right) + \frac{1}{4} B_n \left(\widehat{Z}_{\frac{2}{3}} \right) \right) B_{k,n}(\hat{G}), \quad (3.34)$$

where \hat{G} is defined in eq. (A.11). The first ten coefficients of γ_{qg} stemming from eq. (3.34) read thus:

$$t_0 = 1, \quad (3.35a)$$

$$t_1 = \frac{5}{3}, \quad (3.35b)$$

$$t_2 = \frac{14}{9}, \quad (3.35c)$$

$$t_3 = \frac{82}{81} + 2\zeta_3, \quad (3.35d)$$

$$t_4 = \frac{122}{243} + \frac{25}{6}\zeta_3, \quad (3.35e)$$

$$t_5 = \frac{146}{729} + \frac{14}{3}\zeta_3 + 2\zeta_5, \quad (3.35f)$$

$$t_6 = \frac{2188}{32805} + \frac{287}{81}\zeta_3 + 12\zeta_3^2 + \frac{35}{9}\zeta_5, \quad (3.35g)$$

$$t_7 = \frac{13124}{688905} + \frac{488}{243}\zeta_3 + \frac{515}{21}\zeta_3^2 + \frac{112}{27}\zeta_5 + 2\zeta_7, \quad (3.35h)$$

$$t_8 = \frac{1406}{295245} + \frac{73}{81}\zeta_3 + \frac{55}{2}\zeta_3^2 + \frac{82}{27}\zeta_5 + 32\zeta_3\zeta_5 + \frac{15}{4}\zeta_7, \quad (3.35i)$$

$$t_9 = \frac{11810}{11160261} + \frac{2188}{6561}\zeta_3 + \frac{2665}{126}\zeta_3^2 + 96\zeta_3^3 + \frac{1220}{729}\zeta_5 + \frac{1675}{27}\zeta_3\zeta_5 + \frac{35}{9}\zeta_7 + 2\zeta_9. \quad (3.35j)$$

The coefficients up to t_5 were already known from ref. [62]. We have been able to obtain a large number of coefficients (more than thirty) in an analytical way by solving directly eq. (3.11) order by order, and they coincide with the expansion of the closed form found above, thus providing us with a further confirmation of our all-order result eq. (3.24), and of the self-consistency of the procedures we have followed.

As a marginal comment, we have observed that if we try to expand the function $\hat{\gamma}_{qg}$ in powers of γ_s rather than α_N we obtain a direct expression for the expansion coefficients that is simpler than the two above. We have

$$\hat{\gamma}_{qg}(\alpha_N) = \sum_{n=0}^{\infty} u_n \gamma_s^{n+1}(\alpha_N), \quad (3.36)$$

$$u_n = \frac{1}{n!} \left[\frac{3}{4} B_n \left(\hat{Z}'_2 \right) + \frac{1}{4} B_n \left(\hat{Z}'_{\frac{2}{3}} \right) \right], \quad (3.37)$$

with

$$\hat{Z}'_b^{[k]} = b \left(\delta_{k,1} - (k-1) \sum_{j=1}^{k-1} (-)^{j+1} (j-1)! B_{k-1,j}(Z) \right). \quad (3.38)$$

This form, simpler with respect to that of the h_n coefficients of eq. (3.30), is likely due to the absence of the factor $\chi(\gamma_s(\alpha_N))$ in eq. (3.32), which is compensated by the factor α_N relating $\hat{\gamma}_{qg}$ and h_{qg} , eq. (2.13), thanks to eq. (2.7). As these coefficients u_n are not used anywhere in the text or in the literature, we do not report any of them here.

As we mentioned above, in the context of ref. [47] 36 coefficients have been extracted by solving eq. (3.11) order by order numerically, due to the limited computing resources available at that time that could not allow analytic manipulations up to that order. It is interesting to compare the results of such an extraction with the exact coefficients. We do this at the level of the expansion of h_{qg} , which is better behaved. In fig. 2 we display the ratio of the coefficients h_n as computed in ref. [47] over the exact ones computed here, by plotting the deviation from unity of that ratio, in absolute value and with a logarithmic scale:

$$R_n = \left| 1 - \frac{h_n(\text{ref. [47]})}{h_n(\text{exact})} \right|. \quad (3.39)$$

We observe that above $n \sim 25$ the numerically computed coefficients are completely wrong. This is due to large numerical cancellations among the various terms contributing to these coefficients,

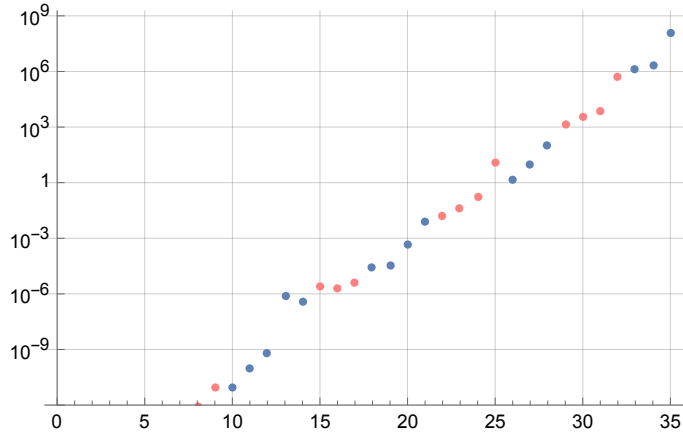


Figure 2. Plot of the relative difference R_n , eq. (3.39), between exact and numerical h_k coefficients in logarithmic scale as a function of n . The blue (red) points feature $h_n(\text{exact}) > 0$ ($h_n(\text{exact}) < 0$).

cancellations which are responsible for increasingly large errors — while the size of these errors is a function of the specific numerical accuracy employed in the calculation, the fact that they increase with n (the coefficient index) is inherently due to the numerical, as opposed to analytical, approach. Having said that, it is reassuring that the lowest-order numerical coefficients are in good agreement with their analytical counterparts; in particular, the agreement is better than permille for all coefficients h_n with $n \leq 20$. The approximate implementation of the resummation of P_{qg} in all of the **HELL** versions prior to that of this paper is based on the first 16 coefficients, and is therefore unaffected by the inaccuracies which plague large- n coefficients²². The actual accuracy of the old approximate implementation of resummation will be studied in sect. 4.3.

3.3 Resummation of subleading running coupling effects

Having computed the function h_{qg} to all orders in sect. 3.1, we now need to use it to obtain a resummed expression for the splitting function P_{qg} , which must include the resummation of subleading running coupling effects as well.

As we discussed in sect. 2.2, the resummation of subleading running coupling effects can be obtained in a number of alternative (equivalent) ways. The most powerful one is given by eq. (2.25), as it allows one to achieve the resummation through the computation of an integral, in a way that would be fully equivalent to what is done in the **HELL** framework for the resummation of coefficient functions. The splitting function would also be straightforwardly obtained as follows

$$P_{qg}^{\text{NLL}'}(\alpha_s(Q^2), x) = \frac{\alpha_s(Q^2)}{3\pi} T_R \int_0^\infty d\xi \frac{d}{d\xi} U(x, Q^2 \xi, Q^2) \mathcal{P}_{qg}(\xi), \quad (3.40)$$

by means of the evolution function $U(x, \mu^2, Q^2)$ in momentum space, which is simply given as the inverse Mellin transform of eq. (2.18)²³. This formulation of resummation requires the generalised function (i.e. a distribution) $\mathcal{P}_{qg}(\xi)$, which is the inverse Mellin transform of $h_{qg}(\gamma)/\gamma$ (see eq. (2.24)). Unfortunately, this Mellin inversion is highly nontrivial. The function is too complicated to allow the analytical computation of its inverse, and even numerically there are issues

²²As was already explained in footnote 13, the choice of this number of coefficients was based on numerical stability checks upon variations of several parameters. At the time of the publication of ref. [56] it was not possible to know that some coefficients were very different from the exact ones.

²³In **HELL**, the evolution function in x space in the ABF approximation (the inverse Mellin transform of eq. (2.22)) is precomputed in grids of values of the arguments (as it is needed for various applications) and readily available for its use in eq. (3.40)

due to the asymptotic behaviour of the function Ω , which makes the numerical convergence very challenging²⁴. In addition to that, a numerical inversion alone is not able to reproduce the nature of $\mathcal{P}_{gg}(\xi)$ as a distribution. We have therefore decided to adopt an alternative approach.

Specifically, we consider the equivalent formulation of the resummation in terms of the series expansion of h_{gg} , eq. (2.17). Also in this case the splitting function can be obtained straightforwardly by means of the evolution function in x space,

$$P_{gg}^{\text{NLL}'}(\alpha_s(Q^2), x) = \frac{\alpha_s(Q^2)}{3\pi} T_R \sum_{k=0}^{\infty} h_k [\partial_\nu^k U(x, Q^2 e^\nu, Q^2)]_{\nu=0}. \quad (3.41)$$

Such a formula depends directly on the coefficients h_k of the expansion of the function h_{gg} , eq. (2.14). We remind the reader that the current formulation of the (approximate) resummation of the gg anomalous dimension in **HELL** is based on this formula, by using just a finite number of coefficients and by extrapolating the others through a Borel-Padé procedure [56]. Here, instead, we manipulate the series to be able to sum it exactly to the now known all-order result of eq. (3.24).

The first step consists in writing the derivatives that appear in eq. (3.41) by using the Cauchy formula, and in expressing the factorial there with the integral representation of the Γ function [66],

$$\begin{aligned} f^{(k)}(0) &= \frac{k!}{2\pi i} \oint \frac{ds}{s} \left(\frac{1}{s}\right)^k f(s) \\ &= \frac{1}{2\pi i} \int_0^\infty dw e^{-w} w^k \oint \frac{ds}{s} \left(\frac{1}{s}\right)^k f(s) \\ &= \frac{1}{2\pi i} \int_0^\infty dw e^{-w} \oint \frac{ds}{s} \left(\frac{1}{s}\right)^k f(ws), \end{aligned} \quad (3.42)$$

which is valid for any function f that is analytic around the origin. In the last step we have rescaled the variable s by w , which is safe as w is positive. The integration contour in the variable s is a closed counterclockwise one that must encircle the origin and avoid other possible singularities of the function f far from $s = 0$. The advantage of this expression is that it converts a k^{th} derivative into a k^{th} power, at the price of introducing two integrals. We can thus rewrite eq. (3.41) as follows

$$\begin{aligned} P_{gg}^{\text{NLL}'}(\alpha_s(Q^2), x) &= \frac{\alpha_s(Q^2)}{3\pi} T_R \sum_{k=0}^{\infty} h_k \frac{1}{2\pi i} \int_0^\infty dw e^{-w} \oint \frac{ds}{s} U(x, Q^2 e^{ws}, Q^2) \left(\frac{1}{s}\right)^k \\ &= \frac{\alpha_s(Q^2)}{3\pi} T_R \frac{1}{2\pi i} \int_0^\infty dw e^{-w} \oint \frac{ds}{s} U(x, Q^2 e^{ws}, Q^2) h_{gg} \left(\frac{1}{s}\right) \\ &= \frac{\alpha_s(Q^2)}{3\pi} T_R \frac{1}{2\pi i} \int_0^\infty dw e^{-w} \oint \frac{dz}{z} U(x, Q^2 e^{w/z}, Q^2) h_{gg}(z), \end{aligned} \quad (3.43)$$

where in the last step we have changed integration variable from s to $z = 1/s$, as this will turn out to be convenient. In Mellin space the result above simply reads

$$\gamma_{gg}^{\text{NLL}'}(\alpha_s(Q^2), N) = \frac{\alpha_s(Q^2)}{3\pi} T_R \frac{1}{2\pi i} \int_0^\infty dw e^{-w} \oint \frac{dz}{z} U(N, Q^2 e^{w/z}, Q^2) h_{gg}(z). \quad (3.44)$$

Note that, after summing the series, the singularity structure in s changes: while there were only singularities in $s = 0$ for each term of the sum, after summing the series more singularities and cuts

²⁴See in particular eq. (B.16). The presence of exponentials of the exponential integral implies that the sought inverse Mellin transform approaches zero (starting at about $\xi \simeq 0.9$) in an incredibly fast way (approximately, by normalising its value to 1 at $\xi = 0.9$, it is equal to 10^{-40} at $\xi = 0.995$). Unfortunately, the full control of the $\xi \rightarrow 1$ region is essential, since the inverse Mellin transform we are talking about is actually a generalised plus distribution, with the function mentioned above as its kernel.

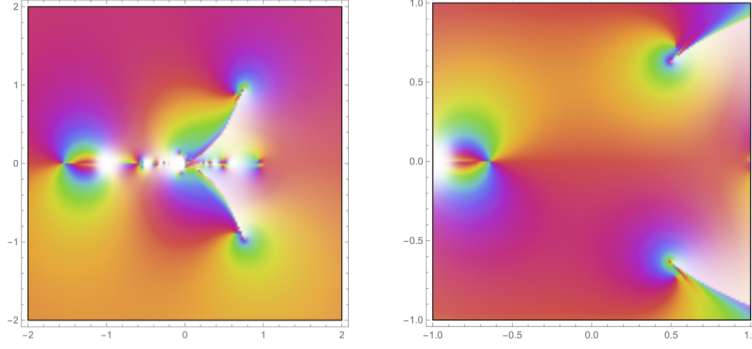


Figure 3. The function $h_{qg}(1/s)$ in the complex s plane (left) and $h_{qg}(z)$ in the complex z plane (right).

appear in the complex s plane. Owing to this new structure, the integration contour in the variable s must be suitably adapted. We observe that all singularities of $h_{qg}(1/s)$ lie in a region around the origin, and get denser as $s = 0$ is approached. Therefore, most of these singularities must lie within the integration contour, lest the contour should cross a branch cut. The simplest option is to encircle them all, which can be easily realized by using for the contour a circle with a large radius — a radius equal to 2 turns out to be sufficient, as one can see from fig. 3. Equivalently, in the variable z one can choose a circle with radius smaller than $1/2$. We stress that inside such a circle in the complex z plane, the function $h_{qg}(z)$ has no singularities (see fig. 3). This makes the formulation that employs the last line of eq. (3.43) convenient for further manipulations, in which the only singularities that contribute to the z integral are those from the function U and the explicit pole at $z = 0$.

In order to assess the goodness of eq. (3.43) and of the choice of the contour, we consider the fixed-coupling limit: in this case, the evolution function is given by eq. (2.19). By plugging eq. (2.19) into eq. (3.44) we obtain

$$\begin{aligned} \gamma_{qg}^{\text{NLL}'}(\alpha_s, N) &\stackrel{\text{f.c.}}{=} \frac{\alpha_s}{3\pi} T_R \frac{1}{2\pi i} \int_0^\infty dw e^{-w} \oint \frac{dz}{z} e^{w\gamma_+(\alpha_s, N)/z} h_{qg}(z) \\ &= \frac{\alpha_s}{3\pi} T_R \frac{1}{2\pi i} \oint \frac{dz}{z - \gamma_+(\alpha_s, N)} h_{qg}(z) \end{aligned} \quad (3.45)$$

$$= \frac{\alpha_s}{3\pi} T_R h_{qg}(\gamma_+(\alpha_s, N)), \quad (3.46)$$

which coincides, as is expected, with the result of eq. (2.13) when $\gamma_+(\alpha_s, N) \rightarrow \gamma_s(\alpha_N)$. Here, in the first step we have computed the w integral which converges only if $\text{Re}(1 - \gamma_+/z) > 0$, and extended the result analytically elsewhere²⁵. Then, we could use in the last step the fact that the only singularity present inside the integration contour is the explicit z pole. This is strictly speaking true only if $|\gamma_+(\alpha_s, N)|$ is sufficiently small to be inside the circle, but the result can be analytically continued elsewhere if that is not the case.

Although this example is not a proof of our assumption on the integration contour, it gives us confidence that our choice is reasonable. In practice though, in order to implement eq. (3.43), (3.44) numerically, we need the evolution operator U with full access to complex values of its second argument. As this is related to the scale at which α_s is computed, it is not straightforward to treat it in a general way. In the following, we thus consider an approximation of the evolution operator that allows us to obtain numerical results, consistently with previous HELL implementation.

Specifically, in order to avoid computing the strong coupling with complex argument, we consider the ABF approximation of the evolution operator that is customarily used in HELL, eq. (2.22).

²⁵A similar procedure is used in appendix A.2 for the manipulations of an integral representation of γ_s .

Plugging it into eq. (3.44) we obtain

$$\begin{aligned}\gamma_{qg}^{\text{NLL}'}(\alpha_s, N) &\stackrel{\text{ABF}}{=} \frac{\alpha_s}{3\pi} T_R \frac{1}{2\pi i} \int_0^\infty dw e^{-w} \oint \frac{dz}{z} \left(1 + \frac{r(\alpha_s, N)w}{z}\right)^{\frac{\gamma_+(\alpha_s, N)}{r(\alpha_s, N)}} h_{qg}(z) \\ &= \frac{\alpha_s}{3\pi} T_R \frac{1}{2\pi i} \oint \frac{dz}{z} e^{\frac{z}{r(\alpha_s, N)}} \left(\frac{r(\alpha_s, N)}{z}\right)^{\frac{\gamma_+(\alpha_s, N)}{r(\alpha_s, N)}} \Gamma\left(1 + \frac{\gamma_+(\alpha_s, N)}{r(\alpha_s, N)}, \frac{z}{r(\alpha_s, N)}\right) h_{qg}(z)\end{aligned}\quad (3.47)$$

in terms of the incomplete Γ function. In deriving this expression we have performed an analytic continuation in z of the w integral thanks to the fact that we have been able to compute the w integral analytically. In order to obtain the splitting function P_{qg} , the inverse Mellin of this result must be computed. However, the integrand of the z integral computed along the inverse Mellin contour has a branch-cut for real negative z values. This means that the original choice of the z integration contour, a circle around the origin, is not suitable anymore, and it must be modified. The most obvious option is to “stretch” the circle to enclose the cut, thereby leading to a Hankel-like contour along the negative real z axis.

It is useful to observe that we can simplify the expression of eq. (3.47) by noting that, for small z , we can expand

$$\begin{aligned}\Gamma\left(1 + \frac{\gamma_+}{r}, \frac{z}{r}\right) &= \Gamma\left(1 + \frac{\gamma_+}{r}\right) - \int_0^{\frac{z}{r}} dt e^{-t} t^{\frac{\gamma_+}{r}} \\ &= \Gamma\left(1 + \frac{\gamma_+}{r}\right) - \mathcal{O}\left(z^{\frac{\gamma_+}{r}+1}\right).\end{aligned}\quad (3.48)$$

Plugging this into eq. (3.47) we obtain

$$\begin{aligned}\gamma_{qg}^{\text{NLL}'}(\alpha_s, N) &\stackrel{\text{ABF}}{=} \frac{\alpha_s}{3\pi} T_R \frac{1}{2\pi i} \oint \frac{dz}{z} e^{\frac{z}{r(\alpha_s, N)}} \left[\left(\frac{r(\alpha_s, N)}{z}\right)^{\frac{\gamma_+(\alpha_s, N)}{r(\alpha_s, N)}} \Gamma\left(1 + \frac{\gamma_+(\alpha_s, N)}{r(\alpha_s, N)}\right) + \mathcal{O}(z)\right] h_{qg}(z) \\ &= \frac{\alpha_s}{3\pi} T_R \Gamma\left(1 + \frac{\gamma_+(\alpha_s, N)}{r(\alpha_s, N)}\right) \frac{1}{2\pi i} \oint \frac{dz}{z} e^{\frac{z}{r(\alpha_s, N)}} \left(\frac{r(\alpha_s, N)}{z}\right)^{\frac{\gamma_+(\alpha_s, N)}{r(\alpha_s, N)}} h_{qg}(z),\end{aligned}\quad (3.49)$$

where we have used the residue theorem to deduce that the $\mathcal{O}(z)$ term has a null integral. Eq. (3.49) represents a significant simplification of eq. (3.47). In particular, the integration along the cut on the real negative z axis converges well for eq. (3.49). We use this representation for the new numerical implementation of the resummation of P_{qg} in **HELL**. Additional details, including the choice of the integration contours in z and N , are given in appendix C.1.

4 Resummed DGLAP evolution to large α_s

Having obtained an all-order expression for P_{qg} , we report in this section new numerical results for the singlet DGLAP evolution matrix, which allow one to handle large values of α_s . For this to be possible, we had to improve some of the core steps of the **HELL** code, which were optimised in the past only for $\alpha_s \lesssim 0.3$. We thus first briefly report on these technical changes.

4.1 Improvements to employ large α_s values in γ_+

The first part of the **HELL** workflow consists in resumming the anomalous dimension γ_+ along the Mellin inversion contour. This procedure is based on the ingredients discussed in sect. 2.1. One of the steps involved is the resummation of collinear poles in the BFKL kernel, obtained through the duality with DGLAP. For this step, **HELL** (from version 2.0 onwards) uses an approximate fixed-order anomalous dimension with the correct small- N structure but with a modified asymptotic behaviour

at large N (see appendix B.3 of ref. [57]). The reason for this is twofold. Firstly, it gives one the possibility of computing the inverse function analytically, which leads to numerical performances which are significantly more stable. Secondly, when using it to resum the collinear ($\gamma = 0$) pole of the BFKL kernel, one does not hit the subleading singularity at $\gamma = -1$ of such a kernel, and thus avoids a problem in the subsequent matching of the resummed anomalous dimension with the fixed order.

However, such approximate fixed-order anomalous dimension does avoid hitting the subleading singularity at $\gamma = -1$ only for sufficiently small values of the coupling constant, namely $\alpha_s \lesssim 0.5$. As we now want to employ larger values of α_s this approximation will have to be improved. We have done this in a minimal way, which retains the advantages of the previous formulation, but also allows us to push the procedure safely to larger α_s values. Moreover, we have introduced our modification in a smooth way, so that for small values of α_s the result is basically unchanged w.r.t. to the original approximation of ref. [57]. Technical details of this procedure are reported in appendix C.2.

An additional issue we have faced when employing large values of α_s is related to the approximation used for implementing the resummation of the subleading running-coupling effects discussed in sect. 2.1. We have noticed that with such an approximation the resummed splitting function behaves at small x in an unexpected way; namely, it decreases, rather than increases, with decreasing x 's. This behaviour is driven by a spurious singularity generated by the aforementioned approximation, which turns out to have a negative residue with large absolute value, and which thus dominates over the leading singularity that has a positive but small residue. We explain this issue in greater detail in appendix C.3.

In order to solve this problem, we propose a very simple modification of the approximation introduced in ref. [57], which is consistent with the original idea, but adds suitable subleading terms that make the spurious pole innocuous. After this modification, which we also argue to lead to a more natural approximation than the original one, the behaviours of the resummed splitting functions are as expected, namely at small x they grow with decreasing x 's. All of the details about these changes are collected in appendix C.3, and their impact is investigated in sect. 4.2.

Finally, another issue which shows up in the computation of the resummed γ_+ at large α_s is a change of branch in the solution of the duality condition with the BFKL kernel. Such a solution is implemented numerically with a zero-finding algorithm in the complex N plane, for values of N along the Mellin inversion contour (we give some details on how this is performed in practice in appendix C.4). The functions involved are very complicated, with rich singularity structures, so it is very natural to expect that when changing the value of α_s the branch selected by the algorithm may change. Luckily, this happens only at large $|\text{Im}(N)|$ values, which impacts the Mellin inversion only at large x , leaving the small- x region, which is the one we are interested in, unaffected by this problem.

In practice, however, having a jump from one branch to another is undesirable because it creates a sudden change in the large- x behaviour of the relevant Mellin inverse (here, the splitting function P_+) when changing α_s . We have therefore decided to adopt a numerical procedure²⁶ in which the large- x behaviour is extrapolated from a lower- x region where the change of branch does not produce any effect. This procedure destroys momentum conservation, which we reimpose manually. In order to do so, we find it convenient to project the splitting function P_+ on a basis of Chebyshev polynomials of the first kind, which we can use to compute the Mellin transform analytically in terms of a small number of coefficients. This approach, that we describe in detail in appendix C.4,

²⁶Note that, in principle, it could be possible to avoid the branch change problem by modifying the BFKL kernel with suitable subleading contributions. The problem of this approach is that without a clear understanding of the analytic structure of the kernel and of the origin of the branch cuts it is very difficult to guess which kind of subleading contributions could fix the problem. Given the complexity of functions involved, we did not pursue this approach.

works very well, and it also allows us to speed up the `HELL` code, thanks to the simpler access to γ_+ .

The only limitation of this procedure is related to the computation of the derivative of γ_+ with respect to α_s , needed for one of the incarnations of the ABF evolution operator given in eq. (2.22) (see the discussion in sect. 2.2). Indeed, the numerical computation of the α_s derivative of the anomalous dimension obviously fails for values of α_s in proximity of the branch-change region. There are different solutions which we may adopt. For instance, we may consider an asymmetric difference quotient on the side where the branch does not change, but it is difficult to implement this approach in an automated way. Given also that we have noticed that the numerical convergence of the integral in eq. (3.49) is problematic when using $r(\alpha_s, N) = \alpha_s^2 \beta_0 \frac{d}{d\alpha_s} \log \gamma_+(\alpha_s, N)$, we have decided to limit ourselves to using the incarnation of the ABF evolution operator of eq. (2.22) which does not require any α_s derivative, namely we set $r(\alpha_s, N) = \alpha_s \beta_0$. Thus, we work exclusively with the latter choice of $r(\alpha_s, N)$, and we postpone further studies of this problem to future work.

4.2 Numerical results for P_{qg} and comparison with previous predictions

We now present some numerical results for the splitting functions that emerge from the procedures discussed thus far. We start by focussing on P_{qg} , and we discuss the comparison with its previous implementation as is included in version 3 of `HELL`.

For the sake of this comparison, we find it more convenient to plot the resummed result after subtracting its expansion at the NNLO [57, 58],

$$\Delta_3 P_{qg}(\alpha_s, x) \equiv P_{qg}^{\text{NLL}'}(\alpha_s, x) - \sum_{k=0}^2 \alpha_s^{k+1} P_{qg}^{\text{NLL}'(k)}(x) \quad (4.1)$$

since this is the default output of `HELL`. We also apply a large- x damping of the form $(1-x)^2(1-\sqrt{x})^4$, as is used in previous versions of `HELL`, to kill the effect of resummation in the large- x region where it is not expected to be accurate.

In fig. 4 we show $2n_f \Delta_3 P_{qg}(\alpha_s, x)$, multiplied by x and divided by α_s^4 for an improved readability, as a function of x in a logarithmic scale. We set $n_f = 3$, which is the value relevant to small scales, where α_s assumes large values. The figure displays four panels, corresponding to four different values of the coupling constant, namely $\alpha_s = 0.2, 0.25, 0.3$, and 0.35 (left to right and top to bottom). Currently, we do not consider larger α_s values since we also want to present the results of `HELL` version 3, which are limited to $\alpha_s \lesssim 0.35$. The plots in each panel have identical layouts, and feature four curves, namely:

- our new best result (thick solid red), obtained according to the procedure we have adopted in this work; in particular, we use the exact form of $h_{qg}(z)$, eq. (3.24), the modified $\gamma_+^{\text{NLL}'}$ as is described in sect. 4.1, and set $r(\alpha_s, N) = \alpha_s \beta_0$;
- the same result as above (thin solid black), except for the fact that we use here $\gamma_+^{\text{NLL}'}$ extracted from `HELL` version 3;
- the old `HELL` 3 result (dot-dashed orange), that uses a Borel-Padé procedure based on a finite number (16) of coefficients of the expansion of $h_{qg}(z)$;
- the old `HELL` 3 result (dashed blue), computed as the previous curve, except that in this case the derivative form of r , namely $r(\alpha_s, N) = \alpha_s^2 \beta_0 \frac{d}{d\alpha_s} \log \gamma_+(\alpha_s, N)$, is used (which was considered the default result in `HELL` 3).

Several comments are in order.

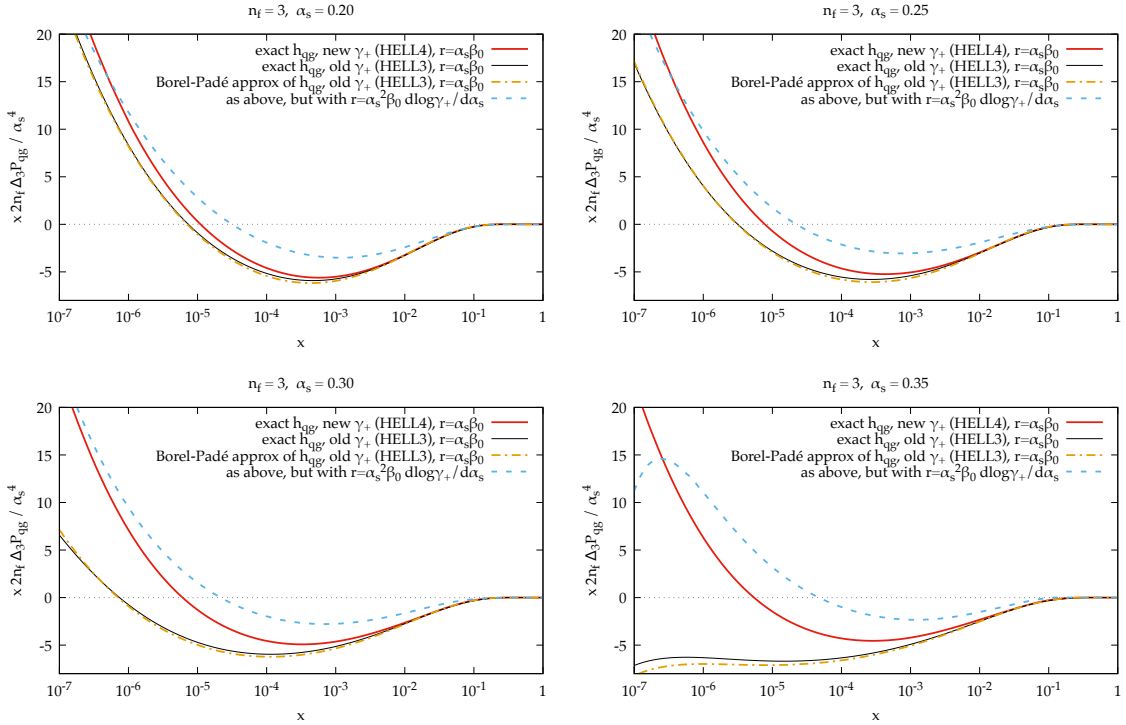


Figure 4. Comparison of $\Delta_3 P_{qg}(\alpha_s, x)$ computed with different combinations of the ingredients and procedure. Each plot corresponds to a different value of α_s , from 0.2 to 0.35 in steps of 0.05.

When comparing the first two curves, we immediately see that the results are very similar at $\alpha_s = 0.2$, and they are increasingly different as α_s gets larger. This is in keeping with the genesis of the difference, namely the modification in the construction of $\gamma_+^{\text{NLL}'}$. The largest part of this effect comes from the modified resummation of the running coupling contributions, as is described in appendix C.3. Indeed, the difference in the new construction amounts to a contribution of $\mathcal{O}(\alpha_s)$, which is thus visible already at intermediate values of α_s , and becomes very significant as α_s gets larger. The other contribution to the difference between the two constructions, discussed in appendix C.2, is instead designed to be a correction of $\mathcal{O}(\alpha_s^2)$, and therefore it has a visible impact only at large α_s . We also note that the new result is very stable across different α_s values, while when using the old $\gamma_+^{\text{NLL}'}$ there is a significant dependence on α_s , with the result bending down at small x already when $\alpha_s = 0.35$. This unexpected (and, we believe, unphysical) behaviour is induced by the spurious pole discussed in appendix C.3, and must be considered as a failure of the previous construction at large α_s values, which is addressed by the modifications we present in this work.

The comparison between the second and third curves is even more interesting. The only difference between these curves is the use of the exact all-order h_{qg} expression in the former, and of its approximation based on the Borel-Padé procedure in the latter. The striking feature of the comparison between these two curves is that the agreement is remarkably good at all α_s values considered. This means that the Borel-Padé procedure devised in ref. [56] works fairly (and even somewhat surprisingly) well, despite being based on just 16 coefficients of the expansion of h_{qg} . Apart from considerations on the procedure itself, this finding shows that results based on previous versions of HELL are fully reliable, if one limits oneself to employing values of α_s compatible with a perturbative expansion.

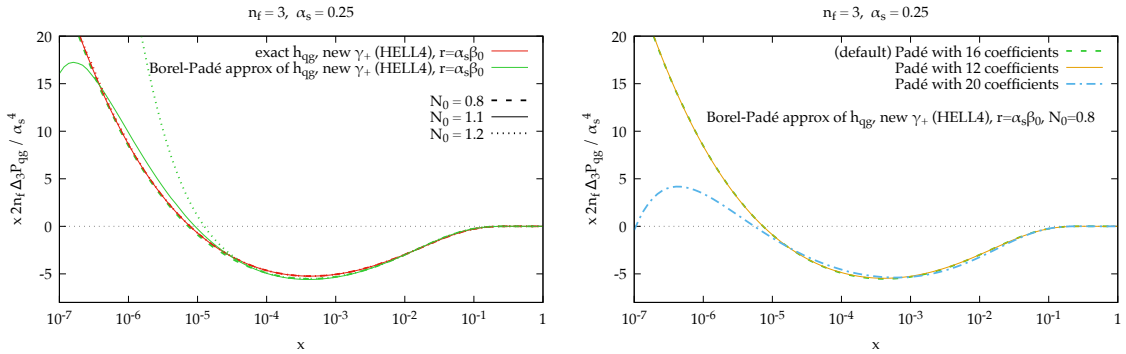


Figure 5. Variations of the Mellin inversion path (left-hand panel) and of the order of the Padé approximant (right-hand panel). The dashed green curve is the same in both plots.

Finally, the comparison between the last two curves shows the impact of varying the approximation on which the construction of the ABF evolution function of eq. (2.22) is based. This difference is not considered here for the first time, as it was already studied in refs. [56–58], in the context of the definition of an uncertainty band. In the previous HELL literature, the last (dashed blue) curve has been considered as the “central” prediction, while the third curve (dot-dashed orange) was used as a variation to construct the uncertainty band. In this work, instead, because of the absence of an exact result obtained with $r(\alpha_s, N) = \alpha_s^2 \beta_0 \frac{d}{d\alpha_s} \log \gamma_+(\alpha_s, N)$, we consider the curve based on $r(\alpha_s, N) = \alpha_s \beta_0$ as the central value. This of course *also* leads to differences with past results, which are in and of themselves sizable. In part, such differences are mitigated by the uncertainty band which we shall construct.

The agreement between the second and third curves which appears in the plots of fig. 4 may raise the question of whether our exact result for the function h_{qg} is phenomenologically useful or not. In order to (positively) answer this question, we consider some “stress tests” of the two implementations of the resummed P_{qg} . While carrying out those, we set the value of α_s equal to a sufficiently moderate value, $\alpha_s = 0.25$, in order to avoid potential problems due to large perturbative corrections at larger α_s values, and consider the following two variations:

- a variation of the path used for Mellin inversion, which path we parametrise as

$$N(u) = N_0 + e^{i\theta} u, \quad \frac{\pi}{2} < \theta < \pi, \quad u \in [0, \infty); \quad (4.2)$$

- a variation of the order of the Padé approximant (obviously applicable only to the “old” implementation).

The results are shown in fig. 5.

In the plot on the left-hand panel, we show $2n_f \Delta_3 P_{qg}(\alpha_s, x)$ multiplied by x and divided by α_s^4 (as in fig. 4) obtained with the exact h_{qg} (red curves) and with the Borel-Padé procedure (green curves) using three different paths for Mellin inversion. In particular, we change the value of the parameter N_0 ²⁷ of eq. (4.2), from its default value $N_0 = 1.1$ (solid curves) to a lower value $N_0 = 0.8$ (dashed curves) and to a higher value $N_0 = 1.2$ (dotted curves). The solid red curve is identical to that of fig. 4. In all cases, we use the new construction for $\gamma_+^{\text{NLL}'}$. We observe that the three red curves are in perfect agreement among themselves: this proves that the implementation based on the exact all-order h_{qg} expression is very stable under variations of the path. Conversely, the result

²⁷We do not show variations due to the slope of the path, i.e. the dependence upon θ of eq. (4.2), as it induces very little differences, mostly at large x where the damping washes out any resummation effects.

based on the Borel-Padé procedure depends significantly on N_0 : it is in good agreement with what is obtained with the exact h_{gg} for small N_0 values (we remark that $N_0 = 0.8$ was the value used in HELL 3), but it deviates from it in the small- x region as N_0 gets larger. This behaviour is likely due to the nature of the Padé approximant, which being a non-linear function may become overly sensitive to small parameter variations.

In the plot on the right-hand panel, we change the order of the Padé approximant while fixing $N_0 = 0.8$, since the latter value underpins the best agreement between the approximate and the exact result. Specifically, from the default $[8/7]$ Padé²⁸ adopted in previous versions of HELL, that uses 16 coefficients of the expansion of h_{gg} , we consider a lower variation $[6/5]$ that uses 12 coefficients, as well as a higher variation $[10/9]$ that uses 20 coefficients. The lower variation (solid yellow curve) is in perfect agreement with the default result (dashed green), in spite of relying on a smaller number of coefficients: this means that either the result is dominated by the first few terms of the expansion of h_{gg} , or the Padé approximant approximates very well the full result even with a small number of terms. The higher variation (dot-dashed blue) predicts a splitting function which is instead rather different w.r.t. the other two. We point out that this difference is not due to the incorrect values of the coefficients, since up to order 20 (which is the maximum considered here) they agree with the exact ones to better than permille (see fig. 2); in fact, we have explicitly verified that by using the exact coefficients in the Padé approximant the result is the same as before. Therefore, this test points to a failure of the procedure itself when one tries and uses too many coefficients which is perhaps paradoxical, but ultimately we interpret it to be due to the fact that a too-complicated rational function becomes increasingly unreliable as a representation of a non-rational function.

The conclusion of these studies is that the Borel-Padé procedure is able to provide one with an essentially correct result for the resummation of P_{gg} , but only in a limited region of the space of parameters involved. Finding this region is not straightforward (one looks for stability under small parameter variations), and ultimately it can only be safely validated by using the exact result, the availability of which of course renders the whole exercise an academic one. Moreover, it is definitely possible that at larger α_s value this region becomes smaller and smaller, thus making it increasingly harder to pin it down. These considerations therefore clearly highlight why our new exact result is crucial.

4.3 Results for the singlet splitting function matrix

Having clarified, by using P_{gg} as a prominent example whose conclusions qualitatively apply to the other splitting functions as well, in which aspects our new results are in keeping with, or differ from, those obtained with the existing version of HELL, we are now in the position to present our predictions for all of the singlet splitting functions, including at large values of α_s . We point out that when constructing the resummed P_{gg} according to eq. (2.2) we must take care of restoring the momentum conservation condition,

$$\int_0^1 dx x [P_{gg}(\alpha_s, x) + 2n_f P_{qg}(\alpha_s, x)] = 0. \quad (4.3)$$

This is in general violated by the large- x damping discussed before (which is applied to all of the resummed splitting functions). The restoration is performed by adding a suitable term to the resummed P_{gg} , as is discussed in detail in refs. [57] (sect. 4.2.2 there). In view of the fact that we adopt the very same procedure here, we do not comment on it any further.

The resummed results matched to NNLO (solid), along with the fixed-order ones (LO: dotted; NLO: dashed; NNLO: dot-dot-dashed), are shown in fig. 6. The plots in the left column display

²⁸We use the standard notation $[n/m]$ to indicate a Padé approximant with numerator of degree n and denominator of degree m .

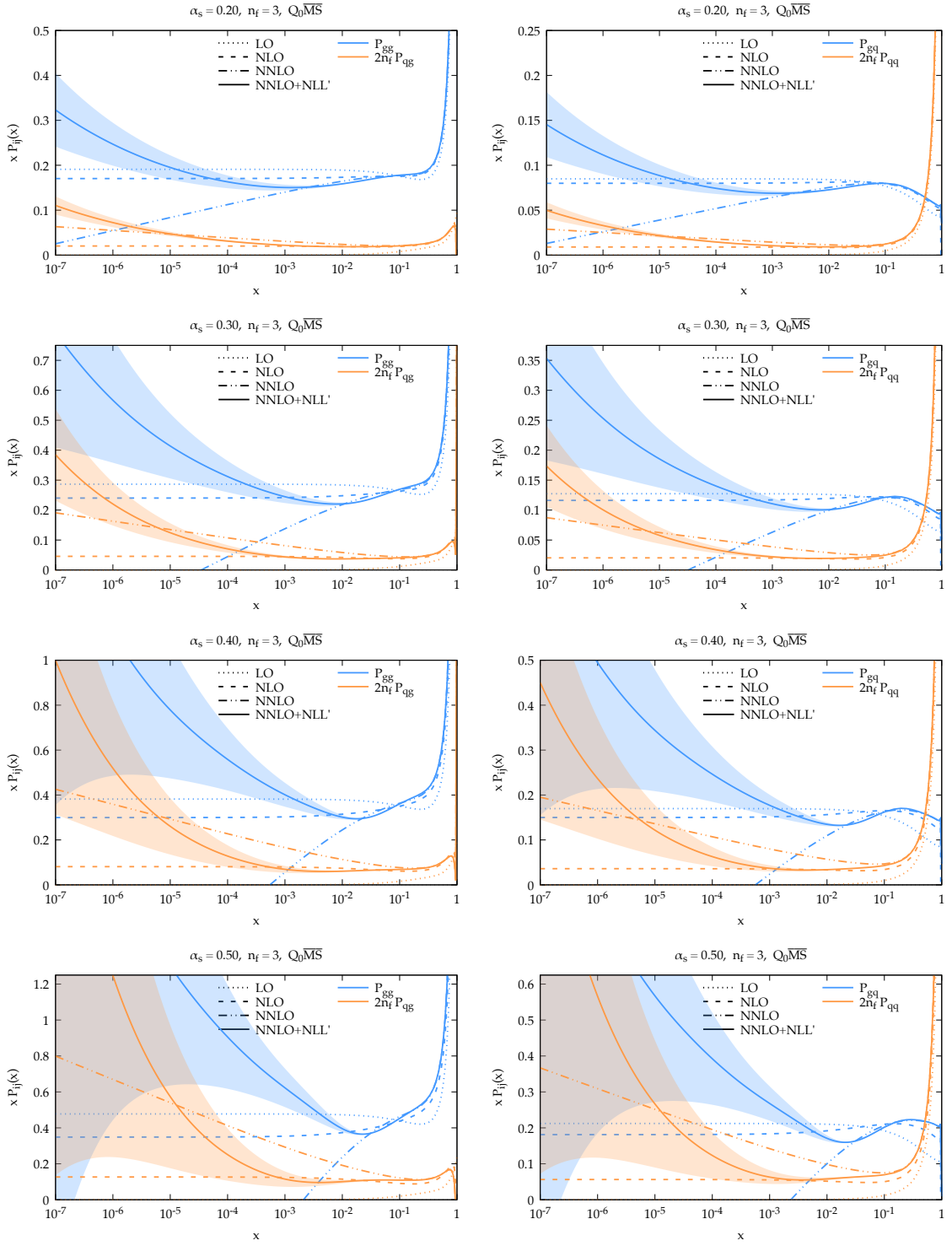


Figure 6. The fixed-order and resummed splitting functions as a function of x . Each row corresponds to a different values of α_s , from 0.2 to 0.5 in steps of 0.1. In each row P_{gg} (blue) and P_{qg} (orange) are shown on the left, and P_{gg} (blue) and P_{qq} (orange) are shown on the right.

the P_{gg} (blue) and $2n_f P_{qg}$ (orange) splitting functions, while those in the right column display the P_{gq} (blue) and $2n_f P_{qq}$ (orange) splitting functions. Each row corresponds to a value of α_s , namely $\alpha_s = 0.2, 0.3, 0.4$, and 0.5 (top to bottom). In all cases we set $n_f = 3$, which is the only value of n_f for which these large α_s values are relevant. The resummed results are supplemented with an uncertainty band (shaded areas). At variance with the previous HELL 3 results, this band is obtained by considering a single variation²⁹ of the anomalous dimension $\gamma_+^{\text{NLL}'}$ which enters the construction of all of the splitting functions. This variation has been described in refs. [57, 58], and is related to the way the resummation of running coupling effects mentioned in sect. 2.1 is implemented (see appendix C.3 for further detail). The final band is obtained by symmetrising the difference of the variation with respect to the central curve.

These results are *qualitatively* similar to those of the existing literature. For example, going from large to small x , the resummed NNLO+NLL' P_{gg} and P_{gq} follow initially the NNLO predictions before dramatically steeping up at a certain x value (which in turn depends on α_s), thus producing the well known and expected dip [46, 50, 67, 68]. Also, the resummed NNLO+NLL' P_{qg} and P_{qq} splitting functions tend to rise in a much milder way w.r.t. their NNLO counterparts, and are thus in a better agreement with the corresponding NLO results in an intermediate range in x , as was observed already in refs. [57, 58].

In addition to known qualitative behaviours, we can now investigate what happens at large α_s values. We first observe that when α_s grows the curves of the resummed results at small x become steeper, and the corresponding rises begin at larger values of x (w.r.t. their small- α_s counterparts) for all of the splitting functions. Moreover, the uncertainty band of the resummed result becomes bigger, which is expected as the impact of subleading terms becomes more important. Keeping in mind that the way this band is constructed is somewhat arbitrary, and it does not necessarily faithfully represent the size of the subleading contributions, it is clear that by going to large α_s values the resummed result becomes less reliable towards small x 's — the uncertainty band becomes huge. A higher logarithmic accuracy would be needed to tame the uncertainty and to obtain a more reliable result, even though there is the concrete possibility that when α_s is too large even the convergence of the resummed expansion is spoiled. The next subsection will present a speculative discussion on this point, and an alternative interpretation which questions its conclusions.

4.4 When subleadingness ceases to be a useful concept

In order to qualitatively understand where we expect the resummed results to be valid, we recall that we are resumming to all orders powers of $\alpha_s \log(1/x)$. This means that the ordering for which this (re)organization of the perturbative series is reliable is the one where

$$\alpha_s \log \frac{1}{x} \sim 1, \quad \alpha_s \ll 1. \quad (4.4)$$

The leftmost condition ensures that the organization of the series as an expansion in powers of α_s of all-order functions of $\alpha_s \log(1/x)$ is meaningful, while the rightmost one ensures that formally-subleading logarithmic corrections are *actually* subleading. Typically, we consider that if the latter condition holds true while the former one does not (i.e. $\alpha_s \log(1/x) \gg 1$), then the logarithmic-ordered expansion of the resummed result is no longer appropriate, and the results thus obtained become unreliable.

We shall argue later that this is not necessarily the case³⁰; but before going into that, we shall briefly elaborate on such a standard interpretation of the logarithmic ordering in the context of small- x physics. Clearly, the border between the regions $\alpha_s \log(1/x) \sim 1$ and $\alpha_s \log(1/x) \gg 1$ is not

²⁹The other variation used in ref. [58] is the choice of the function $r(\alpha_s, N)$, that in our case is set to $r(\alpha_s, N) = \alpha_s \beta_0$, as was previously discussed.

³⁰In this section, for the sake of simplicity the problem of the Landau pole will be ignored, and α_s will be considered as well-defined everywhere.

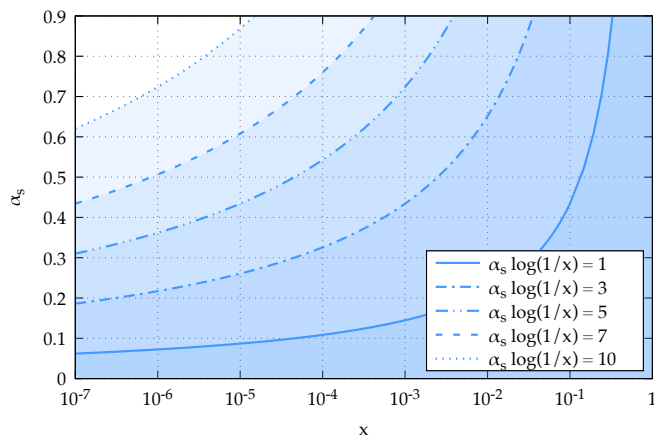


Figure 7. Curves with constant $\alpha_s \log(1/x)$ value. See the text for details.

sharp. We can have a rough idea of the interplay between these regions by looking at figure 7. There, the curves represent the sets of (x, α_s) points for which $\alpha_s \log(1/x)$ assumes a given value, which increases by moving southeast to northwest. Thus, in the context of the standard interpretation of resummed results the bottom right (upper left) corner is the region associated with the most (least) reliable predictions. In particular, the region below and/or to the right of the solid line (for which $\alpha_s \log(1/x) = 1$) poses no problem to the logarithmic ordering of the cross section. If anything, when moving towards large-ish x 's, effects beyond small- x resummation also become important, and indeed the resummed results are damped there. As one moves towards the non-solid curves, the impact of such a damping becomes irrelevant, but at the same time the value of $\alpha_s \log(1/x)$ keeps on growing. Deciding where such a value is uncomfortably large is unfortunately an arbitrary choice. For example, if $\alpha_s \log(1/x) = 5$ is deemed to be acceptable, then resummed predictions are reliable down to $x \sim 10^{-7}$ at $\alpha_s = 0.3$, or $x \sim 10^{-4}$ at $\alpha_s = 0.5$ (clearly, the larger the value of α_s the smaller the “safe” region in x).

In general, *if* we consider the bending down of the results in fig. 4 and fig. 5 as evidence of the start of the breakdown of the logarithmic ordering which underpins the resummed splitting functions, inspection of fig. 7 shows that this indeed corresponds to $\alpha_s \log(1/x) \sim 5$.

However, the very discussion given in the preceding sections implies that the reason for that bending down may actually be more subtle, namely driven in equal measure by the subleading nature of certain contributions and by the way in which those are implemented in the resummed results. In other words, certain classes of resummed results might be such that formally-subleading terms may, or may not, become numerically comparable to the leading ones, depending on the characteristics of different approximations which are all at the same level from a logarithmic standpoint. It is only in this case that the validity of the logarithmic ordering of the resummed results becomes unreliable, and further improvements are necessary to recover sensible predictions.

In order to further the previous point in an over-simplified context, consider a model in which the perturbative expansion in a “small” parameter a is potentially spoiled by large logarithms L that emerge order by order. Suppose also that the LL coefficients associated with such logarithmic terms are well behaved, namely³¹

$$\text{LL} \iff \left\{ a^k L^k \right\}_{k=0}^{\infty} \implies \varsigma_{\text{LL}} = \sum_{k=0}^{\infty} \frac{1}{k!} a^k L^k = e^{aL}, \quad (4.5)$$

³¹All coefficients are understood to be divided by $1/k!$, as is exemplified by eq. (4.5).

with ς any quantity whose resummation is of interest (i.e. the splitting functions here, an observable, and so forth). This simple formula captures the essence of resummation: when $L \sim 1/a$, the coupling a is not a good expansion parameter any longer, and one must use aL instead. By taking into account terms to all orders, one obtains a well-defined expression ς_{LL} . Importantly, ς_{LL} is a perfectly valid result also in the region where $L \gg 1/a$, i.e. where the standard logarithmic-ordered counting loses validity. In other words, by means of resummation one obtains results which are valid regardless of the value assumed by the large logarithm; it is clear that this is strictly an all-order property, and that the conclusion is universally valid only because potentially subleading contributions have been ignored.

We now lift the latter restriction, i.e. we consider the generic NLL, NNLL, etc. contributions

$$\text{N}^i\text{LL} \longleftrightarrow \left\{ c_i(k) a^{k+i} L^k \right\}_{k=0}^{\infty}, \quad i = 1, 2, \dots \quad (4.6)$$

in the following two cases

$$c_1(k) = 1, \quad c_2(k) = \frac{1}{2}, \quad c_3(k) = \frac{1}{6}, \quad \dots \quad \implies \quad c_i(k) = \frac{1}{i!}, \quad (4.7)$$

$$c_1(k) = k, \quad c_2(k) = \frac{k(k-1)}{2}, \quad c_3(k) = \frac{k(k-1)(k-2)}{6}, \quad \dots \quad \implies \quad c_i(k) = \frac{\Gamma(k+1)}{i! \Gamma(k+1-i)}. \quad (4.8)$$

Let us start with eq. (4.7). The resulting resummed quantities are

$$\varsigma_{\text{N}^i\text{LL}} = \sum_{k=0}^{\infty} \frac{1}{k!} c_i(k) a^{k+i} L^k = \frac{1}{i!} a^i e^{aL}, \quad (4.9)$$

and thence

$$\varsigma_{\text{LL}} + \varsigma_{\text{NLL}} + \varsigma_{\text{N}^2\text{LL}} + \varsigma_{\text{N}^3\text{LL}} + \dots = \left(1 + a + \frac{1}{2}a^2 + \frac{1}{6}a^3 + \dots \right) e^{aL}. \quad (4.10)$$

Therefore, here the subleadingness of the various contributions remains a meaningful characteristic, *regardless* of the value of L , which can be arbitrarily large — the only necessary condition is that the coupling constant remain in the perturbative domain. In other words, one may truncate the resummed quantity at any logarithmic accuracy, and be assured that the corresponding prediction is sensible, in the sense that contributions of higher logarithmic accuracy will modify that prediction in an increasingly minimal way.

Conversely, with eq. (4.8) we obtain what follows,

$$\varsigma_{\text{N}^i\text{LL}} = \sum_{k=0}^{\infty} \frac{1}{k!} c_i(k) a^{k+i} L^k = \frac{1}{i!} a^i (aL)^i e^{aL}, \quad (4.11)$$

so that

$$\varsigma_{\text{LL}} + \varsigma_{\text{NLL}} + \varsigma_{\text{N}^2\text{LL}} + \varsigma_{\text{N}^3\text{LL}} + \dots = \left(1 + a^2 L + \frac{1}{2} a^4 L^2 + \frac{1}{6} a^6 L^3 + \dots \right) e^{aL}. \quad (4.12)$$

Now, at variance with what happens with eq. (4.10), if eq. (4.12) truncated at a certain logarithmic order i_0 it does matter whether $aL \sim 1$ or $aL \gg 1$, since in the latter case (in particular, when $aL \gg 1/a$) regardless of how many i_0 resummed contributions one includes the result will not make any physical sense, in spite of the valid definition of each of its components.

The only viable solution is therefore that of considering *all* of the nominally subleading logarithmic terms, i.e. to compute:

$$\text{eq. (4.12)} \quad \longrightarrow \quad \sum_{i=0}^{\infty} \varsigma_{\text{N}^i\text{LL}} = \sum_{i=0}^{\infty} \frac{1}{i!} a^i (aL)^i e^{aL} = e^{a(1+a)L}, \quad (4.13)$$

which is valid for any L , with the behaviour expected on the basis of logarithmic dominance restored (since, regardless of the value of L , $aL > a^2L$ as long as a is sufficiently small). We point out that by playing the same game with eq. (4.10) one does not obtain a result significantly different from a truncated one:

$$\text{eq. (4.10)} \quad \longrightarrow \quad \sum_{i=0}^{\infty} \zeta_{\text{N}^i \text{LL}} = \sum_{i=0}^{\infty} \frac{1}{i!} a^i e^{aL} = e^{a(L+1)}. \quad (4.14)$$

The bottom line is that, depending on the characteristics of the coefficients of the subleading contributions, such contributions may become numerically comparable to or dominant over their leading counterparts, thus spoiling the convergence properties of the resummed quantity of interest, irrespective of the formal logarithmic accuracy which one manages to achieve. In these cases the resummed prediction, if truncated at any given logarithmic accuracy (however large), will be unable to return a sensible physical result, and it must therefore be further improved, for example by finding either an approximation of the neglected subleading terms that can be effectively included in those contributions which have been kept, or a pattern for the neglected subleading terms which allows one to resum them³². The former strategy is clearly the least solid of the two, but in practical cases it may be the only viable one³³.

We conclude this section by stressing that there may be different mechanisms which destroy the logarithmic ordering of resummed quantities, and that we are not implying that small- x resummation is underpinned by geometrically-growing coefficients such as those of eq. (4.8). Nevertheless, we still stress that the commonly-assumed limitations on the validity of resummed quantities may not necessarily be accurate, and a case-by-case assessment is necessary. In our specific situation, it is not unlikely that the improved approximations proposed in this work imply an extended validity of the resummed splitting kernels. Clearly, this improvement (being to some extent heuristic) goes hand-in-hand with large theoretical systematics, and therefore the final evidence of the validity of this approach can only come by means of a comparison to data.

5 Future directions: results for the qg Green function

While this is an aside in the present context, and does not play any role in the numerical results obtained so far, it is worth mentioning the fact that by means of the same techniques employed in sect. 3 we have been able to obtain a closed, all-order form for the $\epsilon = 0$ part of the finite $\hat{\mathcal{G}}_{qg}$ Green function. Some of the details of the derivation are given in appendix B.5; here, we limit ourselves to reporting the results (see sect. 3.1 for the normalisation of the various quantities involved), which read

$$\begin{aligned} \hat{\mathcal{G}}_{qg}(\epsilon \rightarrow 0) = \varphi_0(\Omega(\gamma_s)) + \varphi_1(\gamma_s) \exp & \left[\frac{1}{2} \int_0^1 dy \frac{\gamma_s (\chi_1(y\gamma_s) - \chi'(y\gamma_s))}{\chi(y\gamma_s)} + \gamma_s \psi_0(1) \right. \\ & - \frac{1}{2} \log \Gamma(1 + \gamma_s) + \frac{1}{2} \log \Gamma(1 - \gamma_s) \\ & \left. - \frac{1}{2} \log (\gamma_s \chi(\gamma_s)) - \frac{1}{2} \log (-\gamma_s^2 \chi'(\gamma_s)) \right], \quad (5.1) \end{aligned}$$

³²The analytical inverse Mellin transform of the asymptotic $\xi \rightarrow 1$ form of the weighted exponential of the function $\Omega(s)$ of eq. (B.16) is a case of a resummation with $L = \log(1 - \xi)$ where the coefficients of a logarithmically ordered expansion behave quadratically (as in eq. (4.8)). In spite of having figured out such a behaviour, a double resummation was still not possible, since the coefficients feature several contributions (as opposed to one in the example above) whose number grows with the order, and of which only the first few follow a clear pattern (e.g. the leading ones which, as was just said, behave quadratically).

³³In the context of the simple model discussed here, such a strategy would amount to replacing a with $a + a^2$ in the case of the coefficients of eq. (4.8), and L with $L + 1$ in the case of those of eq. (4.7). The fact that these replacements allow one to recover *exactly* the doubly-resummed quantities of eqs. (4.13) and (4.14), respectively, is due to the simplicity of the model.

with $\chi'(z) = d\chi/dz$, $\gamma_s = \gamma_s(\alpha_N)$ and

$$\varphi_0(z) = -\frac{1}{4} \left(3e^{2z} + e^{\frac{2}{3}z} \right), \quad (5.2)$$

$$\varphi_1(z) = \frac{1}{4} \left[\frac{3}{1-z} + \frac{12}{2-z} - \frac{15}{3-z} \right], \quad (5.3)$$

and where the function χ_1 is defined as follows

$$\chi_1(z) = 2\psi_1(1) - \psi_1(z) - \psi_1(1-z). \quad (5.4)$$

As it is also shown in appendix B.5, this result gives us the possibility of determining a relationship between the finite \mathcal{G}_{qg} and \mathcal{G}_{gg} Green functions. Specifically (see appendix B.5)

$$\hat{\mathcal{G}}_{qg}(\epsilon \rightarrow 0) = \varphi_0(\Omega(\gamma_s)) + \varphi_1(\gamma_s) \frac{\mathcal{G}_{gg}(\epsilon \rightarrow 0)}{\gamma_s \chi(\gamma_s)}. \quad (5.5)$$

Furthermore, from eqs. (3.24), (5.2), (2.13) and (2.7) we obtain:

$$\varphi_0(\Omega(\gamma_s)) = -\frac{h_{qg}(\gamma_s)}{\gamma_s \chi(\gamma_s)} \equiv -\frac{\hat{\gamma}_{qg}}{\gamma_s}. \quad (5.6)$$

Therefore, eq. (5.5) becomes

$$\gamma_s \hat{\mathcal{G}}_{qg}(\epsilon \rightarrow 0) = -\hat{\gamma}_{qg} + \alpha_N \varphi_1(\gamma_s) \mathcal{G}_{gg}(\epsilon \rightarrow 0), \quad (5.7)$$

which gives a direct relationship between the two renormalised Green functions which only involves ϵ -finite contributions. We can also observe what follows: with eqs. (3.6)-(3.8), the derivation of the master equation (3.5) w.r.t. α_N gives

$$\frac{d\hat{\mathcal{G}}_{qg}^{(0)}}{d\alpha_N} = \frac{\gamma_s}{\epsilon\alpha_N} \Gamma_{gg} \hat{\mathcal{G}}_{qg} + \Gamma_{gg} \frac{d\hat{\mathcal{G}}_{qg}}{d\alpha_N} + \frac{\hat{\gamma}_{qg}}{\epsilon\alpha_N} \Gamma_{gg}, \quad (5.8)$$

whence, since \mathcal{G}_{qg} is finite,

$$\gamma_s \hat{\mathcal{G}}_{qg}(\epsilon \rightarrow 0) = -\hat{\gamma}_{qg} + \alpha_N \lim_{\epsilon \rightarrow 0} \left(\frac{\epsilon}{\Gamma_{gg}} \frac{d\hat{\mathcal{G}}_{qg}^{(0)}}{d\alpha_N} \right). \quad (5.9)$$

By equating side-by-side this equation with eq. (5.7) we obtain

$$\lim_{\epsilon \rightarrow 0} \left(\frac{\epsilon}{\Gamma_{gg}} \frac{d\hat{\mathcal{G}}_{qg}^{(0)}}{d\alpha_N} \right) = \varphi_1(\gamma_s) \mathcal{G}_{gg}(\epsilon \rightarrow 0). \quad (5.10)$$

This is an identity whose correctness can be verified perturbatively, by using the explicit results given elsewhere for the quantities that appear in it.

The coefficients of the expansions of the finite Green functions in terms of γ_s can be obtained in a closed form. By defining such coefficients as follows

$$\mathcal{G}_{gg}(\epsilon \rightarrow 0) = \sum_{n=0}^{\infty} r_n \gamma_s^n, \quad (5.11)$$

$$\hat{\mathcal{G}}_{qg}(\epsilon \rightarrow 0) = \sum_{n=0}^{\infty} s_n \gamma_s^n, \quad (5.12)$$

they can be written in term of the complete exponential Bell polynomials,

$$r_n = \frac{1}{n!} B_n \left(\hat{Z}_- \right), \quad (5.13)$$

$$s_n = \frac{1}{n!} B_n \left(\widehat{Z}_+ + \widehat{Z}_R \right) - \frac{1}{n!} \left[\frac{3}{4} B_n \left(\widehat{Z}'_2 \right) + \frac{1}{4} B_n \left(\widehat{Z}'_{\frac{3}{2}} \right) \right]. \quad (5.14)$$

The arguments of the Bell polynomials are given in eq. (3.38) and as follows

$$\widehat{Z}_\pm = \left(0, 0, \left\{ \widehat{Z}_\pm^{[i]} \right\}_{i=3}^\infty \right), \quad (5.15)$$

$$\widehat{Z}_R = \left(\left\{ \frac{(i-1)!}{12^i} (4^i + 6^i - 9^i + 12^i) \right\}_{i=1}^\infty \right), \quad (5.16)$$

$$\begin{aligned} \widehat{Z}_\pm^{[i]} &= -\frac{1}{2} (1 + (-)^{i+1}) \psi_{i-1}(1) + \frac{1}{2} \sum_{j=1}^i (-)^j (j-1)! \left(\pm B_{i,j}(V_1) + B_{i,j}(V_2) \right) \\ &+ \frac{1}{i} \sum_{k=0}^{i-3} \binom{i}{k} (-)^{i-k+1} (i-k-1)(i-k) \psi_{i-k-1}(1) \left(\sum_{j=0}^k (-)^j j! B_{k,j}(V_1) \right), \end{aligned} \quad (5.17)$$

where in turn

$$V_1 = \left(0, \left\{ - (1 - (-)^k) k \psi_{k-1}(1) \right\}_{k=2}^\infty \right), \quad (5.18)$$

$$V_2 = \left(\left\{ (1 - (-)^k) k(k-1) \psi_{k-1}(1) \right\}_{k=1}^\infty \right). \quad (5.19)$$

The numerical values of the first coefficients in eq. (5.11) are

$$r_0 = 1, \quad (5.20a)$$

$$r_1 = 0, \quad (5.20b)$$

$$r_2 = 0, \quad (5.20c)$$

$$r_3 = \frac{8}{3} \zeta_3, \quad (5.20d)$$

$$r_4 = -\frac{3}{4} \zeta_4, \quad (5.20e)$$

$$r_5 = \frac{22}{5} \zeta_5, \quad (5.20f)$$

$$r_6 = \frac{65}{9} \zeta_3^2 - \frac{5}{6} \zeta_6, \quad (5.20g)$$

while the first coefficients of eq. (5.12) are

$$s_0 = 0, \quad (5.21a)$$

$$s_1 = -\frac{7}{12}, \quad (5.21b)$$

$$s_2 = -\frac{41}{72}, \quad (5.21c)$$

$$s_3 = -\frac{157}{1296} + \frac{2}{3} \zeta_3, \quad (5.21d)$$

$$s_4 = \frac{2537}{7776} + \frac{29}{9} \zeta_3 - \frac{3}{4} \zeta_4, \quad (5.21e)$$

$$s_5 = \frac{27595}{46656} + \frac{575}{108} \zeta_3 - \frac{13}{16} \zeta_4 + \frac{12}{5} \zeta_5, \quad (5.21f)$$

$$s_6 = \frac{2960431}{4199040} + \frac{3337}{648} \zeta_3 + \frac{53}{9} \zeta_3^2 - \frac{71}{96} \zeta_4 + \frac{242}{45} \zeta_5 - \frac{5}{6} \zeta_6. \quad (5.21g)$$

These expressions allow one to obtain their analogues in the case of an expansions in α_N , as is explained in eqs. (B.66) and (B.67). We also observe that eq. (5.14) closely mirrors eq. (5.5). More

in details, \widehat{Z}_- (which gives rise to \mathcal{G}_{gg}) is turned into \widehat{Z}_+ by the factor $1/(\gamma_s \chi(\gamma_s))$, while the rational part $\varphi_1(\gamma_s)$ corresponds to \widehat{Z}_R . Finally, the additive piece $\varphi_0(\Omega)$ of eq. (5.5) results in the two terms in square brackets in eq. (5.14), as one expects from eqs. (3.33) and (3.37).

A tribute to ref. [62]

In appendix C of ref. [62], eq. (C.13) gives the rational part of the coefficients of the expansion of γ_{gg} ; it is easy to verify that these are what one obtains by expanding in x the function $\varphi_0(x)$ defined in eq. (5.2) — see eq. (5.6) for the relationship between φ_0 and γ_{gg} , and bear in mind that, by ignoring Riemann ζ 's, $\gamma_s = \alpha_N$. After presenting that result, ref. [62] proceeds to saying, verbatim: “The derivation of the result (C.13) is left as an exercise for the reader”. We therefore find it appropriate, after 30-plus years, to ask the reader to show that the all-order (in ϵ) rational part of the finite gg Green function reads as follows:

$$\begin{aligned} \mathcal{G}_{gg}(z) \Big|_{\substack{\zeta_k \rightarrow 0 \\ \pi^{2k} \rightarrow 0}} &= -\frac{3e^{2z}}{4(1+2\epsilon)} - \frac{3e^{2/3z}}{4(3+2\epsilon)} - \frac{z^2}{4} \\ &+ \frac{3}{4} \left\{ (1+2z+2z^2) \sum_{n=0}^{\infty} (-2\epsilon)^n \right. \\ &\quad \left. + z^3 \sum_{n=0}^{\infty} \epsilon^n \left[\frac{P_n(z)}{(1-z)^{2n+1}} + 2 \sum_{i=1}^n (-2)^i \frac{P_{n-i}(z)}{(1-z)^{2(n-i)+1}} \right] \right\} \\ &+ \frac{3}{8} \left\{ -z(2+z) \sum_{n=0}^{\infty} \left(-\frac{\epsilon}{2}\right)^n \right. \\ &\quad \left. + z^3 \sum_{n=0}^{\infty} (2\epsilon)^n \left[\frac{P_n(z/2)}{(2-z)^{2n+1}} - \sum_{i=1}^n \frac{(-)^i}{2^{2i}} \frac{P_{n-i}(z/2)}{(2-z)^{2(n-i)+1}} \right] \right\} \\ &+ \frac{9+6z+2z^2}{36} \sum_{n=0}^{\infty} \left(-\frac{2\epsilon}{3}\right)^n + \frac{3z+z^2}{18} \sum_{n=0}^{\infty} \left(-\frac{\epsilon}{3}\right)^n \\ &\quad - \frac{5z^3}{36} \sum_{n=0}^{\infty} (3\epsilon)^n \left[\frac{P_n(z/3)}{(3-z)^{2n+1}} - \frac{2}{5} \sum_{i=1}^n \frac{(-)^i (1+2^i)}{3^{2i}} \frac{P_{n-i}(z/3)}{(3-z)^{2(n-i)+1}} \right], \end{aligned} \quad (5.22)$$

with $P_n(z)$ the Eulerian polynomials of the second order. Equation (5.22) is organised, with the exception of the first two terms on its r.h.s., in terms of explicit powers of ϵ . This may or may not be convenient in view of further manipulations. In the case it were not, eq. (5.22) can be rewritten as follows

$$\begin{aligned} \mathcal{G}_{gg}(z) \Big|_{\substack{\zeta_k \rightarrow 0 \\ \pi^{2k} \rightarrow 0}} &= -\frac{3e^{2z}}{4(1+2\epsilon)} - \frac{3e^{2/3z}}{4(3+2\epsilon)} \\ &+ \frac{3}{4} \frac{1-2\epsilon}{1+2\epsilon} \left\{ 1 + \epsilon + z - z^2 \frac{e^{-z/\epsilon}}{\epsilon} \left(-\frac{z}{\epsilon}\right)^{1/\epsilon} \left[\Gamma\left(-\frac{1}{\epsilon}\right) - \Gamma\left(-\frac{1}{\epsilon}, -\frac{z}{\epsilon}\right) \right] \right\} \\ &+ \frac{3}{2} \frac{1+\epsilon}{2+\epsilon} \left\{ 2 + \epsilon + z - z^2 \frac{e^{-z/\epsilon}}{\epsilon} \left(-\frac{z}{\epsilon}\right)^{2/\epsilon} \left[\Gamma\left(-\frac{2}{\epsilon}\right) - \Gamma\left(-\frac{2}{\epsilon}, -\frac{z}{\epsilon}\right) \right] \right\} \\ &- \frac{3}{4} \frac{(1+\epsilon)(5+2\epsilon)}{(3+\epsilon)(3+2\epsilon)} \left\{ 3 + \epsilon + z - z^2 \frac{e^{-z/\epsilon}}{\epsilon} \left(-\frac{z}{\epsilon}\right)^{3/\epsilon} \left[\Gamma\left(-\frac{3}{\epsilon}\right) - \Gamma\left(-\frac{3}{\epsilon}, -\frac{z}{\epsilon}\right) \right] \right\}, \end{aligned} \quad (5.23)$$

in terms of the ordinary Γ function and of its upper incomplete counterpart. Among other things, the equality between eqs. (5.22) and (5.23) is established by means of the identity

$$1 + z \sum_{n=0}^{\infty} t^n \frac{P_n(z)}{(1-z)^{2n+1}} = -\frac{e^{-z/t}}{t} \left(-\frac{z}{t}\right)^{1/t} \left[\Gamma\left(-\frac{1}{t}\right) - \Gamma\left(-\frac{1}{t}, -\frac{z}{t}\right) \right]. \quad (5.24)$$

6 Conclusions

Driven by the original motivation of extending the numerical results of small- x resummation to cases characterised by α_s values of order one, which is necessary in the context of lepton-PDF evolution that also accounts for coloured partons, we have reconsidered the theoretical bases of such resummation, and their use in the computer code [HELL](#).

While doing so, we have found a number of analytical results previously unknown in the literature, that not only help extend the standard small- x treatments to large- α_s cases, but also significantly improve the very basic ingredients of such treatments, thus including those relevant to purely hadronic environments.

In this paper we have therefore focussed on two technical aspects of our work, namely the derivation and presentation of the new analytical results we have obtained, and the novel implementation strategies that they have fostered, which have become the defaults in the new 4.0 version of [HELL](#) and which will be used for hadronic and leptonic PDFs alike; phenomenological applications stemming from these improvements will be presented in forthcoming papers.

Specifically, as far as new analytical results are concerned, we have started with finding several all-order expressions for γ_s , the leading-logarithmic divergent eigenvalue of the singlet anomalous-dimension matrix. Although none of these is in a closed, explicit, non-integral form given in terms of elementary functions, the various expressions we have found offer complementary ways to study the impact of γ_s onto other quantities that employ it as an ingredient. The upshot of this is that, in general, such quantities assume relatively simple forms if expressed in terms of γ_s rather than of α_s ; in other words, γ_s is an inherently complicated object, which helps capture (most of) the complexity of the quantities it enters.

We have then managed to obtain a closed, all-order expression for the qg anomalous dimensions, and closed forms for all of its coefficients relevant to perturbative series in different expansion parameters. Because of this, we have further been able to obtain the first properly resummed expression of the P_{qg} splitting kernel — what had been available up to present was an expression stemming from a Borel-Padé approximation. The difference between the exactly- and the Borel-Padé-resummed results for P_{qg} are seemingly small if one compares the upcoming and previous versions of [HELL](#) which implement them, respectively, but this conclusion is extremely misleading. In fact, we have shown how the Borel-Padé-resummed P_{qg} depends very strongly on the integration path employed to compute the inverse Mellin transform which underpins it — the previous implementation has simply fine-tuned the choice of such a path in order to achieve maximum stability. Conversely, the exactly-resummed splitting kernel is very stable upon path deformation. While studying the numerical consequences of the availability of the latter splitting kernel, we have also taken the opportunity to address some criticalities of the approximations which were present in the [HELL](#) implementation; we propose a new approach which stems from a slightly different definition of $\gamma_+^{\text{NLL}'}$, and which is seen to behave in a more stable manner especially w.r.t. to changes in the value of α_s .

As a final by-product of the analytical work on γ_s and γ_{qg} summarised above we have succeeded in determining the finite $\mathcal{O}(\epsilon^0)$ qg Green function to all orders in γ_s , as well as its relationship with the all-order $\mathcal{O}(\epsilon^0)$ gg Green function. While these results have no immediate consequences and serve no purpose in the upcoming [HELL](#) implementation, they help elucidate the involved $\overline{\text{MS}}$ structure emerging from small- x dynamics, and may pave the way for future improved treatments of contributions beyond leading logarithmic accuracy.

Acknowledgments

We are grateful to Fabio Maltoni, Simone Marzani and Pier Monni for several discussions during

the course of this work. The work of MB is supported by the Italian Ministry of University and Research (MUR) grant PRIN 2022SNA23K funded by the European Union – Next Generation EU, Mission 4, Component 2, CUP I53D23001410006. GS acknowledges financial support from the EU Horizon Europe research and innovation programme under the Marie-Sklódowska Curie Action HIPFLAPP, grant agreement No. 101149076.

A New analytical all-order results for γ_s

For the algebraic manipulations carried out in this appendix, we consider eq. (2.7) expressed in term of a generic complex number a , i.e. we study the function $\gamma_s(a)$ defined as the solution of the equation

$$1 = a \chi(\gamma_s(a)). \quad (\text{A.1})$$

in the complex plane. The physical case corresponds to setting $a = \alpha_N$.

A.1 Perturbative coefficients

In the context of a perturbative approach, eq. (A.1) must be solved for γ_s order by order in a . We employ the ansatz

$$\gamma_s(a) = \sum_{j=0}^{\infty} g_j a^{j+1} = a(1 + \hat{\gamma}_s(a)), \quad g_0 = 1, \quad (\text{A.2})$$

$$\hat{\gamma}_s(a) = \sum_{j=1}^{\infty} g_j a^j, \quad (\text{A.3})$$

and introduce the auxiliary quantities

$$\chi_k = 2\zeta_{k+1} \delta_{\text{mod}(k,2),0}, \quad (\text{A.4})$$

$$f_{-1}(z) = \frac{1}{z}, \quad (\text{A.5})$$

$$f_{\Sigma}(z) = 2\psi_0(1) - \psi_0(1+z) - \psi_0(1-z) \equiv \sum_{k=1}^{\infty} 2\zeta_{2k+1} z^{2k}, \quad (\text{A.6})$$

whence

$$\chi(z) = f_{-1}(z) + f_{\Sigma}(z), \quad (\text{A.7})$$

so that eq. (A.1) becomes

$$1 = f_{-1}(1 + \hat{\gamma}_s(a)) + a f_{\Sigma}(\gamma_s(a)). \quad (\text{A.8})$$

We now expand in series of a the r.h.s. of this equation, by exploiting the Faà di Bruno formula for the composite derivatives of single-variable functions, and obtain the identity,

$$1 = 1 + \sum_{p=1}^{\infty} a^p \left\{ \frac{1}{p!} \sum_{i=1}^p (-)^i \Gamma(i+1) B_{p,i}(G) + \frac{\Theta(p \geq 2)}{(p-1)!} \sum_{i=1}^{p-1} \chi_i \Gamma(i+1) B_{p-1,i}(\hat{G}) \right\}, \quad (\text{A.9})$$

where by $B_{n,k}$ we have denoted the incomplete exponential Bell polynomials, to be computed with the following arguments:

$$G = (0, 0, g_3 3!, \dots, g_n n!, \dots). \quad (\text{A.10})$$

$$\hat{G} = (g_0 1!, g_1 2!, \dots, g_n (n+1)!, \dots) \quad (\text{A.11})$$

$$= (1, 0, 0, g_3 4!, \dots, g_n (n+1)!, \dots). \quad (\text{A.12})$$

Equation (A.9) is solved by the following coefficients:

$$g_p = \sum_{i=1}^p \frac{1}{(p-i+1)!} B_{p,i}(Z), \quad (\text{A.13})$$

where

$$Z = (0, 0, 2\zeta_3 3!, 0, 2\zeta_5 5!, 0, \dots, 2\zeta_{2n+1} (2n+1)!, \dots) \quad (\text{A.14})$$

$$= \left(\left\{ \left. \frac{d^k \hat{\chi}(z)}{dz^k} \right|_{z=0} \right\}_{k=1}^{\infty} \right). \quad (\text{A.15})$$

In eq. (A.15) we have introduced the function

$$\hat{\chi}(z) \equiv z f_{\Sigma}(z) = -z \left[\psi_0(1+z) + \psi_0(1-z) + 2\gamma_{\mathbb{E}} \right], \quad (\text{A.16})$$

which is ubiquitous in our approach, and which is such that

$$1 + \hat{\chi}(z) = z\chi(z). \quad (\text{A.17})$$

The sought perturbative result for $\gamma_s(a)$ is given by eqs. (A.2), (A.3), and (A.13), and reads

$$\gamma_s(a) = a \left(1 + \sum_{k=1}^{\infty} \sum_{i=1}^k \frac{a^k}{(k-i+1)!} B_{k,i}(Z) \right). \quad (\text{A.18})$$

We are unable to find an explicit closed-form, non-integral expression for the series which appears in eq. (A.18) and, for the reasons explained later (see in particular appendix A.3), we doubt that such a form exists. Conversely, after some long and tedious manipulations, we have found an *implicit* closed-form, non-integral expression for γ_s , which reads

$$\log \frac{\gamma_s(a)}{a} = -\log(2a\psi_{0+}(a)) - \frac{2a\psi_{0+}(a)}{2a\psi_{0+}(a) - \delta} \log \left[\frac{1}{\delta} + R \left(\frac{2a\psi_{0+}(a)(1+2a\psi_{0+}(a))}{2a\psi_{0+}(a) - \delta} \right) \right] \Big|^{[\delta^0]}, \quad (\text{A.19})$$

where

$$\psi_{k+}(z) = \frac{1}{2} \left(\psi_k(1+z) + \psi_k(1-z) \right) - \psi_k(1) \Theta(k \leq 1), \quad (\text{A.20})$$

$$\psi_{k-}(z) = \frac{1}{2} \left(\psi_k(1+z) - \psi_k(1-z) \right), \quad (\text{A.21})$$

and

$$R(z) = \frac{\psi_{0+} \left(a - \frac{az}{1+2a\psi_{0+}(a)} \right)}{\psi_{0+}(a)}. \quad (\text{A.22})$$

The notation $[\delta^0]$ in eq. (A.19) implies that only the $\mathcal{O}(\delta^0)$ contribution of the expression preceding it must be kept, which is what prevents one from obtaining an explicit result for γ_s . Perturbatively in a , eqs. (A.18) and (A.19) are fully equivalent, but the structure of the series expansion of the latter is peculiar; we shall return to this point in appendix A.3.

Before moving to the study of the analytical properties of $\gamma_s(a)$, we note that it is also possible to write a as a function of $\gamma_s = \gamma_s(a)$. By means of the vector introduced in eq. (A.14) and owing to eq. (A.15), we have that

$$\log(1 + \hat{\chi}(z)) = \sum_{k=1}^{\infty} \frac{z^k}{k!} \sum_{j=1}^k (-)^{j+1} (j-1)! B_{k,j}(Z), \quad (\text{A.23})$$

whence

$$a^m = (\chi(\gamma_s))^{-m} = \left(\frac{\gamma_s}{1 + \hat{\chi}(\gamma_s)} \right)^m \quad (\text{A.24})$$

$$= \gamma_s^m \left[1 + \sum_{k=1}^{\infty} \frac{\gamma_s^k}{k!} \sum_{j=1}^k \frac{d^j}{dz^j} \frac{1}{(1+z)^m} \Big|_{z=0} B_{k,j}(Z) \right] \quad (\text{A.25})$$

$$= \gamma_s^m \left[1 + \sum_{k=1}^{\infty} \frac{\gamma_s^k}{k!} A_k^{(m)} \right], \quad (\text{A.26})$$

where we have defined:

$$A_k^{(m)} = \sum_{j=1}^k \frac{(-)^j (m-1+j)!}{(m-1)!} B_{k,j}(Z). \quad (\text{A.27})$$

Eqs. (A.26)–(A.27) can be conveniently used to turn a series in a into a series in $\gamma_s = \gamma_s(a)$.

A.2 Integral representations

In order to study the analytical properties of $\gamma_s(a)$ one possibility, lacking a closed-form expression for its perturbative series of eq. (A.18), is that of employing an integral representation. This, we obtain as follows³⁴.

Firstly, we use a Hankel-path representation of the reciprocal of the Γ function,

$$\frac{1}{(n-1-j)!} = \frac{1}{\Gamma(n-j)} = \mp \frac{i}{2\pi} \int_{H^\pm} d\omega e^{\pm\omega} (\pm\omega)^{-n+j}. \quad (\text{A.28})$$

The path H^- (H^+) is counterclockwise (clockwise), starts and ends at $(+\infty \pm i\epsilon)$ ($(-\infty \mp i\epsilon)$), and crosses the real axis at some negative (positive) value. The representation is valid for any integer, real, and complex argument, and the paths can be freely deformed, provided the branch cut of the integrand is not crossed. With eq. (A.28), eq. (A.18) leads to

$$\hat{\gamma}_s(a) = \mp \frac{i}{2\pi} \int_{H^\pm} \frac{d\omega}{(\pm\omega)^2} e^{\pm\omega} \sum_{k=1}^{\infty} \sum_{i=1}^k \left(\frac{a}{\pm\omega} \right)^k (\pm\omega)^i B_{k,i}(Z). \quad (\text{A.29})$$

Next, one Borel-transforms the series whose summation index is k , and thus obtains an integrand whose structure is that of the l.h.s. of the following equation³⁵

$$\exp \left(u \sum_{j=1}^{\infty} x_j \frac{t^j}{j!} \right) = \sum_{n=0}^{\infty} \sum_{k=0}^n B_{n,k}(x_1, \dots, x_n) \frac{t^n}{n!} u^k, \quad (\text{A.30})$$

namely of the generating function of the incomplete exponential Bell polynomials. This allows one to resum the series, and to obtain the exponent on the r.h.s. of eq. (A.30). In turn, the series which appears there is easily resummed since, thanks to eq. (A.15), it is nothing but the series expansion of the function $\hat{\chi}(x)$ at $x=0$ (see eq. (A.16)). Therefore, one ends up with

$$\hat{\gamma}_s(a) = \mp \frac{i}{2\pi} \int_0^\infty dt e^{-t} \int_{H^\pm} \frac{d\omega}{(\pm\omega)^2} e^{\pm\omega} \left\{ \exp \left[\pm\omega \hat{\chi} \left(\frac{at}{\pm\omega} \right) \right] - 1 \right\}. \quad (\text{A.31})$$

³⁴Since the two are trivially related to one another by eq. (A.2), we often deal with $\hat{\gamma}_s$ rather than with γ_s .

³⁵Bar the $k=0$ term, which is absent, and which will be thus subtracted by hand. This is straightforward, since such a term is equal to one ($B_{0,i} = \delta_{i0}$).

In an analogous way, with a procedure that we refrain from reporting here owing to its being fairly technical but without any insights physics-wise, we obtain the following, equivalent, form:

$$\hat{\gamma}_s(a) = \mp \frac{i}{2\pi} \hat{\chi}(a) \int_0^\infty dt e^{-t} \int_{H^\pm} \frac{d\omega}{(\pm\omega)^2} e^{\pm\omega} \exp \left[\frac{\pm\omega}{\hat{\chi}(a)} \left(\hat{\chi} \left(\frac{at}{\pm\omega} \hat{\chi}(a) + a \right) - \hat{\chi}(a) \right) \right]. \quad (\text{A.32})$$

The integral representations of eqs. (A.31) and (A.32) are unusual, in that they feature both a Borel and a Hankel integral. Conceptually, this is not problematic, but it may result in numerical instabilities. It is therefore interesting to further manipulate those results analytically.

Firstly, one notes that eqs. (A.31) and (A.32) have in fact the same functional form. This can be made explicit by observing that

$$\mp \frac{i}{2\pi} \int_0^\infty dt e^{-t} \int_{H^\pm} \frac{d\omega}{(\pm\omega)^2} e^{\pm\omega} = 1. \quad (\text{A.33})$$

Thus, by adding and subtracting $\hat{\chi}(a)$, and by exploiting eq. (A.33) to move the $-\hat{\chi}(a)$ contribution under the integral sign, eq. (A.32) becomes

$$\hat{\gamma}_s(a) = \hat{\chi}(a) \left\{ 1 \mp \frac{i}{2\pi} \int_0^\infty dt e^{-t} \int_{H^\pm} \frac{d\omega}{(\pm\omega)^2} e^{\pm\omega} \left(\exp \left[\frac{\pm\omega}{\hat{\chi}(a)} \left(\hat{\chi} \left(\frac{at}{\pm\omega} \hat{\chi}(a) + a \right) - \hat{\chi}(a) \right) \right] - 1 \right) \right\}, \quad (\text{A.34})$$

whereby the similarity with eq. (A.31) is manifest, with the identification

$$\hat{\chi} \left(\frac{a}{\pm\hat{\omega}} \right) \longleftrightarrow \tilde{G} \left(\frac{a}{\pm\hat{\omega}} \right) \equiv \frac{1}{\hat{\chi}(a)} \hat{\chi} \left(\frac{a}{\pm\hat{\omega}} \hat{\chi}(a) + a \right) - 1. \quad (\text{A.35})$$

By means of the change of variable

$$\omega = t \hat{\omega} \quad (\text{A.36})$$

which preserves the Hankel path for any given $t > 0$, eq. (A.31) reads

$$\hat{\gamma}_s(a) = \mp \frac{i}{2\pi} \int_{H^\pm} \frac{d\hat{\omega}}{(\pm\hat{\omega})^2} I_B \left(\mp\hat{\omega} \mp \hat{\omega} \hat{\chi} \left(\frac{a}{\pm\hat{\omega}} \right), \mp\hat{\omega} \right) \quad (\text{A.37})$$

with

$$I_B(\alpha, \beta) = \int_0^\infty \frac{dt}{t} e^{-t} (e^{-\alpha t} - e^{-\beta t}), \quad (\text{A.38})$$

while eq. (A.34) becomes (see eq. (A.35))

$$\hat{\gamma}_s(a) = \hat{\chi}(a) \left\{ 1 \mp \frac{i}{2\pi} \int_{H^\pm} \frac{d\hat{\omega}}{(\pm\hat{\omega})^2} I_B \left(\mp\hat{\omega} \mp \hat{\omega} \tilde{G} \left(\frac{a}{\pm\hat{\omega}} \right), \mp\hat{\omega} \right) \right\}. \quad (\text{A.39})$$

With an explicit computation we obtain

$$I_B(\alpha, \beta) = \log \frac{1 + \beta}{1 + \alpha}, \quad \text{Re}(\alpha) > -1, \quad \text{Re}(\beta) > -1. \quad (\text{A.40})$$

While the constraints on α and β in eq. (A.40) are essential for the Borel integral to converge, the result is analytical, and can therefore be employed with any values of α and β . We shall therefore ignore those constraints in what follows, but observe that we could not have done that if the Borel integral were computed only numerically — this is not irrelevant, since such constraints are easily violated when increasing the value of a .

In order to proceed in a definite way, let's start with eq. (A.37), and choose the lower signs there. Explicitly,

$$\hat{\gamma}_s(a) = \frac{i}{2\pi} \int_{H^-} \frac{d\hat{\omega}}{\hat{\omega}^2} \log \frac{1 + \hat{\omega}}{1 + \hat{\omega} + \hat{\omega} \hat{\chi}(-a/\hat{\omega})}. \quad (\text{A.41})$$

We now have to bear in mind that the original reason for introducing an Hankel integral was to represent the reciprocal of a factorial (specifically, that in eq. (A.18)). Therefore, the original Hankel path could be chosen arbitrarily close to the real positive axis³⁶, in view of the fact that each summand of the series that leads to $\hat{\gamma}_s(a)$ has a pole at the origin³⁷. When the series is (partly) summed, and one ends up with eq. (A.41), (most of) the poles move away from the origin. However, by assuming the series to be uniformly convergent, they basically do so in a continuous way with a , and one can therefore continuously deform the original Hankel path to keep enclosing those poles. We point out that there may be poles which do not fulfill this condition — in other words, poles that when $a \rightarrow 0$ do not move continuously towards the origin. One example is given by the $\omega = -1$ pole which stems from the numerator of the logarithm in eq. (A.41). This makes sense, since ultimately such a pole is associated with the -1 subtraction term in eqs. (A.31) and (A.34), which is always present, and is independent of the value of a . The bottom line is that, in situations analogous to the present one (where the Hankel integral is associated with the reciprocal of factorials in a well-behaved power series), we can formulate the following ansatz:

- The Hankel path must enclose all of the poles of the integrand which tend continuously to the origin with decreasing values of the expansion parameter of the series. This demands that all branch cuts to which those poles belong be enclosed too, regardless of whether they also feature other poles that do *not* fulfill the previous condition.

We note that there may be situations in which the path defined above cannot be found; in such cases, the integral representation loses validity. For the case at hand, we find that by following the prescription given above the integrals are numerically very stable with an excellent convergent speed. As an example, in the left panel of fig. 8 we show as a dashed line the Hankel path that we have employed with $a = 0.35$ — the crosses, circles, and boxes are singularities of the integrand, and the solid lines are branch cuts. Conversely, in the right panel of the same figure we present the results obtained with eq. (A.41) as solid red circles. These are superimposed over the values of $\hat{\gamma}_s(a)$ (black line), obtained by inverting numerically eq. (A.1) (or, which is equivalent in this range of a , by truncating the series of eq. (A.18) to its first sixty terms); as one can see, we find an excellent agreement.

While it does work in general, the integration-path prescription that has led to the results shown in fig. 8 strictly depends on the integrand: the simpler the latter, the more straightforward the procedure. Therefore, it is convenient to push analytical simplifications as far as one can. In the present case, an obvious simplification stems from rewriting eq. (A.41) as

$$\hat{\gamma}_s(a) = \frac{i}{2\pi} \int_{H^-} \frac{d\hat{\omega}}{\hat{\omega}^2} \log(1 + \hat{\omega}) - \frac{i}{2\pi} \int_{H^-} \frac{d\hat{\omega}}{\hat{\omega}^2} \log\left(1 + \hat{\omega} + \hat{\omega}\hat{\chi}(-a/\hat{\omega})\right). \quad (\text{A.42})$$

By choosing for the leftmost integral a contour around the origin that leaves out the $(-1, 0)$ singularity and the branch cut at $\hat{\omega} < -1$ (which is in keeping with our prescription), one obtains

$$\frac{i}{2\pi} \int_{H^-} \frac{d\hat{\omega}}{\hat{\omega}^2} \log(1 + \hat{\omega}) = -1, \quad (\text{A.43})$$

whence, by employing eq. (A.2), one arrives at

$$\gamma_s(a) = -a \frac{i}{2\pi} \int_{H^-} \frac{d\hat{\omega}}{\hat{\omega}^2} \log\left(1 + \hat{\omega} + \hat{\omega}\hat{\chi}(-a/\hat{\omega})\right). \quad (\text{A.44})$$

³⁶As an aside, one also observes that since one deals with the reciprocal of Γ functions with integer arguments, the Hankel path can in fact be replaced by a closed path (counterclockwise, in the case of H^-) around the origin, and again arbitrarily close to it.

³⁷And a cut along the positive real axis for non-integer Γ -function arguments, which is not the case here.

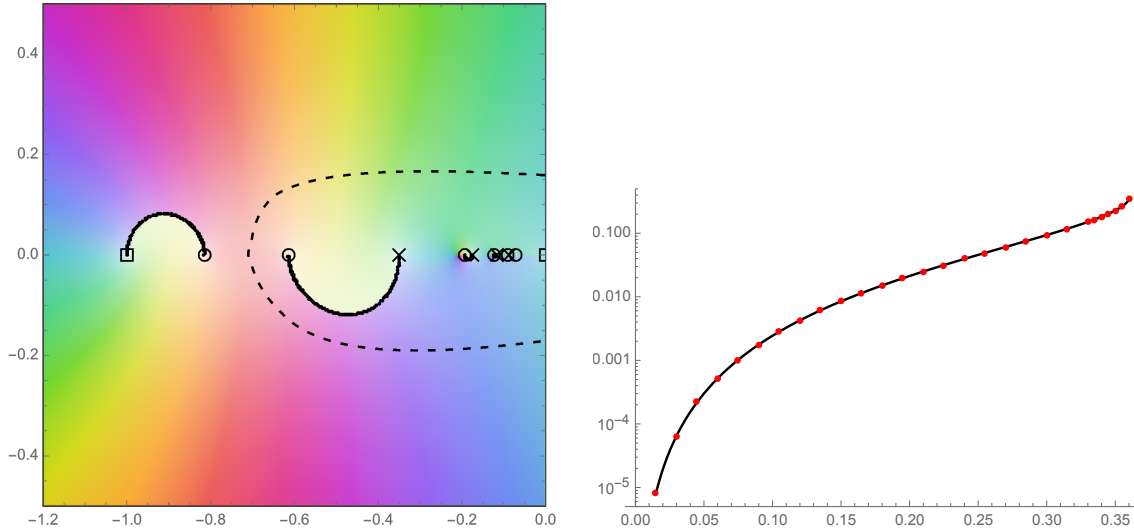


Figure 8. Integrand of eq. (A.41) with $a = 0.35$ (left-hand panel), and the result for $\hat{\gamma}_s(a)$ (right-hand panel). See the text for details.

Equation (A.44) can be expressed in two alternative ways which may be more convenient for numerical evaluations and/or for the study of its analytical behaviour. With a change of variable, and by exploiting the identity in eq. (A.17) we obtain:

$$\gamma_s(a) = -\frac{i}{2\pi} \int_{H^-} \frac{dz}{z^2} \log\left(1 + az + az \hat{\chi}(-1/z)\right) \quad (\text{A.45})$$

$$= -\frac{i}{2\pi} \int_{H^-} \frac{dz}{z^2} \log\left(1 - a \chi(-1/z)\right). \quad (\text{A.46})$$

In this way, having succeeded in rendering the functions $\hat{\chi}$ and χ independent of a , one can then easily compute the integral which is relevant to the definition of Ω , eq. (3.8). Explicitly,

$$\Omega(\gamma_s(\bar{a})) = \int_0^{\bar{a}} \frac{da}{a} \gamma_s(a) = \frac{i}{2\pi} \int_{H^-} \frac{dz}{z^2} \text{Li}_2(\bar{a} \chi(-1/z)). \quad (\text{A.47})$$

In conclusion, we remind the reader what we have observed at the beginning of this section, namely that the two representations given by eqs. (A.31) and (A.32) are functionally identical. Therefore, the manipulations carried out here starting from the former equation can also be applied to the latter one. We have indeed done so, as a further check of the mutual consistency of our results. One interesting aspect of this is presented in fig. 9. The left panel there shows both the real and the imaginary parts of $\hat{\gamma}_s(a)$ and of $\gamma_s(a)$, obtained with eq. (A.41). The results for the former are then employed to compute the ratio $\hat{\gamma}_s(a)/\hat{\chi}(a)$, with $\hat{\chi}(a)$ in the denominator evaluated analytically — this operation results in the red circles displayed in the right panel of the figure. There, they are compared with the values of the same ratio, this time obtained directly from eq. (A.39), i.e. with the alternative integral representation of $\hat{\gamma}_s$. We see that there is a perfect agreement between the two types of predictions.

A.3 Fixed-point representation

Fig. 9, and specifically its right panel, helps us make the following observation: $\hat{\chi}(a)$ is a reasonable approximation for $\hat{\gamma}_s(a)$, precisely as eq. (A.39) suggests. In fact, the structure of that equation,

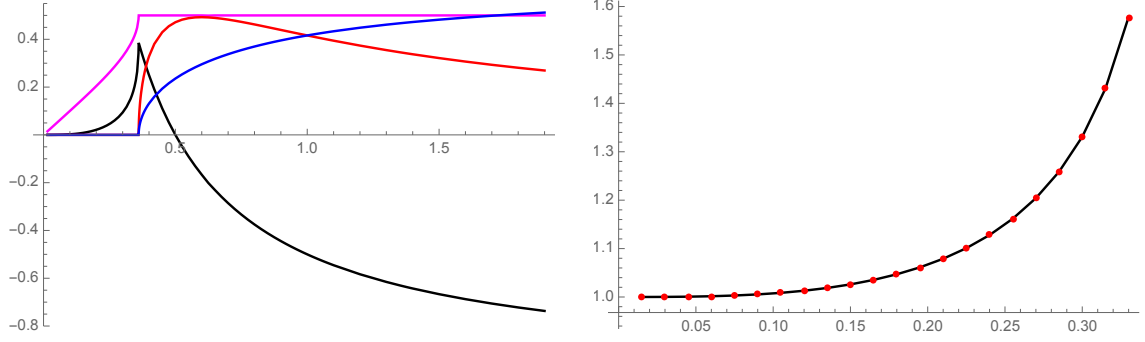


Figure 9. Left-hand panel: integral-representation results for the real and imaginary parts of $\hat{\gamma}_s(a)$ (black and red) and of $\gamma_s(a)$ (magenta and blue), obtained with eq. (A.41). Right-hand panel: ratio $\hat{\gamma}_s(a)/\hat{\chi}(a)$ computed with the results of the left-hand panel (red points), and with the integral representation of the ratio, eq. (A.39).

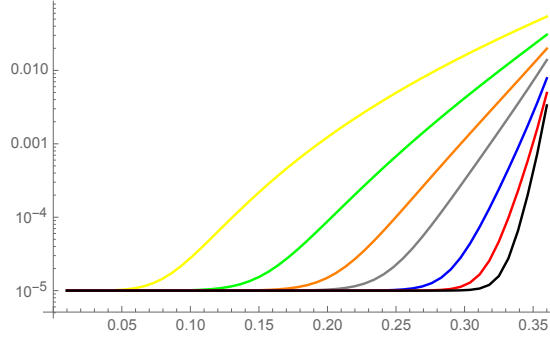


Figure 10. Checks of eq. (A.1) with the elements of the sequence of eq. (A.48).

and of eq. (A.35) in particular, implies that the following sequence is of interest:

$$\{\gamma_s^{(n)}(a)\}_{n=0}^{\infty}, \quad \gamma_s^{(0)}(a) = a, \quad (\text{A.48})$$

where the elements $n \geq 1$ are defined recursively:

$$\gamma_s^{(n+1)}(a) = a[1 + \hat{\chi}(\gamma_s^{(n)}(a))] \quad (\text{A.49})$$

$$= a[1 + \hat{\chi}(a(1 + \hat{\chi}(a(1 + \hat{\chi}(\dots)))))]. \quad (\text{A.50})$$

Equation (A.49) is in the form of a fixed-point sequence; namely, if it converges to $\gamma_s^{(\infty)}(a)$, this is a fixed point of the function $\Phi_a(x)$, with

$$\gamma_s^{(\infty)}(a) = \Phi_a(\gamma_s^{(\infty)}(a)), \quad \Phi_a(x) = a(1 + \hat{\chi}(x)) \equiv ax\chi(x). \quad (\text{A.51})$$

having exploited the identity of eq. (A.17). As the notation suggests, in terms of the fixed-point problem, a is an external parameter. If the convergence point $\gamma_s^{(\infty)}(a)$ exists, it coincides with the sought solution $\gamma_s(a)$, as one can see from the fact that eq. (A.51) becomes an identity upon exploiting eq. (A.1). There is therefore nothing particularly new here, except for the fixed-point observation, and for the related fact that the sequence of eq. (A.48) gives one another approximant

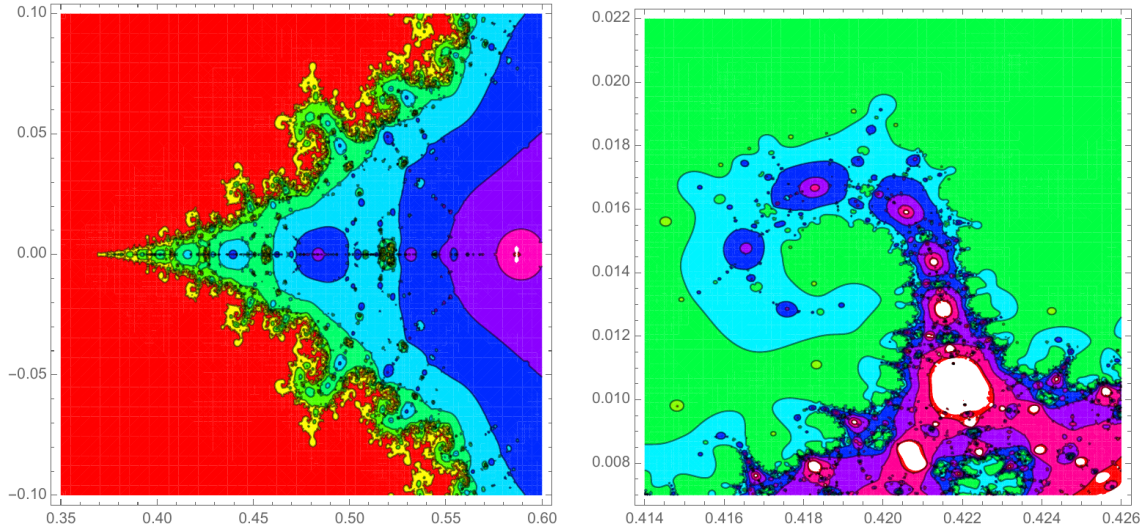


Figure 11. Fractal structures emerging from the recursive fixed-point sequence of eq. (A.49). The plot on the right-hand panel is a zoomed-in version of that on the left-hand panel, with different colour choices.

of $\gamma_s(a)$. The quality of such an approximant is shown in fig. 10, where we plot³⁸

$$a \chi(\gamma_s^{(n)}(a)) - 1 + 10^{-5} \quad (\text{A.52})$$

for n equal to 1 (yellow), 2 (green), 3 (orange), 4 (gray), 6 (blue), 8 (red), and 10 (black). Therefore, at least for values not too close to $a = 1/\log(16)$, the convergence appears to be much faster than that of the original series in eq. (A.2).

We hasten to stress that the positive feature of the fixed-point solution we have just mentioned applies only to real values of a . In the complex plane (and also for larger real values of a) the situation is very different, and the fixed-point recursive sequence becomes very unstable. Indeed, a modern trend in mathematics defines fractal structures by means of the speed of convergence (or lack thereof) of fixed-point sequences associated with given functions. We are indeed able to obtain fractal-type results from eq. (A.49), as is shown in fig. 11, with the uniformly-coloured regions associated with fastly-convergent and stable solutions; unstable, non-converging solution make up the rest of the complex plane.

We conclude this section with the following heuristic observation: the structure of the perturbative expansion of eq. (A.50) is analogous to that of eq. (A.19) (in terms of the functions $\hat{\chi}$ and R , respectively; neither expansion is shown explicitly here). We interpret this as a further evidence that all non-integral-representation results for $\gamma_s(a)$ can be cast as recursive solutions, with the features that we have outlined before.

B Solving equations for the resummation of γ_{qg}

In this appendix, we report the results for some of the quantities of interest in the determination of h_{qg} and of the green function \mathcal{G}_{qg} .

B.1 Determining the function Ω

Here we study in more detail the function Ω introduced in eq. (3.8), which is used in the definition of the transition function Γ_{gg} , eq. (3.7).

³⁸The 10^{-5} factor is there in order for us to use a logarithmic scale in the plot.

We start by performing the change of integration variable $a = 1/\chi(y)$, so that the function $\Omega(z)$ eq. (3.8) becomes

$$\Omega(z) \equiv \int_0^{1/\chi(z)} da \frac{\gamma_s(a)}{a} = - \int_0^z dy y \frac{\chi'(y)}{\chi(y)} \quad (\text{B.1})$$

where we have used eq. (A.1) and we have exploited

$$\frac{da}{dy} = - \frac{\chi'(y)}{\chi^2(y)}. \quad (\text{B.2})$$

As z is in general a complex variable, this integral has to be performed in the complex plane by choosing an integration path. To simplify this aspect, we further change integration variable as $y = wz$, so that eq. (B.1) becomes

$$\Omega(z) = -z^2 \int_0^1 dw \frac{w\chi'(wz)}{\chi(wz)}, \quad (\text{B.3})$$

where now the integration variable w is real. We then perform the following manipulations:

$$\begin{aligned} \Omega(z) &= -z \int_0^1 dw w \frac{d}{dw} \log \chi(wz) \\ &= -z \log \chi(z) + z \int_0^1 dw \log \chi(wz) \\ &= -z \log \chi(z) + z \int_0^1 dw \log \frac{1 + \hat{\chi}(wz)}{wz} \\ &= z - z \log [1 + \hat{\chi}(z)] + z \int_0^1 dw \log [1 + \hat{\chi}(wz)] \end{aligned} \quad (\text{B.4})$$

where we have carried out an integration by parts in the second step and we have made use in the last two steps of the function $\hat{\chi}$ introduced in eq. (A.16), which is related to the LO BFKL kernel function χ as is shown in eq. (A.17). We observe that the integral representations in eq. (B.3) and eq. (B.4) are suitable for numerical implementation for generic complex values of the argument z , and we indeed use them in the `HELL` code. Unfortunately we did not manage to compute the integrals analytically in terms of known functions.

By exploiting eq. (A.23) to rewrite the basic quantity which appears in eq. (B.4), we have

$$\Omega(z) = \sum_{k=0}^{\infty} q_k z^{k+1} = z - \frac{3}{2} \zeta_3 z^4 - \frac{5}{3} \zeta_5 z^6 + \frac{12}{7} \zeta_3^2 z^7 - \frac{7}{4} \zeta_7 z^8 + \frac{32}{9} \zeta_3 \zeta_5 z^9 + \dots, \quad (\text{B.5})$$

where the form of the coefficients is

$$q_0 = 1, \quad q_k = \frac{k}{(k+1)!} \sum_{j=1}^k (-)^j (j-1)! B_{k,j}(Z), \quad (\text{B.6})$$

where Z has been defined in eq. (A.14). Furthermore, by using the Faà di Bruno formula, it is possible to write any power of $\Omega(z)$ as a linear combination of powers of z :

$$\Omega^n(z) = \sum_{k=n}^{\infty} \frac{n!}{k!} B_{k,n} \left(\left\{ l! q_{l-1} \right\}_{l=1}^{k-n+1} \right) z^k. \quad (\text{B.7})$$

The results above can be used to obtain an explicit expression for z in terms of $\Omega(z)$. Indeed, by exploiting known results for the reversion of series, we have

$$z = \sum_{k=0}^{\infty} p_k \Omega^{k+1}(z) = \Omega + \frac{3}{2} \zeta_3 \Omega^4 + \frac{5}{3} \zeta_5 \Omega^6 + \frac{51}{7} \zeta_3^2 \Omega^7 + \frac{7}{4} \zeta_7 \Omega^8 + \frac{193}{9} \zeta_3 \zeta_5 \Omega^9 + \dots \quad (\text{B.8})$$

The closed form of the coefficients is

$$p_0 = 1, \quad p_k = \frac{1}{(k+1)!} \sum_{j=1}^k (-1)^j \frac{(k+j)!}{k!} B_{k,j} \left(\left\{ l! q_l \right\}_{l=1}^{k-j+1} \right), \quad (\text{B.9})$$

and the generic power of z reads thus

$$z^n = \sum_{k=n}^{\infty} \frac{n!}{k!} B_{k,n} \left(\left\{ l! p_{l-1} \right\}_{l=1}^{k-n+1} \right) \Omega^k(z). \quad (\text{B.10})$$

As is discussed immediately after eq. (3.40), the most straightforward way to obtain the resummed qg splitting kernel is through the Mellin inversion of its anomalous-dimension counterpart. In turn, owing to eq. (3.24), this operation requires a complex-plane line integration that involves the function $\Omega(z)$. This is problematic, owing to the behaviour of $\Omega(z)$ at large $|z|$. In order to see this, we choose for simplicity the following integration path, which may be used to carry out the inverse Mellin transform:

$$s = c + \rho (\cos \theta + i \sin \theta) = c + \rho e^{i\theta}. \quad (\text{B.11})$$

We limit ourselves to considering it in the upper half-plane of the complex domain, i.e. for

$$c > 0, \quad \rho \geq 0, \quad 0 < \theta \leq \pi, \quad (\text{B.12})$$

since the arguments that follow can be repeated essentially unchanged in the case of negative imaginary parts. A direct calculation leads us to the following asymptotic behaviour:

$$\Omega(s) \Big|_{s=c+\rho e^{i\theta}} \xrightarrow{\rho \rightarrow \infty} -\frac{1}{2} \log(\gamma_E - i\theta + \log s) - (s-1) \sum_{n=1}^{n_{\max}} \frac{e^{i\hat{\theta}} \Gamma(n, i\hat{\theta})}{(\gamma_E - i\theta + \log s)^n} - (f_R + i f_I), \quad (\text{B.13})$$

where are f_R, f_I two constants (whose forms are irrelevant here), n_{\max} is an integer parameter, and we have defined

$$\hat{\theta} = \frac{\pi}{2} - \theta. \quad (\text{B.14})$$

While the asymptotic behaviour of the inverse Mellin transform of the exponent of eq. (B.13) (times a numerical prefactor equal to either 2 or 2/3, per eq. (3.24)), can be computed analytically, in itself this is not particularly useful since, even for large $|s|$, the agreement between the value of $\Omega(s)$ computed with eq. (B.13) and the one obtained numerically is poor, unless n_{\max} is relatively large ($\gtrsim 8$). Given that the sought configuration-space result is then the convolution of n_{\max} individual inverse-Mellin transforms, it is clear that one ends up with a quantity which does not behave well numerically. A possible solution stems from exploiting the identity

$$-\sum_{n=1}^{\infty} \frac{1}{\log^n \bar{\rho}} e^{i\hat{\theta}} \Gamma(n, i\hat{\theta}) \longrightarrow -\frac{e^{i\hat{\theta}}}{\bar{\rho}} \left(\text{Ei}(\log \bar{\rho} - i\hat{\theta}) + i\pi \right), \quad \bar{\rho} = \rho e^{\gamma_E}, \quad (\text{B.15})$$

by means of which one arrives at the following alternative expression

$$\begin{aligned} \Omega(s) \Big|_{s=c+\rho e^{i\theta}} \xrightarrow{\rho \rightarrow \infty} & -\frac{1}{2} \log(\gamma_E - i\theta + \log s) \\ & - e^{-\gamma_E} e^{i(\hat{\theta}+\theta)} \left[\text{Ei}(\log s + \gamma_E - i(\hat{\theta} + \theta)) + i\pi \right] - (f_R + i f_I) \\ & \xrightarrow{\rho \rightarrow \infty} -\frac{1}{2} \log(\gamma_E - i \text{Arg}(s) + \log s) - i e^{-\gamma_E} \text{Ei}(\log s + \gamma_E - i \frac{\pi}{2}). \end{aligned} \quad (\text{B.16})$$

Here, Ei denotes the exponential integral defined by³⁹

$$\text{Ei}(z) = - \int_{-z}^{\infty} dt \frac{e^{-t}}{t} = -i\pi \left[\frac{\pi + \text{Arg}(z)}{2\pi} \right] + \gamma_E + \log z + \sum_{k=1}^{\infty} \frac{z^k}{kk!}. \quad (\text{B.17})$$

Unfortunately, this manipulation trades one problem for another: eq. (B.16) is a fairly good approximation of the exact $\Omega(s)$, but the inverse Mellin transform of its (weighted) exponential turns out to be very difficult to compute analytically⁴⁰.

B.2 Coefficients of the bare quark Green function $\hat{\mathcal{G}}_{qq}^{(0)}$

We now compute the bare quark Green function $\hat{\mathcal{G}}_{qq}^{(0)}$ as is introduced in eq. (3.1), after having factored out some constant terms as in eq. (3.3b). In particular, we are interested in the expansions in series of ϵ of the coefficients of the $\mathcal{O}(\alpha_s^{k+1})$ terms. The starting point is eq. (4.10) of ref. [62], which we recast as⁴¹

$$\hat{\mathcal{G}}_{qq}^{(0)} = \frac{\alpha_N}{\epsilon} \left(\rho_0(\epsilon) + \sum_{k=1}^{\infty} \frac{\rho_k(\epsilon)}{\epsilon^k} \alpha_N^k \right) \quad (\text{B.18})$$

$$\equiv \frac{\alpha_N}{\epsilon} \sum_{k=0}^{\infty} \sum_{i=0}^{\infty} \frac{\rho_{k,i}}{\epsilon^{k-i}} \alpha_N^k, \quad (\text{B.19})$$

where we have introduced the shorthand notation

$$\rho_{k,i} = \frac{1}{i!} \frac{d^i \rho_k}{d\epsilon^i}(0). \quad (\text{B.20})$$

The coefficients ρ_k are defined as follows:

$$\rho_0(\epsilon) = \frac{e^{\epsilon\psi_0(1)}}{\Gamma(1+\epsilon)} \frac{3(4+\epsilon)}{2(2+\epsilon)(3+\epsilon)}, \quad (\text{B.21})$$

$$\rho_k(\epsilon) = \rho_0(\epsilon) \left(\frac{e^{\epsilon\psi_0(1)}}{\Gamma(1+\epsilon)} \right)^k \frac{\hat{d}_k(\epsilon)}{k}, \quad (\text{B.22})$$

where (note that $\varphi_1(\epsilon) = 1$):

$$\begin{aligned} \hat{d}_k(\epsilon) &= \frac{1}{k+1} \frac{(4+(1-3k)\epsilon) \prod_{i=1}^3 (i+\epsilon)}{(4+\epsilon) \prod_{j=1}^3 (j+(1-k)\epsilon)} \\ &\times \frac{\Gamma(1+\epsilon)^2 \Gamma(1-k\epsilon) \Gamma(1+k\epsilon)}{\Gamma(1+(1-k)\epsilon) \Gamma(1+(1+k)\epsilon)} \hat{c}_k(\epsilon), \end{aligned} \quad (\text{B.23})$$

$$\hat{c}_k(\epsilon) = \hat{c}_{k-1}(\epsilon) \hat{I}_{k-1}(\epsilon) \equiv \hat{c}_{k-1}(\epsilon) \left(\hat{I}_{k-1}^{(A)}(\epsilon) - \hat{I}_{k-1}^{(B)}(\epsilon) \right), \quad (\text{B.24})$$

$$\hat{I}_k^{(A)}(\epsilon) = I_F(\epsilon) \hat{J}_k^{(A)}(\epsilon) \equiv I_F(\epsilon) \frac{\Gamma(1+2\epsilon) \Gamma(k\epsilon) \Gamma(1-k\epsilon)}{\Gamma((1+k)\epsilon) \Gamma(1+(1-k)\epsilon)}, \quad (\text{B.25})$$

$$\hat{I}_k^{(B)}(\epsilon) = I_F(\epsilon) \hat{J}_k^{(B)}(\epsilon) \equiv I_F(\epsilon) \Gamma(1+\epsilon) \Gamma(1-\epsilon), \quad (\text{B.26})$$

$$I_F(\epsilon) = \frac{\Gamma(1+\epsilon)^2}{\Gamma(1+2\epsilon)}. \quad (\text{B.27})$$

³⁹Note that this function coincides with the `ExpIntegralEi` module in Mathematica.

⁴⁰More precisely: such a transform is the sum of two distributions, one of which is a $\delta(1-\xi)$ with an easy-to-compute coefficient. The other contribution is a generalised plus distribution for which we were unable to obtain a closed form (among other things, it requires a double summation of $\log(1-\xi)$ terms, since the nominally subleading contributions have coefficients which scale in a manner that (over)compensates the subleadingness — see also sect. 4.4).

⁴¹Henceforth, without loss of generality, we set $\mu = Q$.

The recursive definition in eq. (B.24) can be made explicit,

$$\hat{c}_k(\epsilon) = I_F^{k-1}(\epsilon) \sum_{q=0}^{k-1} (-)^{k-1-q} \left(\hat{j}^{(B)}(\epsilon) \right)^{k-1-q} \sum_{\{j_1 \dots j_q\}} \hat{j}_{j_1}^{(A)}(\epsilon) \dots \hat{j}_{j_q}^{(A)}(\epsilon). \quad (\text{B.28})$$

Here

$$\{j_1 \dots j_q\} \subseteq \{1, \dots, k-1\} \quad (\text{B.29})$$

is a q -element unordered set, and the rightmost sum in eq. (B.28) is understood to run over all possible such sets — by convention, if $q = 0$ the argument of the sum is set equal to one.

By using eq. (B.28), the coefficients $\rho_k(\epsilon)$ will be given as sums of terms, each of which has a multiplicative structure. Denoting by $f(\epsilon)$ any such term, we shall use the identity⁴²

$$f(\epsilon) = \exp(\log f(\epsilon)), \quad (\text{B.30})$$

so that:

$$\frac{d^n f}{d\epsilon^n}(0) = f(0) B_n \left(\frac{d \log f}{d\epsilon}(0), \dots, \frac{d^n \log f}{d\epsilon^n}(0) \right), \quad (\text{B.31})$$

with B_n the complete exponential Bell polynomials. Thus, each element of the product that defines $f(\epsilon)$ will correspond to a set of inputs to the Bell polynomials, with the set relevant to $f(\epsilon)$ the sum of such sets. The ϵ -dependent terms in eq. (B.21) and (B.22), bar $\hat{d}_k(\epsilon)$, lead us to define

$$\begin{aligned} Z_{56}(k) = & \left(\dots, (-)^{m-1} (m-1)! (1/4^m - 1/3^m - 1/2^m), \dots \right)_{m=1}^n \\ & + (k+1) \left(\dots, (\delta_{1m} - 1) \psi_{m-1}(1), \dots \right)_{m=1}^n. \end{aligned} \quad (\text{B.32})$$

The ϵ -dependent terms in eq. (B.23), bar $\hat{c}_k(\epsilon)$, gives instead:

$$\begin{aligned} Z_{34}(k) = & \left(\dots, (-)^{m-1} (m-1)! ((1-3k)^m - 1)/4^m, \dots \right)_{m=1}^n \\ & - \left(\dots, (-)^{m-1} (m-1)! (1 + 1/2^m + 1/3^m) ((1-k)^m - 1), \dots \right)_{m=1}^n \\ & + \left(\dots, (2 + (1 + (-1)^m) k^m - (1+k)^m - (1-k)^m) \psi_{m-1}(1), \dots \right)_{m=1}^n. \end{aligned} \quad (\text{B.33})$$

Equations (B.25)–(B.27) give

$$Z_A(k) = \left(\dots, (2^m + (1 + (-1)^m) k^m - (1-k)^m - (1+k)^m) \psi_{m-1}(1), \dots \right)_{m=1}^n, \quad (\text{B.34})$$

$$Z_B = \left(\dots, (1 + (-1)^m) \psi_{m-1}(1), \dots \right)_{m=1}^n, \quad (\text{B.35})$$

$$Z_F = \left(\dots, (2 - 2^m) \psi_{m-1}(1), \dots \right)_{m=1}^n, \quad (\text{B.36})$$

respectively. With these, eq. (B.31) leads to the sought results⁴³

$$\frac{d^n \rho_0}{d\epsilon^n}(0) = B_n \left(Z_{56}(0) \right), \quad (\text{B.37})$$

$$\frac{d^n \rho_1}{d\epsilon^n}(0) = \frac{1}{2} B_n \left(Z_{34}(1) + Z_{56}(1) \right), \quad (\text{B.38})$$

$$\begin{aligned} \frac{d^n \rho_k}{d\epsilon^n}(0) = & \frac{1}{k(1+k)} \sum_{q=0}^{k-1} (-)^{k-1-q} \sum_{\{j_1 \dots j_q\}} \hat{j}_{j_1}^{(A)}(0) \dots \hat{j}_{j_q}^{(A)}(0) \\ & \times B_n \left(Z_{34}(k) + Z_{56}(k) + (k-1)Z_F + (k-1-q)Z_B + Z_A(j_1) + \dots + Z_A(j_q) \right). \end{aligned} \quad (\text{B.39})$$

⁴²Clearly, no manipulation is necessary for terms that are already in an exponential form, of which there is only one here, namely $\exp(\epsilon \psi_0(1))$.

⁴³Which are actually valid also for $n = 0$.

Note that

$$\hat{j}_j^{(A)}(0) = \frac{1+j}{j}, \quad (\text{B.40})$$

and that the arguments of the Bell polynomials in eqs. (B.37)–(B.39) do not feature $\psi_0(1)$, i.e. the results are independent of the Euler-Mascheroni constant. In these arguments, the only irrational numbers are $\psi_i(1)$ with $i \geq 1$, i.e. Riemann's ζ_{i+1} of either parity. We expect significant cancellations in the sums on the right-hand side of eq. (B.39); bear in mind that this structure stems from the difference on the rightmost side in eq. (B.24), which leads to a proliferation of terms upon recursion.

An alternative result can be obtained by starting from the observation that the n^{th} coefficient of the series expansion in ϵ of the product of $m+1$ functions $f_q(\epsilon)$ reads

$$\frac{1}{n!} \frac{d^n f_0 \dots f_m}{d\epsilon^n}(0) = \frac{1}{n!} \sum_{\substack{j_0 \dots j_m=0 \\ j_0 + \dots + j_m = n}}^n \binom{n}{j_0 \dots j_m} \frac{d^{j_0} f_0}{d\epsilon^{j_0}}(0) \dots \frac{d^{j_m} f_m}{d\epsilon^{j_m}}(0), \quad (\text{B.41})$$

with the usual definition of the multinomial coefficient:

$$\binom{n}{j_0 \dots j_m} = \frac{n!}{j_0! \dots j_m!} = \binom{j_0}{j_0} \binom{j_0 + j_1}{j_1} \dots \binom{j_0 + \dots + j_m}{j_m}. \quad (\text{B.42})$$

By applying eq. (B.41) to the computation of the derivatives of $\rho_k(\epsilon)$ ($k \geq 2$), with $m = k-1$ and

$$f_0 = \frac{\rho_k(\epsilon)}{\hat{c}_k(\epsilon)} I_F^{k-1}(\epsilon), \quad (\text{B.43})$$

$$f_q = \hat{j}_q^{(A)}(\epsilon) - \hat{j}_q^{(B)}(\epsilon), \quad 1 \leq q \leq k-1, \quad (\text{B.44})$$

and by bearing in mind the definitions in eqs. (B.32)–(B.36), we arrive at:

$$\begin{aligned} \frac{d^n \rho_k}{d\epsilon^n}(0) &= \frac{1}{k(1+k)} \sum_{\substack{j_0 \dots j_{k-1}=0 \\ j_0 + \dots + j_{k-1} = n}}^n \binom{n}{j_0 \dots j_{k-1}} B_{j_0}(Z_{34}(k) + Z_{56}(k) + (k-1)Z_F) \\ &\quad \times \prod_{q=1}^{k-1} \left[\hat{j}_q^{(A)}(0) B_{j_q}(Z_A(q)) - B_{j_q}(Z_B) \right]. \end{aligned} \quad (\text{B.45})$$

The equivalence of eqs. (B.39) and (B.45) can be shown by using the rightmost expression of eq. (B.42) in eq. (B.45), and by repeatedly applying the Binomial identity

$$B_n(x_1 + y_1, \dots, x_n + y_n) = \sum_{i=0}^n \binom{n}{i} B_{n-i}(x_1, \dots, x_{n-i}) B_i(y_1, \dots, y_n) \quad (\text{B.46})$$

of the complete exponential Bell polynomials.

B.3 Extraction of the h_k coefficients and construction of the function h_{qg}

In the literature, the all-order result for h_{qg} we have presented in sect. 3.1 was unknown, and therefore the determination of its perturbative coefficients necessarily followed a different procedure with respect to we have adopted in sect. 3.2. Here, we derive the coefficients employing a more traditional approach; still, we stress that the emerging results, at variance with those in the literature, are entirely analytical *and* not recursive (in other words, the perturbative-index dependence is completely parametrical).

The relevant quantity is $\hat{\gamma}_{qg}$, which enters the integral in eq. (3.6), and whose perturbative expansion in terms of α_N is given by eq. (3.33), that we report here for convenience:

$$\hat{\gamma}_{qg}(\alpha_N) = \sum_{k=0}^{\infty} t_k \alpha_N^{k+1}. \quad (\text{B.47})$$

The t_k will be determined order-by-order by means of an expansion of eq. (3.11), bearing in mind that the left-hand side there is finite.

One starts by computing Γ_{gg} , according to its definition in eq. (3.7), in a way which emphasises the role of α_N as the expansion parameter. With eq. (A.2) we have

$$\Gamma_{gg}(\alpha_N, \epsilon) = \exp \left[\frac{1}{\epsilon} \sum_{j=0}^{\infty} g_j \int_0^{\alpha_N} \frac{da}{a} a^{j+1} \right] = \exp \left[\frac{1}{\epsilon} \sum_{k=1}^{\infty} \frac{g_{k-1}}{k} \alpha_N^k \right]. \quad (\text{B.48})$$

By employing the properties of the Bell polynomials (in particular, their generating function and the homogeneous behaviour of the incomplete ones), we arrive at the following expression:

$$\Gamma_{gg}(\alpha_N, \epsilon) = \sum_{n=0}^{\infty} \Gamma_{gg}^{(n)}(\epsilon) \alpha_N^n, \quad (\text{B.49})$$

$$\Gamma_{gg}^{(n)}(\epsilon) = \frac{1}{n!} \sum_{k=0}^n \frac{1}{\epsilon^k} B_{n,k}(G_0), \quad (\text{B.50})$$

where

$$G_0 = (g_0 0!, g_1 1!, g_2 2!, \dots, g_n n!, \dots). \quad (\text{B.51})$$

By replacing eqs. (B.49) and (B.47) into eq. (3.6), after performing the integration and changing summation indices we arrive at

$$\hat{\Gamma}_{gg}(\alpha_N, \epsilon) = \frac{1}{\epsilon} \sum_{n=0}^{\infty} \frac{\alpha_N^{n+1}}{n+1} \sum_{k=0}^n t_{n-k} \Gamma_{gg}^{(k)}(\epsilon). \quad (\text{B.52})$$

Thus eq. (3.11), thanks to eqs. (B.19), (B.52), and (B.49), becomes

$$\begin{aligned} \hat{\mathcal{G}}_{gg}(\alpha_N, \epsilon) = \frac{1}{\epsilon} \sum_{n=0}^{\infty} \alpha_N^{n+1} \sum_{k=0}^n \frac{1}{(n-k)!} & \left[\left(\sum_{i=0}^{\infty} \frac{\rho_{k,i}}{\epsilon^{k-i}} \right) \left(\sum_{p=0}^{n-k} \frac{(-)^p}{\epsilon^p} B_{n-k,p}(G_0) \right) \right. \\ & \left. - \frac{1}{k+1} \sum_{j=0}^k \frac{t_{k-j}}{j!} \left(\sum_{i=0}^j \frac{1}{\epsilon^i} B_{j,i}(G_0) \right) \left(\sum_{p=0}^{n-k} \frac{(-)^p}{\epsilon^p} B_{n-k,p}(G_0) \right) \right]. \end{aligned} \quad (\text{B.53})$$

The singular structure of the two terms in squared brackets in eq. (B.53) is manifest. For a given $\mathcal{O}(\alpha_N^n)$ term, and ignoring the $1/\epsilon$ prefactor, the singular terms are

$$1/\epsilon^{k+p-i}, \quad -\infty < k+p-i \leq n, \quad (\text{B.54})$$

$$1/\epsilon^{i+p}, \quad 0 \leq i+p \leq n. \quad (\text{B.55})$$

Since $\hat{\mathcal{G}}_{gg}$ is a finite quantity, this implies that at $\mathcal{O}(\alpha_N^n)$ we shall have to impose that the residues of the n poles and the constant term (owing to the $1/\epsilon$ prefactor) vanish; the corresponding equations must be solved for the t_i coefficients. With tedious but straightforward manipulations of the sums, eq. (B.53) can be recast in the following form:

$$\begin{aligned} \hat{\mathcal{G}}_{gg} = \frac{1}{\epsilon} \sum_{n=0}^{\infty} \alpha_N^{n+1} \sum_{m=-\infty}^n \frac{1}{\epsilon^m} \sum_{k=0}^n \frac{1}{(n-k)!} & \left[\sum_{p=0}^{n-k} (-)^p \Theta(p \geq m-k) \rho_{k,k+p-m} B_{n-k,p}(G_0) \right. \\ & \left. - \frac{1}{k+1} \sum_{i=0}^m \sum_{j=i}^k (-)^{m-i} \Theta(m-n+k \leq i \leq k) \frac{t_{k-j}}{j!} B_{j,i}(G_0) B_{n-k,m-i}(G_0) \right]. \end{aligned} \quad (\text{B.56})$$

Since at $\mathcal{O}(\alpha_N^n)$ the absence of divergencies in eq. (B.56) gives $(n+1)$ conditions, there is a lot of redundancy as far as the determination of the t_i coefficients is concerned. It turns out, for example,

that the $(n + 1)$ conditions at a given n feature all t_j coefficients with $0 \leq j \leq n$. However, it is actually more convenient to consider the $m = 0$ contributions associated with different n 's. This is because eq. (B.56) in that case leads to

$$m = 0 \implies \dots \sum_{k=0}^n \frac{1}{(n-k)!} \left[\sum_{p=0}^{n-k} (-)^p \rho_{k,k+p} B_{n-k,p}(G_0) - \frac{1}{k+1} \sum_{j=0}^k \frac{t_{k-j}}{j!} B_{j,0}(G_0) B_{n-k,0}(G_0) \right] \quad (\text{B.57})$$

whence

$$\begin{aligned} \frac{t_n}{n+1} &= \sum_{k=0}^n \frac{1}{(n-k)!} \sum_{p=0}^{n-k} (-)^p \rho_{k,k+p} B_{n-k,p}(G_0) \\ &= \sum_{i=0}^n \sum_{k=0}^i \frac{(-)^{i-k}}{(n-k)!} \rho_{k,i} B_{n-k,i-k}(G_0). \end{aligned} \quad (\text{B.58})$$

Equation (B.58) is remarkable, because it tells us that it is not even necessary to solve (recursively or otherwise) a system of linear equations in order to arrive at the t_i coefficients, since these are already in a closed form.

We now focus on an alternative determination of h_{qg} , which we remind the reader to be implicitly defined by

$$\hat{\gamma}_{qg}(\alpha_N) = \alpha_N h_{qg}(\gamma_s(\alpha_N)), \quad (\text{B.59})$$

with expansion

$$h_{qg}(z) = \sum_{n=0}^{\infty} h_n z^n. \quad (\text{B.60})$$

The coefficients h_n are obtained by exploiting the variable replacement of eq. (A.26) inside eq. (B.47) and by using the results of eq. (B.58). After having computed in this way a few of the h_n coefficients, we trade z for $\Omega \equiv \Omega(z)$ by employing the relationships in eqs. (B.8)–(B.10), whence

$$h_{qg}(z) = 1 + \frac{5}{3}\Omega + \frac{14}{9}\Omega^2 + \frac{82}{81}\Omega^3 + \frac{122}{243}\Omega^4 + \frac{146}{729}\Omega^5 + \mathcal{O}(\zeta_i) + \dots \quad (\text{B.61a})$$

$$= 1 + \sum_{k=1}^{\infty} \frac{2^{k-2}}{k!} \left(3 + \frac{1}{3^k} \right) \Omega^k + \mathcal{O}(\zeta_i) \quad (\text{B.61b})$$

$$= \frac{1}{4} \left(3e^{2\Omega} + e^{\frac{2}{3}\Omega} \right) + \mathcal{O}(\zeta_i) \quad (\text{B.61c})$$

$$= \frac{1 + \hat{\chi}(z)}{4} \left(3e^{2\Omega} + e^{\frac{2}{3}\Omega} \right), \quad (\text{B.61d})$$

which coincides with eq. (3.24). In eq. (B.61a), by $\mathcal{O}(\zeta_i)$ we have denoted all of the terms with coefficients which are not rational numbers, in that they feature (also) Riemann's ζ 's. In the same equations, the dots indicate terms of higher powers of Ω , of which we have computed a few, although obviously not all of them. However, by induction we have established that their general form is that reported in eq. (B.61b). The resulting series can be easily summed, leading to eq. (B.61c). Then, crucially, eq. (B.61d) shows that all terms with non-rational coefficients can in fact be accounted for by simply including a z -dependent prefactor, while keeping the same exponential structure. The key message to take home here is that most of the inherent complications of the function h_{qg} are captured by replacing the dependence on α_N in its rational part with that on $\Omega(\gamma_s(\alpha_N))$ — essentially, Ω collects the non-rational behaviour of the result we sought, up to some residual non-rational dependence which, in turn, is completely accounted for by an almost trivial γ_s -dependent prefactor (which confirms, once again, the role of γ_s in the significant simplifications of the analytical results with respect to their α_N -expanded counterparts).

B.4 Alternative closed-form expression for t_n coefficients

If one assumes to know the coefficients h_n as in eq. (3.30), one can obtain a different, more compact, closed-form expressions for the coefficients t_n eq. (B.58). This is done by realizing that eq. (B.60) and eq. (B.47) imply that

$$\sum_{k=0}^{\infty} t_k \alpha_N^k = \sum_{n=0}^{\infty} h_n \gamma_s^n(\alpha_N), \quad (\text{B.62})$$

and then

$$t_k = \frac{1}{k!} \frac{d^k}{d\alpha_N^k} h_{gg} \Big|_{\alpha_N=0} = \frac{1}{k!} \sum_{n=0}^k h_n \frac{d^k \gamma_s^n}{d\alpha_N^k} \Big|_{\alpha_N=0}, \quad (\text{B.63})$$

The derivative on the right-hand side of this equation is computed by employing the Faà di Bruno formula, whence

$$\frac{d^k \gamma_s^n}{d\alpha_N^k} \Big|_{\alpha_N=0} = n! B_{k,n}(\hat{G}), \quad (\text{B.64})$$

with the argument of the Bell polynomial defined in eq. (A.11) (note that this is the list of the derivatives of γ_s computed at $\alpha_N = 0$). Therefore

$$t_k = \frac{1}{k!} \sum_{n=0}^k h_n n! B_{k,n}(\hat{G}) = \frac{1}{k!} \sum_{n=0}^k \left(\frac{3}{4} B_n(\hat{Z}_2) + \frac{1}{4} B_n(\hat{Z}_{\frac{2}{3}}) \right) B_{k,n}(\hat{G}), \quad (\text{B.65})$$

having used eq. (3.30) and the fact that $B_{k,n}() = 0$ for any $n > k$, which allows one to set the upper bound of the summation over n equal to k .

Eq. (B.65) is in fact a blueprint for expressing the coefficients of the expansion in α_N of a quantity whose coefficients of the expansion in γ_s are known. Explicitly, if

$$\sum_{n=0}^{\infty} c_n \gamma_s^n(\alpha_N) = \sum_{k=0}^{\infty} c'_k \alpha_N^k \quad (\text{B.66})$$

then

$$c'_k = \frac{1}{k!} \sum_{n=0}^k c_n n! B_{k,n}(\hat{G}). \quad (\text{B.67})$$

B.5 Construction of finite quark Green function \mathcal{G}_{qq}

The method employed in sect. 3.1 for the determination of h_{gg} can be used to compute the other non-divergent component of eq. (3.11), namely $\hat{\mathcal{G}}_{qq}$ (or, more precisely, its $\epsilon \rightarrow 0$ limit). Note that, according to eqs. (3.15), (3.17), and (3.18), we have

$$\lim_{\epsilon \rightarrow 0} \hat{\mathcal{G}}_{qq} = A_0 = B_0 = F^0. \quad (\text{B.68})$$

As a power series, F^0 can be directly determined by taking the $\mathcal{O}(\epsilon^0)$ term of $F(\Omega)$ from its definition in eq. (3.12). In order to do this, one needs to exploit the series expansion of $\hat{\mathcal{G}}_{qq}^{(0)}$, eq. (B.19), and of Γ_{gg}^{-1} (eq. (B.49), with $\epsilon \rightarrow -\epsilon$ there). The former is a series in α_N , which is turned into a series in $\gamma_s(\alpha_N)$ by means of eq. (A.26). As far as Γ_{gg}^{-1} is concerned, we can simply employ eq. (B.7).

From its definition in eqs. (3.12) and (3.18), and the results for $\hat{\mathcal{G}}_{qq}^{(0)}$ and Γ_{gg} , we have

$$F^0 \equiv \lim_{\epsilon \rightarrow 0} \hat{\mathcal{G}}_{qq}^{(0)} \Gamma_{gg}^{-1} = \lim_{\epsilon \rightarrow 0} \sum_{k=0}^{\infty} \sum_{i=0}^{\infty} \sum_{j=0}^{\infty} \frac{\epsilon^i}{\epsilon^j \epsilon^{k+1}} \rho_{k,i} \alpha_N^{k+1} \frac{(-\Omega)^j}{j!}, \quad (\text{B.69})$$

The $\epsilon \rightarrow 0$ limit then is simply taken by selecting the $\mathcal{O}(\epsilon^0)$ terms on the right-hand side of this equation by constraining

$$i - j - k - 1 = 0. \quad (\text{B.70})$$

Owing to eqs. (A.26) and (B.7), this implies that the i^{th} ϵ -derivative of a ρ_k coefficient must be computed only up to $\mathcal{O}(\gamma_s^{j+k+1})$. Therefore, if the overall accuracy one is interested in is some $\mathcal{O}(\gamma_s^M)$, then

$$F^0 = \sum_{k=0}^{M-1} \sum_{j=0}^{M-1-k} \rho_{k,j+k+1} \alpha_N^{k+1} \frac{(-\Omega)^j}{j!}. \quad (\text{B.71})$$

Before proceeding, we point out that in view of the attempt to find a functional expression for F^0 , it is crucially important that the derivatives of polygamma functions be treated symbolically, and not converted into their equivalent real-number expressions. Specifically, the problem affects the derivatives with odd indices, since for example $\pi^4 \propto \psi_3(1)$ but also $\pi^4 \propto \psi_1(1)^2$. In any case, following what has been done in other, simpler, cases, the first step is the determination of the rational part of F^0 . The explicit calculation of the right-hand side of eq. (B.71) leads to

$$F^0 = -\frac{7}{12} \gamma_s - \frac{41}{72} \gamma_s^2 - \frac{157}{1296} \gamma_s^3 + \frac{2537}{7776} \gamma_s^4 + \frac{27595}{46656} \gamma_s^5 + \dots + \mathcal{O}(\psi_2(1)\gamma_s^3) + \mathcal{O}(\psi_3(1)\gamma_s^4). \quad (\text{B.72})$$

The arguments of the $\mathcal{O}()$ symbols on the right-hand side denote the instances of the Riemann ζ at the lowest order in γ_s where they start to appear — only the first with even and odd indices are reported. This implies that F^0 features neither $\psi_0(1) = -\gamma_E$ nor $\psi_1(1) = \pi^2/6$ (but higher powers of π will be present). By computing a sufficiently large number of terms of the series, one finds that the sequence of rational coefficients is

$$\left\{ -\frac{7}{12}, -\frac{41}{72}, -\frac{157}{1296}, \frac{2537}{7776}, \dots \right\} = \left\{ -\frac{2^{k-2}}{k!} \left(3 + \frac{1}{3^k} \right) \right\}_{k=1}^{\infty} + \left\{ \frac{3}{4} + \frac{3}{2^{k+1}} - \frac{5}{4 \cdot 3^k} \right\}_{k=1}^{\infty}. \quad (\text{B.73})$$

We note that the two sequences on the right-hand side of eq. (B.73) computed in $k = 0$ would give -1 and 1 respectively, thus summing up to zero. For subsequent manipulations, it will turn out to be convenient to include such harmless $k = 0$ contributions in the definitions of the following functions, already reported in the main text as eqs. (5.2) and (5.3):

$$\begin{aligned} \varphi_0(z) &\equiv -\sum_{k=0}^{\infty} \frac{2^{k-2}}{k!} \left(3 + \frac{1}{3^k} \right) z^k \\ &= -\frac{1}{4} \left(3e^{2z} + e^{\frac{2}{3}z} \right), \end{aligned} \quad (\text{B.74})$$

$$\begin{aligned} \varphi_1(z) &\equiv \sum_{k=0}^{\infty} \left(\frac{3}{4} + \frac{3}{2^{k+1}} - \frac{5}{4 \cdot 3^k} \right) z^k \\ &= \frac{1}{4} \left(\frac{3}{1-z} + \frac{12}{2-z} - \frac{15}{3-z} \right), \end{aligned} \quad (\text{B.75})$$

so that

$$F^0 = \varphi_0(\gamma_s) + \varphi_1(\gamma_s) + \mathcal{O}(\psi_2(1)\gamma_s^3) + \mathcal{O}(\psi_3(1)\gamma_s^4). \quad (\text{B.76})$$

Then, one finds a crucial property of F^0 by assuming, in keeping with eq. (B.61b), that the natural argument of the φ_0 function is $\Omega(\gamma_s)$ rather than simply γ_s . This results in the following identity:

$$\frac{F^0 - \varphi_0(\Omega)}{\varphi_1(\gamma_s)} = 1 + \delta_1 F^0 + \delta_2 F^0 + \dots \quad (\text{B.77})$$

The defining characteristic of the functions $\delta_i F^0$ is that they feature monomials that contain exactly i instances of Riemann's ζ , each *uniquely* associated with a power of γ_s . In other words, if one finds some term $\psi_a(1)\gamma_s^b$ in $\delta_1 F^0$, then $\psi_a(1)$ will not appear anywhere else in $\delta_1 F^0$. This simplifies significantly the task of finding the structures of the functions $\delta_i F^0$, an operation that requires

their explicit computations for the lowest values of i in the attempt to find a pattern for larger i values. Obviously, one starts with $i = 1$, and by trial and errors one finds

$$\delta_1 F^0 = d_1^e(\gamma_s) + d_1^o(\gamma_s), \quad (\text{B.78})$$

$$d_1^e(\gamma_s) = -2\gamma_s \int_0^1 dy \psi_{0+}(y\gamma_s) + 2\gamma_s \psi_{0+}(\gamma_s) - \gamma_s^2 \psi_{1-}(\gamma_s), \quad (\text{B.79})$$

$$d_1^o(\gamma_s) = -\gamma_s^2 \int_0^1 dy y \psi_{1+}(y\gamma_s), \quad (\text{B.80})$$

where we have used the definitions eqs. (A.20)–(A.21). Then, eq. (B.77) becomes

$$\frac{F^0 - \varphi_0(\Omega)}{\varphi_1(\gamma_s)} = 1 + d_1^e(\gamma_s) + d_1^o(\gamma_s) + \delta_2 F^0 + \dots \quad (\text{B.81})$$

$$\equiv \exp \left[d_1^e(\gamma_s) + d_1^o(\gamma_s) \right] + \bar{\delta}_2 F^0 + \dots \quad (\text{B.82})$$

In other words, while eq. (B.81) is simply equal to our starting point, eq. (B.77), in eq. (B.82) we have made the further crucial assumption that the contributions of d_1^e and d_1^o exponentiate: this does not change the structure of the single-Riemann- ζ terms in F^0 (which is why this operation is legitimate), but it does change that of the terms with multiple ζ 's, hence the change of notation $\delta_2 F^0 \rightarrow \bar{\delta}_2 F^0$. Ultimately, whether this exponentiation is appropriate or not is determined by the capability of finding a pattern in the (iteratively modified) $\bar{\delta}_i F^0$ sequence. This indeed turns out to be the case — by computing exactly the contributions up to and including those that feature monomial with four Riemann's ζ , we could establish the existence of a clear pattern, and thence to resum the resulting series. Eq. (B.82) becomes

$$\frac{F^0 - \varphi_0(\Omega)}{\varphi_1(\gamma_s)} = \exp \left[\sum_{n=1}^{\infty} \left(d_n^e(\gamma_s) + d_n^o(\gamma_s) \right) \right], \quad (\text{B.83})$$

while eqs. (B.79) and (B.80) generalise as follows

$$\begin{aligned} \sum_{n=1}^{\infty} d_n^e(\gamma_s) &= - \int_0^1 dy \frac{\gamma_s \psi_{0+}(y\gamma_s)}{1 - 2y\gamma_s \psi_{0+}(y\gamma_s)} - \gamma_s \int_0^1 dy \psi_{0+}(y\gamma_s) \\ &\quad - \log \left(1 - 2\gamma_s \psi_{0+}(\gamma_s) \right) - \frac{1}{2} \log \left(1 + 2\gamma_s^2 \psi_{1-}(\gamma_s) \right), \end{aligned} \quad (\text{B.84})$$

$$\sum_{n=1}^{\infty} d_n^o(\gamma_s) = - \int_0^1 dy \frac{y\gamma_s^2 \psi_{1+}(y\gamma_s)}{1 - 2y\gamma_s \psi_{0+}(y\gamma_s)}, \quad (\text{B.85})$$

where the quantities defined in eqs. (A.20) and (A.21) emerge in a natural manner.

By computing analytically the second integral on the right-hand side of eq. (B.84), and by exploiting some obvious identities among the $\psi_{k\pm}(z)$ functions, eq. (B.83) leads us to the sought result

$$\begin{aligned} F^0 = \varphi_0(\Omega) + \varphi_1(\gamma_s) \exp &\left[\int_0^1 dy \frac{y\gamma_s^2 (\psi_1(1) - \psi_1(1 - y\gamma_s))}{1 - 2y\gamma_s \psi_{0+}(y\gamma_s)} + \gamma_s \psi_0(1) \right. \\ &\quad - \frac{1}{2} \log \Gamma(1 + \gamma_s) + \frac{1}{2} \log \Gamma(1 - \gamma_s) \\ &\quad \left. - \frac{1}{2} \log \left(1 - 2\gamma_s \psi_{0+}(\gamma_s) \right) - \frac{1}{2} \log \left(1 + 2\gamma_s^2 \psi_{1-}(\gamma_s) \right) \right]. \end{aligned} \quad (\text{B.86})$$

This expression can also be rewritten in terms of quantities which have already played a prominent role. One starts by observing that (see eq. (A.17))

$$1 + \hat{\chi}(\gamma_s) \equiv \gamma_s \chi(\gamma_s) = 1 - 2\gamma_s \psi_{0+}(\gamma_s), \quad (\text{B.87})$$

and that

$$1 + \hat{\chi}(\gamma_s) - \gamma_s \hat{\chi}'(\gamma_s) \equiv -\gamma_s^2 \chi'(\gamma_s) = 1 + 2\gamma_s^2 \psi_{1-}(\gamma_s), \quad (\text{B.88})$$

having denoted by a prime the first derivative of a function. Since $\hat{\chi}(z)$ is an odd function of z , its series expansion features only $\psi_i(1)$ terms with even i , and therefore not all terms in eq. (B.86) can be expressed by means of it. We can therefore employ a function which we define by analogy to eq. (2.6), namely:

$$\chi_1(z) = 2\psi_1(1) - \psi_1(z) - \psi_1(1-z). \quad (\text{B.89})$$

We then have

$$\frac{1}{2}(\chi_1(z) - \chi_1'(z)) = \psi_1(1) - \psi_1(1-z). \quad (\text{B.90})$$

By means of these relationships we obtain the final form reported in the main text, eq. (5.1).

At this point, one notes that the structure of the exponential in eq. (B.86) is quite similar (although not identical) to that of the function R_N in eq. (3.17) of ref. [62]; this is relevant, since R_N is the $\mathcal{O}(\epsilon^0)$ term of the renormalised \mathcal{G}_{gg} Green function, in keeping with F^0 being the $\mathcal{O}(\epsilon^0)$ term of the renormalised $\hat{\mathcal{G}}_{gg}$ Green function, eq. (B.68). As a matter of fact, one can manipulate the formulae so that indeed R_N emerges, since owing to eq. (B.90):

$$\begin{aligned} R_N(\text{eq. (3.17) of [62]}) = \exp & \left[\frac{1}{2} \gamma_s \int_0^1 dy \frac{\chi_1(y\gamma_s) - \chi_1'(y\gamma_s)}{\chi(y\gamma_s)} + \gamma_s \psi_0(1) \right. \\ & - \frac{1}{2} \log \Gamma(1 + \gamma_s) + \frac{1}{2} \log \Gamma(1 - \gamma_s) \\ & \left. + \frac{1}{2} \log(\gamma_s \chi(\gamma_s)) - \frac{1}{2} \log(-\gamma_s^2 \chi'(\gamma_s)) \right]. \quad (\text{B.91}) \end{aligned}$$

It is then a matter of trivial algebra to arrive at eq. (5.5).

C Details on numerical implementation

C.1 Numerical integrations for P_{gg}

The numerical implementation of the resummed P_{gg} requires the computation of the inverse Mellin transform of eq. (3.49), which is in turn given by an integral in the complex z plane. We now review the strategy adopted in the HELL code.

The integration in z , at fixed N , must be performed along a Hankel-like contour enclosing the negative real axis. We find it convenient to parametrise the contour as

$$z(t) = A - t + iB \left(1 - \frac{1}{1+t} \right), \quad t \in [0, \infty), \quad (\text{C.1})$$

for the upper part of the contour, while the lower part is given by complex conjugation, $\bar{z}(t)$, to be traveled in the opposite direction. Suitable values for the parameters are $A = 0.2$, $B = 2$. In particular the latter ensures that we travel sufficiently far from the negative real axis, otherwise oscillations may show up. Conversely, A must be small in order to avoid the singularities of h_{gg} . The contour is shown in fig. 12.

Then, we also need to compute the inverse Mellin transform. For this, we can use a typical Mellin inversion path parametrised as

$$N(u) = N_0 + e^{i\theta} u, \quad \frac{\pi}{2} < \theta < \pi, \quad u \in [0, \infty), \quad (\text{C.2})$$

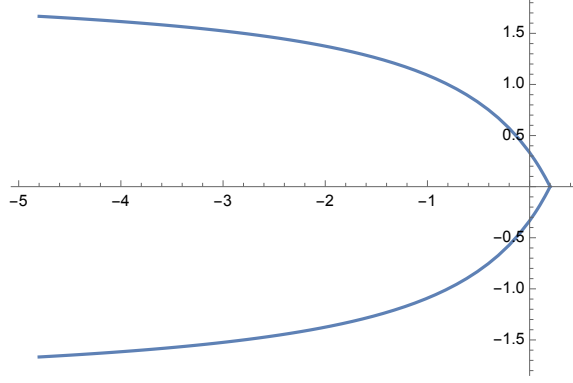


Figure 12. Contour used for the computation of the z integral.

for the upper part, and its complex conjugate (in the opposite direction) for the lower part. Here, $N_0 = 1$ and $\theta = \frac{2}{3}\pi$ are reasonable values. Now, defining⁴⁴

$$H(z, N) \equiv \Gamma \left(1 + \frac{\gamma_+(N, \alpha_s)}{r(N, \alpha_s)} \right) \frac{1}{z} e^{\frac{z}{r(N, \alpha_s)}} \left(\frac{r(N, \alpha_s)}{z} \right)^{\frac{\gamma_+(N, \alpha_s)}{r(N, \alpha_s)}} h_{qg}(z), \quad (\text{C.3})$$

we can rewrite eq. (3.49) as

$$\begin{aligned} \gamma_{qg}^{\text{NLL}'}(\alpha_s, N) &= \frac{\alpha_s}{3\pi} T_R \frac{1}{2\pi i} \oint dz H(z, N) \\ &= \frac{\alpha_s}{3\pi} T_R \frac{1}{2\pi i} \int_0^\infty dt \left[\frac{dz}{dt} H(z(t), N) - \frac{d\bar{z}}{dt} H(\bar{z}(t), N) \right] \end{aligned} \quad (\text{C.4})$$

and thus its inverse Mellin transform as (the bar denotes complex conjugation)

$$\begin{aligned} P_{qg}^{\text{NLL}'}(\alpha_s, x) &= \frac{\alpha_s}{3\pi} T_R \frac{1}{2\pi i} \int_0^\infty du \left\{ \frac{dN}{du} x^{-N(u)} \frac{1}{2\pi i} \int_0^\infty dt \left[\frac{dz}{dt} H(z(t), N(u)) - \frac{d\bar{z}}{dt} H(\bar{z}(t), N(u)) \right] \right. \\ &\quad \left. - \frac{d\bar{N}}{du} x^{-\bar{N}(u)} \frac{1}{2\pi i} \int_0^\infty dt \left[\frac{dz}{dt} H(z(t), \bar{N}(u)) - \frac{d\bar{z}}{dt} H(\bar{z}(t), \bar{N}(u)) \right] \right\} \\ &= -\frac{\alpha_s}{3\pi} T_R \frac{1}{4\pi^2} \int_0^\infty du \int_0^\infty dt \left\{ \frac{dN}{du} x^{-N(u)} \left[\frac{dz}{dt} H(z(t), N(u)) - \frac{d\bar{z}}{dt} H(\bar{z}(t), N(u)) \right] \right. \\ &\quad \left. + \frac{d\bar{N}}{du} x^{-\bar{N}(u)} \left[\frac{d\bar{z}}{dt} H(\bar{z}(t), \bar{N}(u)) - \frac{dz}{dt} H(z(t), \bar{N}(u)) \right] \right\} \\ &= -\frac{\alpha_s}{3\pi} T_R \frac{1}{2\pi^2} \int_0^\infty du \int_0^\infty dt \operatorname{Re} \left\{ \frac{dN}{du} x^{-N(u)} \left[\frac{dz}{dt} H(z(t), N(u)) - \frac{d\bar{z}}{dt} H(\bar{z}(t), N(u)) \right] \right\}, \end{aligned} \quad (\text{C.5})$$

which gives a simple and stable numerical implementation.

One practical aspect that we have to consider is that the function $h_{qg}(z)$, eq. (3.24), depends on the function $\Omega(z)$, eq. (3.8), which is given by an integral appearing at the exponent. Unfortunately we have not been able to compute the integral analytically, so by computing it during integration

⁴⁴We remind the reader that the quantity $r(N, \alpha_s)$ has been introduced in sect. 2.2 in the context of the definition of the approximation of the anomalous dimension, eq. (2.21), used for the resummation of the running coupling contributions.

in z, N one would end up with nested integrals, which are very slow to evaluate. In order to achieve a sufficiently fast numerical implementation, our strategy consists in precomputing the function $\Omega(z)$ along the z contour, eq. (C.1), so that $h_{qg}(z)$ can be quickly evaluated by performing a simple interpolation. For the computation of $\Omega(z)$ along the contour we use one of the expressions derived in appendix B.1, specifically eq. (B.3) or eq. (B.4), which have similar performances.

C.2 Approximate fixed-order anomalous dimension at large α_s

As was mentioned in section 4.1, the HELL construction of the resummed anomalous dimension $\gamma_+^{(N)LL}$ requires an approximation of the fixed-order anomalous dimension used to resum the collinear singularities of the BFKL kernel. The inverse of this fixed-order anomalous dimension (called χ_s in ref. [57]) must be added to the fixed-order BFKL kernel, after subtracting the double counting. This procedure removes the singular behaviour at $\gamma = 0$ of the kernel $\chi_0(\gamma)$, eq. (2.5). However, the kernel has an additional, subleading, singularity at $\gamma = -1$. When computing the inverse to obtain the resummed anomalous dimension (after the symmetrisation procedure) this singularity would dominate the asymptotic behaviour at large N , in disagreement with the logarithmically divergent behaviour of the actual anomalous dimension.

Therefore, in order for this procedure not to spoil the original large- N behaviour, in ref. [57] it has been suggested to replace the exact fixed-order anomalous dimension with an approximation that, while preserving the physical small- N features, behaves asymptotically as a (negative) constant. This is helpful because, when this constant is larger than -1 , the dual of the approximate anomalous dimension dominates over the subleading pole of the BFKL kernel, thus determining the asymptotic form of the resummed anomalous dimension, which then coincides with the one we started from. At this point, in order to restore the physical logarithmic large- N behaviour, one can simply subtract the approximate fixed-order prediction from the resummed anomalous dimension (which have the same asymptotic form), and add back the exact one.

For this procedure to work the constant must be greater than -1 , but its value depends on α_s . Let us review the construction of the approximation. The LO and NLO anomalous dimensions close to $N = 0$ behave as

$$\begin{aligned}\gamma_0(N) &= \frac{a_{11}}{N} + a_{10} + \mathcal{O}(N), \\ \gamma_1(N) &= \frac{a_{22}}{N^2} + \frac{a_{21}}{N} + a_{20} + \mathcal{O}(N),\end{aligned}\tag{C.6}$$

where $a_{22} = 0$ (accidental zero). The approximation proposed in ref. [57] is

$$\gamma^{\text{approx}}(N) = \frac{a_1}{N} + a_0 - (a_1 + a_0) \frac{2N}{N+1},\tag{C.7}$$

which is valid both at the LO and the NLO with appropriate coefficients. At the NLO these are given by

$$\begin{aligned}a_1 &= \alpha_s a_{11} + \alpha_s^2 a_{21}, \\ a_0 &= \alpha_s a_{10} + \alpha_s^2 a_{20},\end{aligned}\tag{C.8}$$

and at the LO one simply neglects the $\mathcal{O}(\alpha_s^2)$ terms; the coefficients are thus given by

$$\begin{aligned}a_{11} &= \frac{C_A}{\pi}, \\ a_{21} &= n_f \frac{26C_F - 23C_A}{36\pi^2}, \\ a_{10} &= -\frac{11C_A + 2n_f(1 - 2C_F C_A + 4C_F^2)}{12\pi},\end{aligned}$$

$$a_{20} = \frac{1}{\pi^2} \left[\frac{1643}{24} - \frac{33}{2} \zeta_2 - 18 \zeta_3 + n_f \left(\frac{4}{9} \zeta_2 - \frac{68}{81} \right) + n_f^2 \frac{13}{2187} \right]. \quad (\text{C.9})$$

The last term of eq. (C.7) is needed to restore the constraint $\gamma^{\text{approx}}(N=1) = 0$ due to momentum conservation, and it is thus largely arbitrary. The choice of the specific functional form of this term is dictated by simplicity, as one additional requirement of the approximation is the possibility of computing the inverse function analytically.

We propose here to modify this function so that the functional form remains simple but the asymptotic value at large N is larger. We thus generalize eq. (C.7) as

$$\gamma^{\text{approx}}(N) = \frac{a_1}{N} + a_0 - (a_1 + a_0) \frac{(1 + \lambda)N}{N + \lambda}, \quad (\text{C.10})$$

where $0 < \lambda \leq 1$ is a parameter that controls the asymptotic behaviour. At large N , eq. (C.10) behaves as a constant,

$$\gamma(N) \xrightarrow{N \rightarrow \infty} -(1 + \lambda)a_1 - \lambda a_0. \quad (\text{C.11})$$

By modifying the original value ($\lambda = 1$) into a smaller value we see that the asymptotic limit of $\gamma(N)$ becomes larger, as desired.

In practice, rather than choosing a specific value of λ , we have decided to promote it to a function of α_s . A simple form that gives satisfactory results is

$$\lambda = \frac{1}{1 + 6\alpha_s^2}. \quad (\text{C.12})$$

In this way at small α_s this reproduces the original value $\lambda = 1$, where it is sufficient, but as α_s increases λ decreases, reaching e.g. $\lambda \sim 1/5$ at $\alpha_s = 0.8$.

The inverse (i.e. the dual) of eq. (C.10) can be computed analytically

$$\chi_s(M) = \frac{a_1 + \lambda a_0 - \lambda M + \sqrt{(\lambda M + a_1 - \lambda a_0)^2 + 4\lambda(1 + \lambda)a_1(a_1 + a_0)}}{2[(1 + \lambda)a_1 + \lambda a_0 + M]}, \quad (\text{C.13})$$

which of course reduces to the result of ref. [57] for $\lambda = 1$.

C.3 A modified approximation for the resummation of running coupling effects in γ_+

The resummation of running-coupling effects to the duality relation between the BFKL kernel and the DGLAP anomalous dimension is obtained by solving the BFKL evolution equation with running coupling, and then by deriving from its solution the desired anomalous dimension [46, 52–54]. A convenient way of performing this task is that of considering an approximation of the kernel such that the sought solution can be computed analytically, simplifying the numerical implementation of this procedure. Originally, an approximation was proposed in ref. [46], which was later used in the first version of HELL [56]. Then, a different form of the approximation has been introduced in ref. [57], which has solved some problems of the original approximation, leading to a more reliable result which has been implemented in HELL from version 2 onwards. In this appendix, we shall briefly review this approximation, and propose a simple modification of it which allows us to avoid an undesired effect showing up at large α_s .

Without giving a thorough explanation (for more detail, see section 3 of ref. [57]), we recall that the approximation of the BFKL kernel $\chi(\alpha_s, \gamma)$ which we consider here has two aspects: an approximation of the α_s dependence, and an approximation of the γ dependence. As far as the former is concerned, a linear approximation in α_s is employed,

$$\chi(\alpha_s, \gamma) = \chi(\alpha_0, \gamma) + (\alpha_s - \alpha_0)\chi'(\alpha_0, \gamma), \quad (\text{C.14})$$

where the prime denotes a derivative with respect to α_s . In the equation above, α_0 is a reference value for α_s around which the linear approximation is computed, and it is typically given by α_s computed at the hard scale. A simpler approximation is also considered,

$$\chi(\alpha_s, \gamma) = \alpha_s \frac{\chi(\alpha_0, \gamma)}{\alpha_0}, \quad (\text{C.15})$$

which is used as an alternative implementation for the resummation of these running coupling effects, to construct an uncertainty band on the result, see sect. 4.3.

Then, the γ dependence of the kernel is approximated as

$$\begin{aligned} \chi(\alpha_s, \gamma) &\simeq \chi_{\text{coll}}(\alpha_s, \gamma) \\ &= c(\alpha_s) + \frac{\gamma_{\text{min}}^3(\alpha_s) \kappa(\alpha_s)}{4} \left[\frac{1}{\gamma} + \frac{1}{2\gamma_{\text{min}}(\alpha_s) - \gamma} - \frac{2}{\gamma_{\text{min}}(\alpha_s)} \right] \\ &= c(\alpha_s) + \frac{\kappa(\alpha_s)}{2} (\gamma - \gamma_{\text{min}}(\alpha_s))^2 + \mathcal{O}((\gamma - \gamma_{\text{min}})^3), \end{aligned} \quad (\text{C.16})$$

which is a symmetric form with respect to $\gamma = \gamma_{\text{min}}(\alpha_s)$ based on two poles such that its expansion around the symmetry point coincides with the one of the double-leading kernel up to second order. Indeed, the parameters $c(\alpha_s)$ and $\kappa(\alpha_s)$, as well as the position of the minimum $\gamma_{\text{min}}(\alpha_s)$, are computed from the double-leading kernel, and used in the construction of the approximation. This is the key property of this approximation, as the region around the minimum encodes the leading behaviour at small x , which then must be correctly reproduced.

For reasons upon which we shall comment in a moment, we propose here a simple modification of this approximation, where the two poles are shifted by some amount η in mutually opposite directions to preserve the symmetry:

$$\begin{aligned} \chi(\alpha_s, \gamma) &\simeq \chi_{\text{coll, new}}(\alpha_s, \gamma) \\ &= c(\alpha_s) + \frac{(\gamma_{\text{min}}(\alpha_s) + \eta)^3 \kappa(\alpha_s)}{4} \left[\frac{1}{\gamma + \eta} + \frac{1}{2\gamma_{\text{min}}(\alpha_s) - \gamma + \eta} - \frac{2}{\gamma_{\text{min}}(\alpha_s) + \eta} \right]. \end{aligned} \quad (\text{C.17})$$

The parameters of the approximation have been adapted such that its expansion around the minimum coincides with the previous approximation, eq. (C.16). Therefore, this approximation has all the properties of the previous one, but the poles are located in different places. The solution to the running-coupling duality equation within this new approximation is

$$\gamma_{\text{rc}}(\alpha_s, N) = \gamma_{\text{min}} + \beta_0 \bar{\alpha}_s \left[z \frac{k'_\nu(z)}{k_\nu(z)} - 1 \right], \quad (\text{C.18})$$

with (omitting the dependence on α_s for improved readability)

$$\frac{1}{\bar{\alpha}_s} = \frac{1}{\alpha_s} + \frac{\kappa' - 2c' / (\gamma_{\text{min}} + \eta)^2}{\kappa - \alpha_s \kappa' + 2(N - c + \alpha_s c') / (\gamma_{\text{min}} + \eta)^2} \quad (\text{C.19a})$$

$$z = \frac{1}{\beta_0 \bar{\alpha}_s} \sqrt{\frac{N - c + \alpha_s c'}{(\kappa - \alpha_s \kappa') / 2 + (N - c + \alpha_s c') / (\gamma_{\text{min}} + \eta)^2}} \quad (\text{C.19b})$$

$$\nu = \left(\frac{c'}{N - c + \alpha_s c'} + \frac{\kappa' - 2c' / (\gamma_{\text{min}} + \eta)^2}{\kappa - \alpha_s \kappa' + 2(N - c + \alpha_s c') / (\gamma_{\text{min}} + \eta)^2} \right) \bar{\alpha}_s z. \quad (\text{C.19c})$$

and where $k_\nu(z)$ is a Bateman function. This solution tends to the one of ref. [57] in the limit $\eta \rightarrow 0$. We also clearly see that the overall effect of having introduced the parameter η amounts to a global⁴⁵ shift in $\gamma_{\text{min}} \rightarrow \gamma_{\text{min}} + \eta$, which is thus very easy to implement numerically.

⁴⁵Except in the first term of eq. (C.18), which remains γ_{min} . This is however irrelevant, as this term is subtracted as a double-counting contribution when combining this solution with the double-leading result.

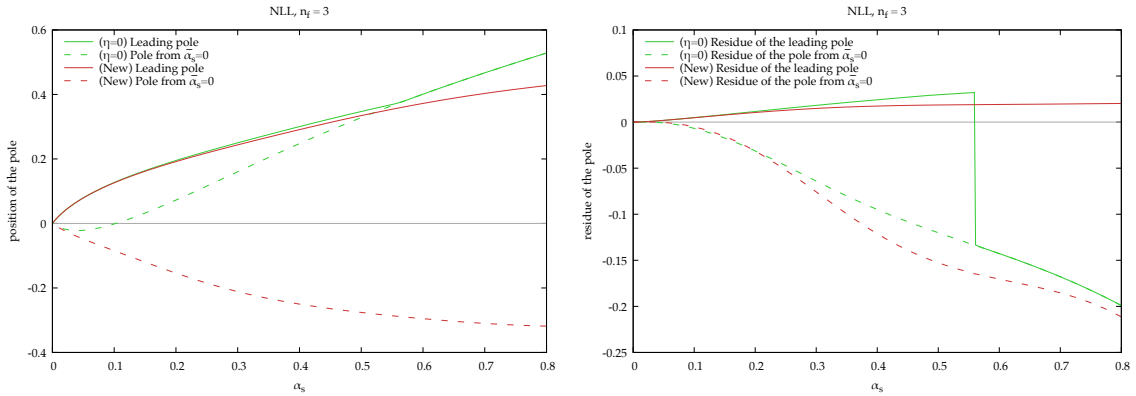


Figure 13. The left-hand side panel shows the leading (i.e. rightmost) pole of $\gamma_{\text{rc}}(\alpha_s, N)$ (solid lines) and the pole due to $\bar{\alpha}_s = 0$, eq. (C.20) (dashed lines), in the original configuration with $\eta = 0$ (green curves) and with the new suggested value of η , eq. (C.22) (red curves). The right-hand side panel shows the corresponding residues using curves with the same styles. In the $\eta = 0$ case the pole due to $\bar{\alpha}_s = 0$ becomes the leading one at $\alpha_s \sim 0.55$, thus inducing a jump in the residue of the leading pole; with the new choice for η the pole due to $\bar{\alpha}_s = 0$ is always negative.

The reason for the new approximation resides in the singularities of this solution. When α_s is sufficiently small, the leading (rightmost) singularity in N is dictated by the rightmost zero of the Bateman function $k_\nu(z)$ appearing in the denominator of eq. (C.18). However, there are other poles not due to the Bateman function but to the factors $\bar{\alpha}_s$ and z . The former in particular gives a pole at

$$N = N_-(\alpha_s) \equiv c(\alpha_s) - \frac{\kappa(\alpha_s)}{2} (\gamma_{\min}(\alpha_s) + \eta)^2 \quad (\text{C.20})$$

with residue

$$r_-(\alpha_s) \equiv -\alpha_s \beta_0 \left[\alpha_s c'(\alpha_s) - \frac{\alpha_s \kappa'(\alpha_s)}{2} (\gamma_{\min}(\alpha_s) + \eta)^2 \right]. \quad (\text{C.21})$$

This residue is typically negative, and typically larger in absolute value than the positive residue due to the Bateman pole. Moreover, in the original $\eta = 0$ case, this pole becomes the leading one at sufficiently large α_s , see fig. 13.

Having a pole with a large negative residue which becomes even the dominant one as α_s increases has the effect of producing splitting functions which decrease with decreasing x at small x 's. This is unexpected, based on the features seen at the LL and at smaller values of α_s , as well as from general Regge theory considerations. In fact, the presence of this singularity is strongly related to the specific functional form that we have used to construct the approximation of the kernel, and as such it does not necessarily represent a true physical feature.

This is where the η parameter comes to help. Owing to the positivity of $\kappa(\alpha_s)$, a positive value of η reduces the value of N_- , eq. (C.20), pushing the pole to the left and thus making it less dangerous. A positive parameter η is also natural. Indeed, the actual double-leading kernel does no longer have the collinear pole at $N = 0$, because it has been resummed by duality with the (approximate) fixed-order anomalous dimension discussed in sect. C.2. Rather, after resummation the leading pole to the left of the minimum is positioned by construction in the asymptotic value of the approximate anomalous dimension at large N , eq. (C.11). The shape of the actual double-leading kernel is thus better reproduced by setting

$$\eta = (1 - \lambda)a_1 + \lambda a_0, \quad (\text{C.22})$$

in terms of the parameters introduced in sect. C.2. In this way, η becomes a function of α_s , which begins at $\mathcal{O}(\alpha_s)$. As such, this change with respect to the previous implementation is “perturbative”, and thus it has a smaller effect at small α_s . At the large values of α_s that we have considered in this work, the introduction of η with the form eq. (C.22) solves the issue found at $\eta = 0$. In particular, the leading pole is always the one coming from the Bateman function, while for the considered α_s values the spurious pole N_- , eq. (C.20), is always negative (see figure 13).

In particular, as one can see from the figure, the leading pole is basically unchanged after the introduction of the η parameter, up until the point where the spurious pole from $\bar{\alpha}_s = 0$ dominates in the $\eta = 0$ case. This confirms that the rightmost pole coming from the Bateman function is stable upon changes of unphysical parameters, and represents a physical property of the result. On the contrary, the spurious pole from $\bar{\alpha}_s = 0$ is strongly dependent on the choice of η , which confirms its unphysical nature. The use of η from eq. (C.22) strongly reduces the impact of this unphysical pole, and thus represents a significant improvement over the previous $\eta = 0$ implementation, which is necessary to deal reliably with the region of large α_s .

C.4 Solution to the branch-change problem in γ_+

We give here some detail on how we solved the branch-change problem discussed in section 4.1. First of all, we want to clarify how the duality is solved along the inverse Mellin contour. This contour is typically given by eq. (C.2) in the upper half-plane $\text{Im}(N) \geq 0$, and by its complex conjugate path in the lower half-plane. As the function $\gamma_+(\alpha_s, N)$ is real, namely $\gamma_+(\alpha_s, \bar{N}) = \overline{\gamma_+(\alpha_s, N)}$, it is sufficient to consider it on the upper half-plane.

The original HELL approach consisted in starting from the computation of $\gamma_+(\alpha_s, N_0)$, with N_0 lying on the real axis where we can use robust numerical zero-finding methods, and then moving along the contour in small steps, using every time the value of γ_+ from the previous step as an initial guess for the Secant method, which is a variant of the well known Newton method where the derivative of the function is replaced by a numerically computed difference quotient. The only change we have made to this procedure is related to the choice of the starting point. Any of these zero-finding algorithms require a reasonably good guess of the result, and it is much easier to find it if N is real and large. Indeed, in this limit, the solution of the duality should, by construction, correspond to the fixed-order anomalous dimension that was used to resum the kernel, i.e. the one discussed in appendix C.2. In order to exploit this property, we take a starting real value of N which is sufficiently large (we currently use $N = 15$ in the code), and from there we move towards N_0 in small steps along the real axis, using the result at the previous step as an initial guess. For this procedure to be even more robust, along this path on the real axis we perform for each value of N a scan of the (real) function to be set to zero in order to make sure that there is a single sign flip in the region under consideration, and then apply the Regula Falsi method⁴⁶ in that region. Note that this path along the real axis is ignored in the end — it is just used to provide the correct starting point N_0 for the original procedure.⁴⁷

As was mentioned, it may happen at large values of $|\text{Im}(N)|$ that for two values of α_s even very close to one another the duality condition selects two different branches of the anomalous dimension along the N contour. This is normal because we expect this function to have branch cuts, but undesirable because it produces different large- x behaviours after Mellin inversion. One possible workaround is to modify the contour such that the duality always selects the same branch. This works up to a point: indeed, in order to avoid switching branch, the contour must become very steep as α_s gets larger, leading to numerical instabilities in the Mellin inversion. Therefore,

⁴⁶If there is a single zero in the considered range, the Regula Falsi method finds it in a very robust and fast way.

⁴⁷This is important at large α_s , because at $N_0 \sim 1$ the resummed anomalous dimension is no longer so similar to the fixed-order one.

we have decided to keep the contour fixed (we employ $N_0 = 1.1$ and $\theta = \frac{2}{3}\pi$ in eq. (C.2)) and to adopt the procedure discussed in section 4.1, which is articulated in a number of steps:

- Firstly, the resummed contribution to the anomalous dimension (the actual resummed result minus its fixed-order expansion), that we denote here by $\Delta\gamma_+(\alpha_s, N)$, is computed along the Mellin inversion contour.
- Then, its inverse Mellin transform, denoted by $\Delta P_+(\alpha_s, x)$, is numerically computed ignoring the issue of the change-of-branch.
- Since the large- x behaviour of such $\Delta P_+(\alpha_s, x)$ is unstable (due to the changing of the branch) and is in any case inaccurate (as we are resumming small- x logarithms without control on the large- x region), we replace it with a cubic extrapolation (in $\log x$) for $x > x_{\text{extr}}$ based on the values of x below this boundary of the large- x region. In the code we currently use $x_{\text{extr}} = 0.02$. We call the result of this procedure $\Delta P_+^{\text{extr}}(\alpha_s, x)$.
- The extrapolation destroys momentum conservation, which we have to impose back by adding a suitable contribution. In order to do so, we need to know the integral of $x\Delta P_+^{\text{extr}}(\alpha_s, x)$ after the extrapolation is performed. This cannot be done analytically, so we have to revert to numerical methods. Rather than simply computing the integral numerically, we find it more convenient to approximate the entire function with a suitable polynomial basis, so that the integral (and in general, the Mellin transform) can be computed analytically. Therefore, the fourth step consists in performing this polynomial approximation.
- Once this projection onto polynomials is performed, not only we can easily restore momentum conservation, but we also have a simple parametrisation available for the Mellin transform of the patched ΔP_+ . We thus use it as a substitute of the original γ_+ for all the remaining tasks in HELLY, e.g., for the computation of the resummed γ_{qg} from eq. (3.49).

It is instructive to give some extra detail on the last two steps. First of all, we recall that the dominant behaviour of the function ΔP_+ at low x is given by x^{-1-N_B} , where $N_B = N_B(\alpha_s) > 0$ is the position of the leading pole of eq. (C.18). We thus find it more convenient to apply the approximation procedure to the function

$$f(\alpha_s, x) = x^{1+N_B(\alpha_s)+p} \Delta P_+^{\text{extr}}(\alpha_s, x), \quad (\text{C.23})$$

which has a flatter behaviour at small x when $p \sim 0$. We introduced p to be able to slightly modify the asymptotic small- x behaviour, in order to have a handle to possibly improve the polynomial approximation. For such an approximation, we considered Chebyshev polynomials of the first kind, which are very convenient from a numerical point of view, as they provide accurate approximations with fast routines. It is important however to choose a proper functional form of x to be used as the variable in these polynomials. The simplest option is to consider polynomials in $\log x$, which would allow us to express, after the projection onto the basis and further manipulations,

$$f^{\text{cheb,log}}(\alpha_s, x) = \sum_{k=0}^n c_k \log^k x, \quad (\text{C.24})$$

whose Mellin transform is easily computed,

$$\tilde{f}^{\text{cheb,log}}(\alpha_s, N) = \sum_{k=0}^n c_k \frac{(-)^k k!}{(N+1)^{k+1}}. \quad (\text{C.25})$$

Here, n is the order of the polynomial approximation. In practice, we found it more convenient to use another functional form for the argument of the polynomials, namely a fractional power of x , so that

$$f^{\text{cheb,pow}}(\alpha_s, x) = \sum_{k=0}^n c_k x^{k/q}, \quad (\text{C.26})$$

whose Mellin transform is even simpler than that of eq. (C.25),

$$\tilde{f}^{\text{cheb,pow}}(\alpha_s, N) = \sum_{k=0}^n \frac{c_k}{N+1+k/q}. \quad (\text{C.27})$$

In both cases, we perform the projection onto the Chebyshev polynomials in the range $x_{\min} \leq x \leq 1$, with $x_{\min} = 10^{-7}$. We observe that the extrapolation below x_{\min} is better behaved when using a power, so we adopt this choice, with $q = 6$, $n = 12$ and $p = -0.1$. The Mellin transform of $\Delta P_+^{\text{extr}}(\alpha_s, x)$ is thus approximated by

$$\begin{aligned} \int_0^1 dx x^N \Delta P_+^{\text{extr}}(\alpha_s, x) &= \int_0^1 dx x^{N-1-N_B-p} f(\alpha_s, x) \\ &\simeq \tilde{f}^{\text{cheb,pow}}(\alpha_s, N-1-N_B-p) \\ &= \sum_{k=0}^n \frac{c_k}{N-N_B-p+k/q}. \end{aligned} \quad (\text{C.28})$$

We can now restore momentum conservation by defining

$$\Delta P_+^{\text{new}}(\alpha_s, x) \equiv \frac{f^{\text{cheb,pow}}(\alpha_s, x)}{x^{1+N_B+p}} - c_{\text{mc}} \quad (\text{C.29})$$

with

$$c_{\text{mc}} = 2\tilde{f}^{\text{cheb,pow}}(\alpha_s, -N_B-p) \quad (\text{C.30})$$

such that

$$\int_0^1 dx x \Delta P_+^{\text{new}}(\alpha_s, x) = 0. \quad (\text{C.31})$$

The corresponding anomalous dimension is

$$\begin{aligned} \Delta\gamma_+^{\text{new}}(\alpha_s, N) &= \tilde{f}^{\text{cheb,pow}}(\alpha_s, N-1-N_B-p) - \frac{c_{\text{mc}}}{N+1} \\ &= \sum_{k=0}^n c_k \left(\frac{1}{N-N_B-p+k/q} - \frac{1}{(N+1)(-N_B-p+k/q)} \right). \end{aligned} \quad (\text{C.32})$$

This anomalous dimension is now used in all of the subsequent manipulations in [HELL](#). This is very convenient, as with a limited number of parameters (13 coefficients for $n = 12$) we can reconstruct the anomalous dimension at any N in a very fast way, as opposed to the previous implementation that required the sampling of the anomalous dimension on a specific N -space path with many (~ 2000) points.

References

- [1] V. N. Gribov and L. N. Lipatov, *Deep inelastic e p scattering in perturbation theory*, *Sov. J. Nucl. Phys.* **15** (1972) 438.
- [2] Y. L. Dokshitzer, *Calculation of the Structure Functions for Deep Inelastic Scattering and e+ e- Annihilation by Perturbation Theory in Quantum Chromodynamics.*, *Sov. Phys. JETP* **46** (1977) 641.

- [3] G. Altarelli and G. Parisi, *Asymptotic Freedom in Parton Language*, *Nucl. Phys. B* **126** (1977) 298.
- [4] S. Moch, J. A. M. Vermaseren and A. Vogt, *The Three loop splitting functions in QCD: The Nonsinglet case*, *Nucl. Phys. B* **688** (2004) 101 [[hep-ph/0403192](#)].
- [5] A. Vogt, S. Moch and J. A. M. Vermaseren, *The Three-loop splitting functions in QCD: The Singlet case*, *Nucl. Phys. B* **691** (2004) 129 [[hep-ph/0404111](#)].
- [6] J. Davies, A. Vogt, B. Ruijl, T. Ueda and J. A. M. Vermaseren, *Large- n_f contributions to the four-loop splitting functions in QCD*, *Nucl. Phys. B* **915** (2017) 335 [[1610.07477](#)].
- [7] S. Moch, B. Ruijl, T. Ueda, J. A. M. Vermaseren and A. Vogt, *Four-Loop Non-Singlet Splitting Functions in the Planar Limit and Beyond*, *JHEP* **10** (2017) 041 [[1707.08315](#)].
- [8] G. Falcioni, F. Herzog, S. Moch and A. Vogt, *Four-loop splitting functions in QCD – The gluon-to-quark case*, *Phys. Lett. B* **846** (2023) 138215 [[2307.04158](#)].
- [9] G. Falcioni, F. Herzog, S. Moch and A. Vogt, *Four-loop splitting functions in QCD – The quark-quark case*, *Phys. Lett. B* **842** (2023) 137944 [[2302.07593](#)].
- [10] G. Falcioni, F. Herzog, S. Moch, J. Vermaseren and A. Vogt, *The double fermionic contribution to the four-loop quark-to-gluon splitting function*, *Phys. Lett. B* **848** (2024) 138351 [[2310.01245](#)].
- [11] T. Gehrmann, A. von Manteuffel, V. Sotnikov and T.-Z. Yang, *Complete N_f^2 contributions to four-loop pure-singlet splitting functions*, *JHEP* **01** (2024) 029 [[2308.07958](#)].
- [12] T. Gehrmann, A. von Manteuffel, V. Sotnikov and T.-Z. Yang, *The $N_f CF_3$ contribution to the non-singlet splitting function at four-loop order*, *Phys. Lett. B* **849** (2024) 138427 [[2310.12240](#)].
- [13] G. Falcioni, F. Herzog, S. Moch, A. Pelloni and A. Vogt, *Four-loop splitting functions in QCD – The quark-to-gluon case*, *Phys. Lett. B* **856** (2024) 138906 [[2404.09701](#)].
- [14] G. Falcioni, F. Herzog, S. Moch, A. Pelloni and A. Vogt, *Four-loop splitting functions in QCD – the gluon-gluon case –*, *Phys. Lett. B* **860** (2025) 139194 [[2410.08089](#)].
- [15] B. A. Kniehl, S. Moch, V. N. Velizhanin and A. Vogt, *Flavor Nonsinglet Splitting Functions at Four Loops in QCD: Fermionic Contributions*, *Phys. Rev. Lett.* **135** (2025) 071902 [[2505.09381](#)].
- [16] G. Falcioni, F. Herzog, S. Moch, A. Pelloni and A. Vogt, *Additional results on the four-loop flavour-singlet splitting functions in QCD*, [[2512.10783](#)].
- [17] V. Bertone, M. Cacciari, S. Frixione and G. Stagnitto, *The partonic structure of the electron at the next-to-leading logarithmic accuracy in QED*, *JHEP* **03** (2020) 135 [[1911.12040](#)].
- [18] V. Bertone, M. Cacciari, S. Frixione, G. Stagnitto, M. Zaro and X. Zhao, *Improving methods and predictions at high-energy e^+e^- colliders within collinear factorisation*, *JHEP* **10** (2022) 089 [[2207.03265](#)].
- [19] S. Frixione, *Initial conditions for electron and photon structure and fragmentation functions*, *JHEP* **11** (2019) 158 [[1909.03886](#)].
- [20] M. Stahlhofen, *NNLO electron structure functions (PDFs) from SCET*, [[2508.16964](#)].
- [21] M. Schnubel and R. Szafron, *Electron and Photon Structure Functions at Two Loops*, [[2509.09618](#)].
- [22] J. Blumlein, A. De Freitas and W. van Neerven, *Two-loop QED Operator Matrix Elements with Massive External Fermion Lines*, *Nucl. Phys. B* **855** (2012) 508 [[1107.4638](#)].
- [23] T. Han, Y. Ma and K. Xie, *Quark and gluon contents of a lepton at high energies*, *JHEP* **02** (2022) 154 [[2103.09844](#)].
- [24] F. Garosi, D. Marzocca and S. Trifinopoulos, *LePDF: Standard Model PDFs for high-energy lepton colliders*, *JHEP* **09** (2023) 107 [[2303.16964](#)].
- [25] S. Frixione and G. Stagnitto, *The muon parton distribution functions*, *JHEP* **12** (2023) 170 [[2309.07516](#)].

- [26] Y. V. Kovchegov and E. Levin, *Quantum Chromodynamics at High Energy*, vol. 33. Oxford University Press, 2013, [10.1017/9781009291446](https://doi.org/10.1017/9781009291446).
- [27] J. R. Forshaw and D. A. Ross, *Quantum Chromodynamics and the Pomeron*, vol. 9. Oxford University Press, 1998, [10.1017/9781009290111](https://doi.org/10.1017/9781009290111).
- [28] L. N. Lipatov, *Reggeization of the Vector Meson and the Vacuum Singularity in Nonabelian Gauge Theories*, *Sov. J. Nucl. Phys.* **23** (1976) 338.
- [29] V. S. Fadin, E. A. Kuraev and L. N. Lipatov, *On the Pomeron Singularity in Asymptotically Free Theories*, *Phys. Lett. B* **60** (1975) 50.
- [30] E. A. Kuraev, L. N. Lipatov and V. S. Fadin, *Multiregge processes in the Yang-Mills theory*, *Sov. Phys. JETP* **44** (1976) 443.
- [31] E. A. Kuraev, L. N. Lipatov and V. S. Fadin, *The Pomeron singularity in nonabelian gauge theories*, *Sov. Phys. JETP* **45** (1977) 199.
- [32] I. I. Balitsky and L. N. Lipatov, *The Pomeron Singularity in Quantum Chromodynamics*, *Sov. J. Nucl. Phys.* **28** (1978) 822.
- [33] V. S. Fadin and L. N. Lipatov, *BFKL pomeron in the next-to-leading approximation*, *Phys. Lett. B* **429** (1998) 127 [[hep-ph/9802290](https://arxiv.org/abs/hep-ph/9802290)].
- [34] M. Ciafaloni and G. Camici, *Energy scale(s) and next-to-leading BFKL equation*, *Phys. Lett. B* **430** (1998) 349 [[hep-ph/9803389](https://arxiv.org/abs/hep-ph/9803389)].
- [35] F. Caola, A. Chakraborty, G. Gambuti, A. von Manteuffel and L. Tancredi, *Three-Loop Gluon Scattering in QCD and the Gluon Regge Trajectory*, *Phys. Rev. Lett.* **128** (2022) 212001 [[2112.11097](https://arxiv.org/abs/2112.11097)].
- [36] G. Falcioni, E. Gardi, N. Maher, C. Milloy and L. Vernazza, *Disentangling the Regge Cut and Regge Pole in Perturbative QCD*, *Phys. Rev. Lett.* **128** (2022) 132001 [[2112.11098](https://arxiv.org/abs/2112.11098)].
- [37] G. Falcioni, E. Gardi, N. Maher, C. Milloy and L. Vernazza, *Scattering amplitudes in the Regge limit and the soft anomalous dimension through four loops*, *JHEP* **03** (2022) 053 [[2111.10664](https://arxiv.org/abs/2111.10664)].
- [38] F. Buccioni, F. Caola, F. Devoto and G. Gambuti, *Investigating the universality of five-point QCD scattering amplitudes at high energy*, *JHEP* **03** (2025) 129 [[2411.14050](https://arxiv.org/abs/2411.14050)].
- [39] S. Abreu, G. De Laurentis, G. Falcioni, E. Gardi, C. Milloy and L. Vernazza, *The two-loop Lipatov vertex in QCD*, *JHEP* **04** (2025) 161 [[2412.20578](https://arxiv.org/abs/2412.20578)].
- [40] E. P. Byrne, V. Del Duca, L. J. Dixon, E. Gardi and J. M. Smillie, *One-loop central-emission vertex for two gluons in $\mathcal{N} = 4$ super Yang-Mills theory*, *JHEP* **08** (2022) 271 [[2204.12459](https://arxiv.org/abs/2204.12459)].
- [41] E. P. Byrne, V. Del Duca, E. Gardi, Y. Mo and J. M. Smillie, *Regge factorization of tree-level QCD amplitudes using a minimal set of lightcone variables*, [[2506.10644](https://arxiv.org/abs/2506.10644)].
- [42] R. D. Ball and S. Forte, *Summation of leading logarithms at small x* , *Phys. Lett. B* **351** (1995) 313 [[hep-ph/9501231](https://arxiv.org/abs/hep-ph/9501231)].
- [43] R. D. Ball and S. Forte, *Asymptotically free partons at high-energy*, *Phys. Lett. B* **405** (1997) 317 [[hep-ph/9703417](https://arxiv.org/abs/hep-ph/9703417)].
- [44] G. Altarelli, R. D. Ball and S. Forte, *Factorization and resummation of small x scaling violations with running coupling*, *Nucl. Phys. B* **621** (2002) 359 [[hep-ph/0109178](https://arxiv.org/abs/hep-ph/0109178)].
- [45] G. Altarelli, R. D. Ball and S. Forte, *An Anomalous dimension for small x evolution*, *Nucl. Phys. B* **674** (2003) 459 [[hep-ph/0306156](https://arxiv.org/abs/hep-ph/0306156)].
- [46] G. Altarelli, R. D. Ball and S. Forte, *Perturbatively stable resummed small x evolution kernels*, *Nucl. Phys. B* **742** (2006) 1 [[hep-ph/0512237](https://arxiv.org/abs/hep-ph/0512237)].
- [47] G. Altarelli, R. D. Ball and S. Forte, *Small x Resummation with Quarks: Deep-Inelastic Scattering*, *Nucl. Phys. B* **799** (2008) 199 [[0802.0032](https://arxiv.org/abs/0802.0032)].

- [48] G. P. Salam, *A Resummation of large subleading corrections at small x* , *JHEP* **07** (1998) 019 [[hep-ph/9806482](#)].
- [49] M. Ciafaloni, D. Colferai and G. P. Salam, *Renormalization group improved small x equation*, *Phys. Rev. D* **60** (1999) 114036 [[hep-ph/9905566](#)].
- [50] M. Ciafaloni, D. Colferai, G. P. Salam and A. M. Stasto, *Renormalization group improved small x Green's function*, *Phys. Rev. D* **68** (2003) 114003 [[hep-ph/0307188](#)].
- [51] M. Ciafaloni, D. Colferai, G. P. Salam and A. M. Stasto, *A Matrix formulation for small- x singlet evolution*, *JHEP* **08** (2007) 046 [[0707.1453](#)].
- [52] R. S. Thorne, *Explicit calculation of the running coupling BFKL anomalous dimension*, *Phys. Lett. B* **474** (2000) 372 [[hep-ph/9912284](#)].
- [53] R. S. Thorne, *NLO BFKL equation, running coupling and renormalization scales*, *Phys. Rev. D* **60** (1999) 054031 [[hep-ph/9901331](#)].
- [54] R. S. Thorne, *The Running coupling BFKL anomalous dimensions and splitting functions*, *Phys. Rev. D* **64** (2001) 074005 [[hep-ph/0103210](#)].
- [55] C. D. White and R. S. Thorne, *A Global Fit to Scattering Data with NLL BFKL Resummations*, *Phys. Rev. D* **75** (2007) 034005 [[hep-ph/0611204](#)].
- [56] M. Bonvini, S. Marzani and T. Peraro, *Small- x resummation from HELL*, *Eur. Phys. J. C* **76** (2016) 597 [[1607.02153](#)].
- [57] M. Bonvini, S. Marzani and C. Muselli, *Towards parton distribution functions with small- x resummation: HELL 2.0*, *JHEP* **12** (2017) 117 [[1708.07510](#)].
- [58] M. Bonvini and S. Marzani, *Four-loop splitting functions at small x* , *JHEP* **06** (2018) 145 [[1805.06460](#)].
- [59] B. R. Webber, *QCD power corrections from a simple model for the running coupling*, *JHEP* **10** (1998) 012 [[hep-ph/9805484](#)].
- [60] M. Bonvini, S. Frixione and G. Stagnitto, *Lepton parton distribution functions with a mixed QED+QCD evolution and small- x resummation*, to appear.
- [61] S. Catani, M. Ciafaloni and F. Hautmann, *High-energy factorization in QCD and minimal subtraction scheme*, *Phys. Lett. B* **307** (1993) 147.
- [62] S. Catani and F. Hautmann, *High-energy factorization and small x deep inelastic scattering beyond leading order*, *Nucl. Phys. B* **427** (1994) 475 [[hep-ph/9405388](#)].
- [63] M. Ciafaloni and D. Colferai, *Dimensional regularisation and factorisation schemes in the BFKL equation at subleading level*, *JHEP* **09** (2005) 069 [[hep-ph/0507106](#)].
- [64] S. Marzani, R. D. Ball, P. Falgari and S. Forte, *BFKL at next-to-next-to-leading order*, *Nucl. Phys. B* **783** (2007) 143 [[0704.2404](#)].
- [65] R. D. Ball, *Resummation of Hadroproduction Cross-sections at High Energy*, *Nucl. Phys. B* **796** (2008) 137 [[0708.1277](#)].
- [66] M. Bonvini and S. Marzani, *Resummed Higgs cross section at N^3LL* , *JHEP* **09** (2014) 007 [[1405.3654](#)].
- [67] M. Ciafaloni, D. Colferai, G. P. Salam and A. M. Stasto, *The Gluon splitting function at moderately small x* , *Phys. Lett. B* **587** (2004) 87 [[hep-ph/0311325](#)].
- [68] G. Altarelli, R. D. Ball and S. Forte, *Resummation of singlet parton evolution at small x* , *Nucl. Phys. B* **575** (2000) 313 [[hep-ph/9911273](#)].